The eco-hydrology of drought: What are the survival mechanisms of trees?

Exploring the hypothesis that trees will create deep fine root mass to prevent carbon loss under severe drought.

E.E. (Emma) Daniels (0448257)
Student Utrecht University (UU)
Master programme: System Earth Modelling (Earth Sciences)
Email: *amme@hccnet.nl*

Supervisors:
Prof. dr. ir. M.F.P. (Marc) Bierkens
Utrecht University, Physical Geography
Email: m.*biekens@geo.uu.nl*

Dr. S.C. (Stefan) Dekker
Utrecht University, Copernicus Institute
Email: *s.dekker@geo.uu.nl*

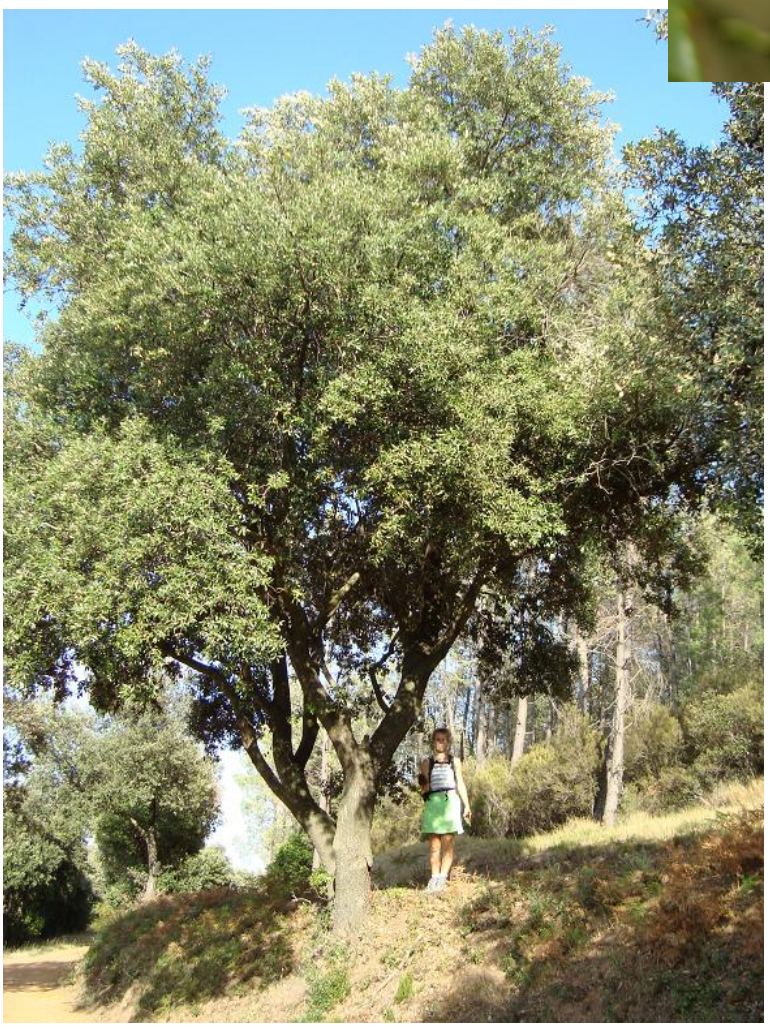

Abstract

Trees play an important role in the biosphere on earth, both in the ecosystems they are part of and through the role they play in the biosphere-atmosphere interaction as a source of water to the atmosphere by transpiration. Global climate change will increase the magnitude and frequency of droughts in many parts of the world among which Southern Europe, therefore increasing our knowledge of the drought resistance and vulnerability of tree species is most pressing. Evaporation observations of forests in the Netherlands during periods of regular drought show that trees are able to evaporate almost at full potential, while surrounding crops and grasses show an evaporation reduction. This reduction in transpiration indicates a reduction in the carbon uptake of vegetation, because these processes are linked. There are doubts whether the underlying process that causes this phenomenon is taken into account correctly in current simulation models. The hypothetical mechanism that will be investigated during this research project is that trees can relocate fine root mass under drought to utilize water stored deeper in the soil and retain transpiration under limiting soil moisture conditions. To correctly simulate the hydrological consequences of climate change, under the foreseen increase in droughts, it is important to investigate this adaptation mechanism and potentially make it part of eco-hydrological models. The key assumption is that a tree will maximize its energy (i.e. carbon) gain by the optimal choice of the following trade-off strategies: (1) keeping photosynthesis going by investing in replacement of fine root mass and extracting water from deeper down the profile or (2) decreasing maintenance respiration by decreasing leave area.

This hypothesis is investigated with a Vegetation Optimality Model that simulates vertical carbon and water fluxes. The underlying assumption of the optimality approach is that vegetation maximizes its 'Net Carbon Profit' (NCP) to be most fit from an evolutionary perspective. The hypothetical root optimization strategy proposed in this research project was modelled as to achieve maximum NCP for the tree. The assumption that NCP is maximized by vegetation, allows formulating a single objective function accounting for both productivity and "water stress". The model was run using half-hourly Eddy covariance measurement data made available by the CarboEurope Integrated Project Ecosystem Component Database. The model was used for the Hainich forest site (DE-Hai) in Central Germany, where it was calibrated for the tree species *Fagus sylvatica L.* (european beech), and for Puechabon (FR-Pue) in the Herault region in France, calibrated for *Quercus ilex L* (holm oak). Root distribution and the maximal electron transport capacity (J_{max}) are allowed to adapt dynamically during a model run, while ce and me (unitless empirical parameters that define the slope of the curve between photosynthesis and evapotranspiration), c_{Rl} (leaf respiration coefficient), J_{maxtop} (electron transport capacity at the top of the canopy) and phenology were optimized off-line for the year 2005.

The model's simulations were compared to the flux measurements of carbon (Net Ecosystem Exchange) and water (latent heat) and validated for the summer of 2005. Phenology was simulated using a degree-day method based solely on temperature. The difference between measurements and model outcome was minimized by an unconstrained nonlinear optimization function, taking into account the difference in measurement errors by weighing the carbon and water components. Off-line stochastic optimization of the 4 parameters (ce, me, c_{Rl}, J_{maxtop}) was done with the DiffeRential Evolution Adaptive Metropolis (DREAM) algorithm. The results for the half hourly simulations in the summer (JJA) at the Hainich site showed very good agreement with the observed data both in magnitude and dynamics. In most of the model runs the root water uptake flux (Qr) and consequently the internal water storage of the tree (Mq) fluctuate strongly, from unrealistically high to low values with each time step, possibly as a

result of numerical instability. Yearly results from the optimized model show some discrepancy in both carbon and water fluxes, as the simulated fluxes are generally overestimated in spring and for a short period during summer. Overall, the yearly dynamics of soil moisture for the year 2003-2007 give realistic results and water and carbon fluxes show good agreement with the observations. The difference between observed and simulated fluxes results from the late onset and early decline of leaves as prescribed by the phenology, since fluxes are overestimated during the period of full vegetative cover to balance the underestimation without the presence of leaves.

To test the hypothesis and examine the feasibility of investing in the relocation of fine root mass, the simulated cumulative NCP was evaluated after 1 to 7 days. The results for the summer of 2003, during the extreme drought, show that the root mechanism does not take place when evaluation of NCP is done after 1 or 2 days at all and only starts to make a difference after an evaluation period of 4 days or more. The simulations of the water flux increase after roots have been repositioned to deeper soil layers, allowing for higher water uptake and consequently carbon assimilation. Thus, it is beneficial to relocate fine root mass since the NCP is higher with the mechanism in place. The hypothetical root mechanism allows trees to continue transpiration after soil moisture has been depleted from the top soil layers. Currently, most hydrological models will simulate a decrease of evapotranspiration for forests during moderate droughts, whereas it should only occur if droughts are severe enough. The main conclusions, with the hypothetical root mechanism implemented in the model, are that there is indeed an increase in NCP, but there is no proof that this gives a better fit to the data, because the phenology, onset and decline of Leaf Area Index (LAI), is not simulated correctly. The model that was used during this project would benefit from (1) a better representation of the root water uptake flux. To further investigate the hypothetical root mechanism it is advised to (2) change the cost of creating new fine root mass and/or the vascular system respiration. Whereas nearly all eco-hydrological model simulations could be improved from (3) building a better phenology model.

1. Introduction

In the face of global warming and future predictions on the increase of more extreme weather events, this research project will focus on the adaptation of trees to drought. There is a general consensus that global climate change will increase the magnitude and frequency of droughts in Southern Europe and other parts of the world. The Intergovernmental Panel on Climate Change (IPCC) has concluded with high confidence that anthropogenic warming over the last three decades has had a discernible influence on many physical and biological systems (IPCC, 2007). Increases in CO_2 and other green house gasses (GHGs) have direct and indirect effects on the hydrological cycle, local precipitation and evapotranspiration through interactions with global temperature and other feedback mechanisms. As a consequence of droughts large reductions in carbon storage by vegetation and forests are expected to occur. Facing an increase in droughts in the future as a consequence of climate change, increasing our knowledge of the drought resistance and vulnerability of tree species is most pressing (Verkaik *et al.*, 2009). Local changes in the soil moisture because of drought can lead to unexpected rises in carbon emissions from forests and organic matter in the soil. In the drier conditions predicted in the Mediterranean area in the frame of climate change, an important reduction of growth rates in tree species can be expected, accompanied by a shift towards more drought-tolerant species such as *Phillyrea latifolia* instead of more mesic species such as *Quercus ilex* (Ogaya *et al.*, 2003). Local drought is expected to form regular problems in Western, Eastern and Southern Europe. The European Union has funded studies and is already setting up programs to combat forest dieback (Requardt *et al.*, 2009), trying to reduce the impact of climate change on terrestrial ecosystems. The predicted changes in environmental conditions would lead to a reduction in carbon uptake by forests while GHGs are still on the rise.

In 2003 an extreme drought event occurred throughout Europe. This year has been used as an example in many studies assessing the consequences of droughts. For example, Ciais *et al.* (2005) estimate a 30 per cent reduction in gross primary productivity over Europe caused by the heat and drought in 2003. From this and other studies it is clear that vegetation will have reduced carbon storage and growth under conditions of less water availability, but it is hard to determine the point in time when this will take place. Next to their impact on carbon uptake, trees play an important role in the biosphere on earth through the role they play in the biosphere-atmosphere interaction as a source of water to the atmosphere by transpiration. Evapotranspiration is the combined process of vegetation water uptake from the soil into the atmosphere by evaporation (physical water loss), and transpiration (biological water loss). Evaporation observations of forests in the Netherlands during periods of regular drought show that trees are able to evaporate almost at full potential, while surrounding crops and grasses show an evaporation reduction (Schuurmans, 2008). However, some species of trees are more sensitive to drought than others and several mechanisms have been proposed to account for this sensitivity. The hypothetical mechanism that will be investigated during this research project is that trees can relocate fine root mass under drought to utilize water stored deeper in the soil. Water availability will be reduced in the top soil first because of evaporation and uptake from shallow roots of understory vegetation. However, under dry conditions, trees might be able to create new fine root mass deeper in the soil. The hypothesis is that trees keep on exploring water at greater depth until the carbon costs of this deeper water extraction become higher than the carbon gain by continued assimilation. At that moment, the trees decrease their maintenance cost by shedding leaves (increasing temperatures will increase the carbon cost of maintaining leaves). So the tree maximizes its net carbon gain by adapting to the most optimal trade-off strategy. It can keep assimilation going by extracting water from deeper down the profile or decrease maintenance respiration by decreasing leave area. To correctly simulate the hydrological consequences of climate change, under the foreseen increase in droughts, it is important to investigate this tree adaptation mechanism and potentially make it part of eco-hydrological models. Currently, most existing hydrological models simulate a decrease of evaporation for forests during moderate droughts, whereas it should only occur if droughts are severe enough (M. Bierkens, personal communication, 2010). This is amplified by the absence of dynamic vegetation which implies that the effect of climate variability in modifying physiological characteristics of vegetation is not taken into account (Arora, 2002).

For several crop systems, which have been more extensively studied, is has been shown that soil water is extracted from greater depth under prolonged soil moisture deficit (e.g. Gallardo *et al.*, 1996; Yadav and Singh, 1981) resulting from decreased irrigation. Next to a change in the frequency of drought events, there are other aspects that are expected to change in the future climate. Anticipated temperature increase will affect the growing season, possibly eroding the health and productivity of ecosystems, reversing sinks to sources (IPCC, 2007). Also, the increased CO_2 content of the atmosphere is expected to have a beneficial effect on ecosystem productivity by a phenomenon called CO_2 fertilization (Tubiello and Ewert, 2002). The increased CO_2 concentration in the air, resulting in a larger gradient between atmosphere-leaf concentrations, enhances the uptake of carbon through the stomata of plants when these are fully opened during day time. The increased growth from enhanced CO_2 uptake is expected to have a larger effect on deciduous trees (trees that shed and produce new leaves every year) compared to evergreen trees, because they assimilate their carbon over a shorter time period (Bala *et al.*, 2007). Forests and other plants could become more water efficient due to the higher concentration of CO_2 in the atmosphere as less water is lost from the stomata through transpiration while the same biomass increase is accomplished. Combined with the expected increase in temperature under climate change though it is not sure whether this increase in carbon uptake will exceed the increase in carbon losses due to higher temperatures. When temperatures rise and drought is experienced, plants will shed their leaves to reduce maintenance costs and transpiration, thereby reducing biomass accumulation and carbon uptake. In the Netherlands, Kruijt *et al.* (2008) have shown that the projected effects of climate change and moisture deficits are strongly sensitive to the change of stomatal conductance by altered ambient CO_2 concentrations.

During this research project an optimality model simulating tree growth was developed. The optimality approach based on the carbon benefit is based on the Vegetation Optimality Model by Schymanski (2007). Optimality principles have long been used in ecophysiology, for example to make predictions of gas exchange at the leaf scale. Cowan and Farquhar (1977) assumed a priori that plants would optimize stomatal conductivity dynamically in order to maximize total photosynthesis for a given amount of transpiration. This research project combines both ecophysiological and ecohydrological optimality approaches. It accounts explicitly for the nonlinear coupling between CO_2 uptake and water uptake/loss, adopting a biochemical model of photosynthesis, while at the same time, it also considers the dynamics of soil water and carbon costs of maintaining roots and water transport tissues. The underlying assumption of the optimality approach is that vegetation maximises its 'Net Carbon Profit' to be most fit from an evolutionary perspective. A tree will maximize its net carbon (i.e. energy) gain by the optimal choice of the following trade-off strategies: (1) keeping assimilation going by replacing fine root mass and extracting water from deeper down the profile or (2) decreasing maintenance respiration by decreasing leave area. Vegetation optimality modeling has in recent years mainly been done to predict fluxes such as transpiration and CO2 assimilation in ungauged basins without the need for site specific model calibration.

In the next chapter an overview of relevant processes in eco-hydrology as described in the literature will be given for vegetation interactions with the immediate environment and internal trade-offs, such as water availability, carbon allocation, root distribution and survival mechanisms under drought. In chapter 3 the current state of models and possible ways of including vegetation and feedback mechanisms will be discussed and the basis for the model that will be used during this project is explained. Both chapter 2 and 3 were written before a start was made with the actual programming of the model, thus they are more general and do not give specific information on the utilized model. The equations given in chapter 4 are the fundament of the model and are programmed as such. Chapter 5 gives a brief introduction to the sites for which the model was used site specific parameters. Furthermore, in the remainder of the chapter the models initialization and optimization strategies are explained and possible validation strategies explored. Chapter 6 gives the results of the optimization procedures and some model adjustments as the initial simulations were not acceptable. It continues with the off-line parameter calibration, optimization and validation simulation for the summer of 2005 at the Hainich site. The last chapter shows and discusses the final simulations of soil moisture, water and carbon fluxes for the years 2003-2007. The chapter finishes with the simulations of the extremely dry year 2003 with the hypothetical root mechanism in place.

2. Theoretical background: Processes and interactions influencing local hydrology and carbon storage

Tree growth depends on water availability and will consequently be affected by drought. The strength and duration of the drought are governed by local climatic conditions which arise from hydrological processes acting on local, regional and global scales. Locally, soil moisture is the most important environmental factor linking climate and vegetation. Trees take up water from the soil through their roots and loose water from their leaves during photosynthesis. Drought is basically the imbalance between incoming water, mainly in the form of precipitation, and water loss in the area from the soil and areas of open water (evaporation) and vegetation (transpiration). Evaporation, the physical process of water loss, and transpiration are often combined into evapotranspiration as there is almost no information about the partitioning between these processes (Lauenroth and Bradford, 2006). Climate change influences tree growth through changes in the hydrological regime and the carbon budget. Increases in GHGs are expected to increase tree growth and carbon storage as an effect of CO_2 fertilization, while increases in temperature will lead to decreases in soil moisture, increases in evaporation and duration of the growth season of vegetation. The net effect of climate change on carbon allocation and the local hydrology are highly uncertain and/or unknown. This research project will to contribute to our knowledge on drought survival strategies of trees under water limited conditions and tries to find an explanation for the observed phenomenon that trees are able to transpire much longer than understory vegetation under drought. First, an overview of relevant processes (see also Figure 1) and recent literature will be given, starting with the physical and biological processes that influence the water availability, governed by precipitation and evapotranspiration. Next the main processes controlling carbon storage in trees will be explained. More specifically, areas of carbon allocation and root distribution in trees are reviewed and linked to variations in the stem diameter. Since the model that will be developed during the course of this project might be validated using tree rings.

2.1. Drought and soil moisture

Water availability for plants is determined by solar radiation, temperature, precipitation, groundwater level, and local topographic and soil characteristics. However the contribution of future changes in temperature and precipitation to changes in drought occurrence under future climates is not straightforward because of the complex interactions between these forcing variables and hydrologic processes at the earth's surface and in the pedosphere. The type of soil, porosity and the amount of organic matter in the soil determine the water retention capacity of the soil and therefore the amount of water available for uptake by plants through their roots. This is complicated further by changes in mean precipitation versus changes in precipitation frequency and intensity and the seasonality of these changes, especially in snow dominated regions where spring temperatures determine when water, deposited during winter as snow, will become available for plants. An agricultural drought is defined as the occurrence of an extended period of anomalously low soil moisture. Soil moisture provides a useful indicator of drought as it reflects the aggregate effect of all hydrologic processes from changes in short-term precipitation events and temperature swings to long-term changes in climate (Sheffield and Wood, 2008) thus it can be used to assess the water availability for plants, drainage from the soil and potential recharge to rivers and reservoirs. Drought occurrence can vary highly on temporal and spatial scales as the result of an imbalance between local precipitation and atmospheric demand. Precipitation, evaporation, snow melt and soil moisture also have strong seasonal components. Under future climate change, droughts are expected to occur more often both at high latitudes and in dry Mediterranean or arid climates. At high latitudes where snow processes play a dominant role drought is expected to occur more frequently as a redistribution of soil moisture from spring to winter is forced by earlier spring melt and a likely increased rain to snow ratio during the cooler seasons (Wang, 2005). These droughts are amplified during the summer when reduced soil moisture persistence from the spring is coupled with increased evaporative demand from increased temperature. Worldwide, increases in temperature will increase transpiration and direct evaporation from the soil through increased atmospheric demand, leading to more extreme situations in drought prone areas. Decreases in temperature and precipitation will tend to increase and decrease soil

moisture respectively, the relationship between temperature and precipitation however is very uncertain and depends on local topography and atmospheric circulation patterns. In general higher temperatures will lead to enhanced atmospheric moisture contents and convective systems that might increase cloud formation and potentially precipitation. These mechanisms are poorly understood and local feedbacks or anthropogenic influences may disturb the balance and cause local differences

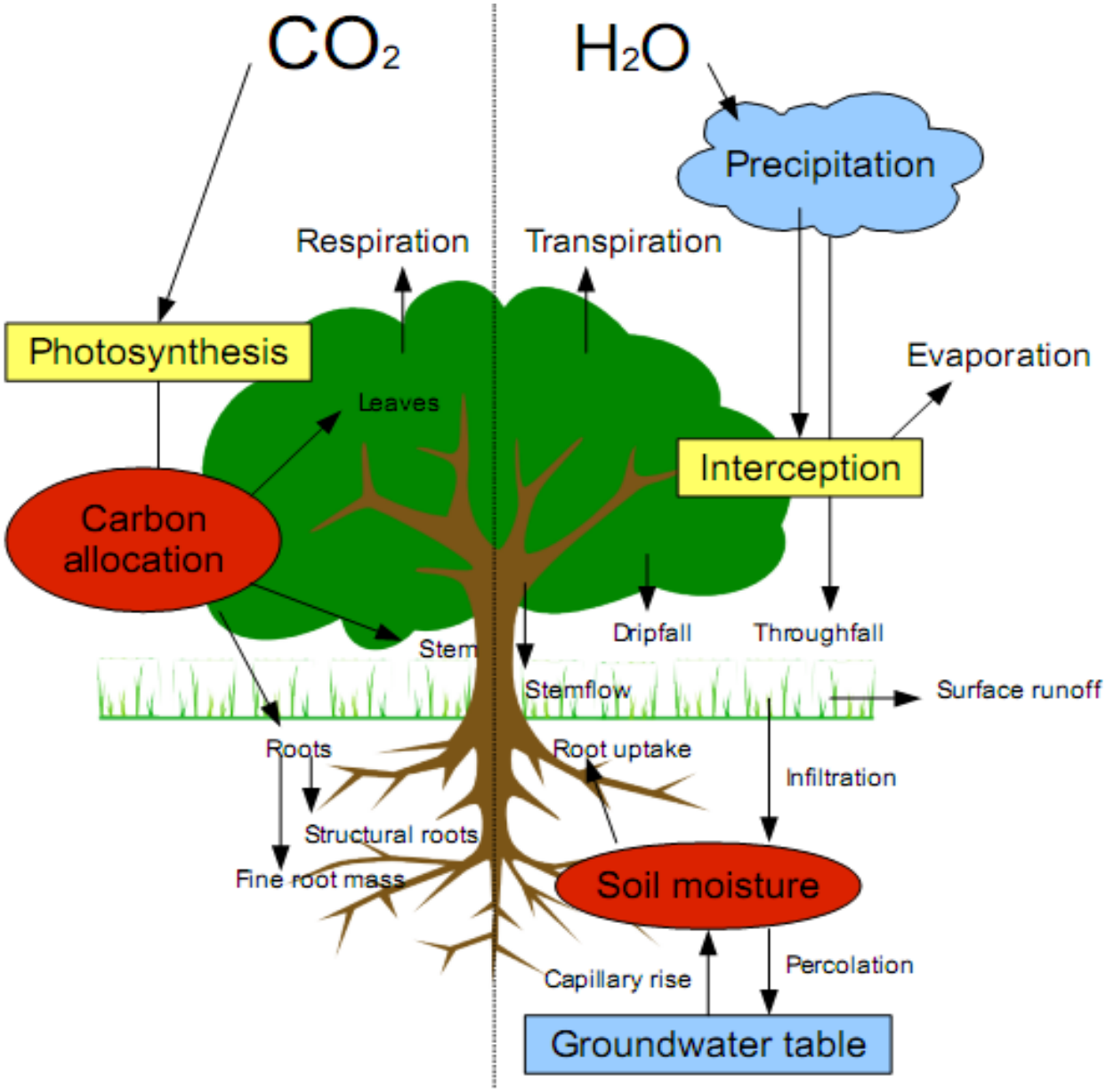

Figure 1: *A simplified schematic overview of the most important processes affecting tree growth through the carbon (left) and the hydrological cycle (right).The model developed during this research project includes most of these processes, however it used a simplified equation that combines the effects of interception and throughfall without using dripflow and stemflow separately. Also the root mass in the model can be seen to represent fine root mass only as this is the most important for water uptake and the model does not take into account capillary rise from the groundwater table, since this was deemed inappropriate for the selected sites.*

Drought associated with greenhouse gas induced climate change has the potential to cause rapid vegetation change through drought-induced forest dieback (Guarin and Taylor, 2005) as different types of vegetation will be able to inhabit the areas that were previously occupied by forests. Under the influence of rising temperatures, tree mortality has also been associated with fire and insect outbreaks resulting in increased forest disappearance (Requardt *et al.*, 2009). Soils have a 'memory' of prior rain events that can last several months until the soil is totally dry again. Because of such memory effects, the effects of precipitation cannot be understood either at the level of single rainfall events or at the level of seasonal or annual precipitation totals. However, the memory for recent rainfall events is the basis for ecosystem

sensitivity to intra-seasonal precipitation patterns (Schwinning *et al.*, 2004). Summarizing, drought and differences in soil moisture have direct and indirect effects on vegetation and tree growth. Soil moisture is directly linked to vegetation and root systems through water uptake and the positive influence on water infiltration and water retention capacity of the soil. Indirectly, drought has been linked to tree death by acting as a trigger for insect or pathogen outbreaks (Ferrell, 1996).

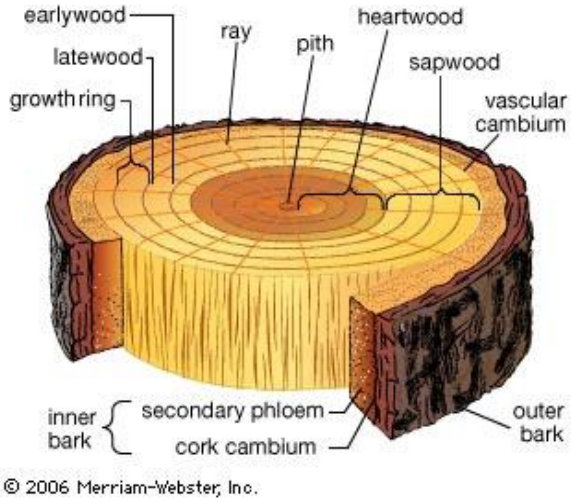

Figure 2: *Cross-section of a tree (image taken from Merriam–Webster, a subsidiary of Encyclopaedia Britannica, Inc.). Transpiration from leaves drives the movement of water and minerals in the stem, this is important because many plant cells need the minerals as nutrients and water is needed for photosynthesis. Xylem tissue is the main transport path of water and is usually found close to the other transport tissue in plants, phloem, which transports sugars and amino acids. In trees transport is mainly provided by secondary xylem and phloem found in the vascular cambium.*

The direct process linking vegetation to changes in the surrounding soil moisture is evaporation. Plants influence the local water budget through their roots; water is removed from the soil through suction and lost trough stomata in the leaves during photosynthesis. Root suction in trees is created from the transport of water from the roots to the leaves through the xylem in the stem (figure 2). This upward transport of water and nutrients is driven by a combination of transpirational pull from above and possibly root pressure from below. Whether such a force as root pressure exists is an ongoing debate, since it is impossible to measure in a real system and the flux could also result from osmotic differences between the water in the root system and the soil. Transpiration is the water loss of plants that occurs during photosynthesis when plants open their stomata to exchange CO_2 with the atmosphere. The transpiration rate depends on the humidity gradient between the atmosphere and the leaves internal space and the diffusion resistance provided by the stomatal pores to water loss through the openings in the leaves (stomatal resistance). There are many processes and feedback mechanisms that link climate and vegetation. The local weather conditions and evapotranspiration from plants determine the soil moisture regime and drought occurrence. Local water availability in turn determines the type of vegetation that is capable of growing in a region. The depth of the roots of plants is important for their individual moisture availability. Plants need water for CO_2 assimilation, internal nutrient transport and leaf vigour. Transpiration depends on the amount of leafs and their stomatal resistance, along with the surrounding energy intensity, temperature, humidity, and wind speed. Evapotranspiration is the coupled water loss term for vegetation combining evaporation from the plants surface with the plants internal water loss. The soil evaporation is often included in local evapotranspiration terms as well. The energy exchanges at the surface drive local climate through input of heat and water to the atmosphere. Hence, any differences in the energy partitioning among sites could lead to distinctly different local climates. Moisture in the soil will support transpiration but result in only a small increase in forest floor evaporation because of the shading from the overstory canopy. Beringer *et al.* (2005) for example have also shown that differences in evapotranspiration are more strongly controlled by larger scale meteorological parameters such as vapour pressure deficit (VPD) than by local soil moisture.

Other direct effects of vegetation on the surrounding soil moisture are positive feedback mechanisms that increase the water availability. A positive feedback mechanism enhances itself leading to large increases in its interacting components. In nature these processes are usually balanced by negative feedback mechanisms that limit growth. Eugster *et al.* (2000) for example, suggest that, under future warming, a vegetation change from tundra to shrub or

shrub to forest would cause a positive feedback to atmospheric temperature but a negative feedback to atmospheric water vapor. Both the infiltration and water retention capacity of the soil improve under root presence. These processes are part positive feedback mechanisms as they increase soil moisture, increased soil moisture raises the amount of vegetation and roots, which in turn increases soil moisture. Also enhanced evaporation from vegetation can be involved in a feedback mechanism increasing local precipitation (Dekker *et al.*, 2007).

Local climatic and soil conditions determine the available water for uptake by plants. Precipitation is intercepted by the present vegetation and is returned to the atmosphere as water vapour by evapotranspiration. Water that reaches the ground as through-, stem- or dripfall replenishes the soil moisture and eventually recharges the ground water table. Vegetation increases the infiltration capacity of the soil and the amount of water that can be stored in the area through the carbon organic matter and its root system. Excess precipitation that is not able to infiltrate the soil will leave the catchment in the form of surface runoff. The vegetation's tolerance to water stress and root density profile are factors that have to be taken into account for in the estimation of the root uptake capacity and the contribution of the water table to water extracted by trees from their surroundings (Vincke and Thiry, 2008). There is a strong positive relationship between water storage in the soil and stems and there are some indications that this relationship is also present in roots and leaves of trees. The stem-soil moisture relationship is observed among others by Hernandez-Santana *et al.* (2008), as a seasonal trend in stem water content that drops when the available water in the soil decreases. This relationship might be used in the future to estimate the amount of soil moisture when direct measurements are not possible.

2.2. Photosynthesis and CO_2 fertilization

Water is essential for plants to gain energy provided by photosynthesis. During photosynthesis carbon is assimilated under the influence of solar radiation that provides the energy for plants to convert inorganic CO_2 into carbohydrates in the form of sugar and other organic compounds. Plants can only use part of the incoming solar radiation within the visible light, this is called the photosynthetically active radiation (PAR). Carbon enters the plant in the form of CO_2 by turbulent diffusion through the stomatal leave openings under the pressure gradient of atmospheric and internal CO_2. Surrounding cells use CO_2 and water to form glucose and more complicated organic material and as a by-product produce oxygen. The assimilated carbon is allocated to different parts of the plant and stored there during its lifetime, making the plant a net carbon sink. In young plants most carbon is used for growth, older plants allocate more to their stem and branches for stability, reproductive organs and seeds. Like all other living organisms, plants and trees respire CO_2 that is formed during growth and for maintaining tissue. Respiration is the excretion of CO_2 as a waste product from metabolic reactions. Respiration is often separated into growth respiration, used to synthesize new plant material, and maintenance respiration, used to keep existing tissue alive and functioning. Maintenance respiration is a function of the total biomass and environmental stress (e.g. temperature), while growth respiration depends on the total growth. Autotrophic respiration is the combination of growth and maintenance respiration. The proportion of respiration for growth and maintenance is not constant and primarily depends on the age of plants. Generally, when plants are young and growing rapidly, seasonal growth respiration is higher than maintenance respiration. As plants age, maintenance respiration increases, owing to the increasing mass of the living tissue.

The currently experienced and predicted rise of GHGs influences trees indirectly through a temperature rise and soil moisture decrease and directly through the elevated CO_2 concentration in the atmosphere. In forests, the influence of increased CO_2 levels is not well understood at the ecosystem level and is, in many regions, masked by other direct and indirect effects of human activity (Easterling and Apps, 2005). Several studies have been conducted to examine the response of vegetation to elevated CO_2 levels, because this is expected to have a fertilizing effect on plant growth. However, it has only been possible to study responses at the level of individual plants by elevating CO_2 concentrations artificially or in relatively small Free Atmosphere Carbon Experiments (FACE). The results of these studies remain difficult to extrapolate to large areas in the field where other factors like moisture and nutrient availability play an important role. The increase in CO_2 is expected to have a larger effect on plants that

are only capable of capturing CO_2 at the same time they are photosynthesising (C3 plants) and deciduous trees that lose their leaves seasonally. Welp *et al.* (2007) report an increased net carbon uptake by 40% at the deciduous forest and 3% at the evergreen forest in 2004 as compared with 2002. These results suggest that deciduous forests may react disproportionately to the rise in atmospheric CO_2 concentrations.

2.3. Drought survival mechanisms and water use efficiency

The water use efficiency (WUE) is a concept used in ecology to express the relative amount of carbon that different species assimilate compared to the amount of water that is lost through transpiration. It is defined as the amount of carbon gained per unit amount of water lost. Water is lost during photosynthesis trough the stomata under conditions of low atmospheric humidity when the stomata are opened to sequester carbon. The stomatal resistance is a function of local environmental conditions and atmospheric CO_2 concentration and limits the outflow of water. Plant growth is often limited by water availability, especially in Mediterranean and arid climates. To reduce the amount of water lost, plants are able to close their stomata, minimizing water loss but at the same time however, stopping the uptake of CO_2 and the ability to assimilate carbon. Experimental evidence shows that elevated atmospheric CO_2 concentrations tend to reduce stomatal opening in plants (Kruijt *et al.*, 2008), leading to lower transpiration rates and higher WUE. These reductions are, however, of comparable but opposite magnitude to predicted temperature-induced increases in evapotranspiration.

Generally water use efficiency is higher for C4 plants that are capable of storing CO_2 at a different time than assimilating it. Water loss can be reduced as the stomata can open during colder or more humid hours and close during the middle of the day when VPD is highest. All trees however are C3 plants and only able to assimilate CO_2 while their stomata are open. Drought tolerance is generally associated with an efficient use of water and it has generally been considered that herbs are less drought tolerant species than woody plants and trees. However, in a recent study by Medrano *et al.* (2009) herbaceous species presented the highest relative increase in leaf intrinsic water use efficiency (leaf WUE) as drought progressed, suggesting that the capacity of withstanding water limitation may be an adaptation of all Mediterranean plants regardless of their growth form and leaf habit . Furthermore they found no clear relationship between leaf WUE and soil water content among Mediterranean plants. Leaf WUE (AN/G_s) is in their study defined as the ratio of net CO_2 assimilation rate (AN) to the stomatal conductance (G_s). Especially for woody evergreen shrubs Medrano et al. (2009) relate strong increases in specific leaf area (SLA) during drought and insignificant changes in leaf WUE to the high stomatal conductance value. The high stomatal conductance value of woody Mediterranean plants and trees reduces the range of measured leaf WUE because changes in the net assimilation rate are small compared to the value of G_s. A high stomatal conductance could be an adaptation strategy of woody Mediterranean vegetation to drought, because less water is lost during the uptake of carbon for photosynthesis.

Another suggested drought survival mechanism is the ability of trees to store water in their stems that can be used for several days when soil moisture conditions are insufficient. De Swaef *et al.* (2009) only observed a difference in sap flow rates in the stem of trees during drought experiments 4 days after drought stress induction. This retarded response suggests that trees could initially maintain normal growth rates because they deplete water stored internally in the surrounding bark tissue. Tree death under drought is also induced by other stress factors such as insect outbreaks and increased water competition between plants. In the dense stands of Yosemite forest, increased water stress during drought increases the susceptibility of trees to mortality (Guarin and Taylor, 2005). The frequency of tree death is associated with decreased moisture conditions over periods of 2–5 years, but not for single years. Guarin and Taylors results indicate that co-occurring periods of high spring and summer temperatures and low annual and seasonal precipitation triggered high tree mortality. However, mortality was not simply associated with dry years. Statistically significant associations between low moisture and high tree mortality were only found for multi-year periods. This indicates that although any annual drought may be severe, tree death is mainly associated with dry conditions over extended periods of several years. This suggests that the soil moisture memory in the deeper layers of the soils that trees have access to is much longer compared to the top soil. Or that trees have a survival mechanism that allows them to adapt to dryer

conditions for several years, but fails after a persisting period of drought. This survival mechanism could be the related to the mortality mechanism of carbon starvation reported by others (e.g. Adams *et al.*, 2009). Under drought trees close their stomata to retain safe levels of xylem pressure, hereby stopping photosynthesis, during this time they rely on stored carbohydrates for maintenance respiration. Their internal carbon store is slowly depleted if it is not replenished during the remainder of the season or in the next growing season. If severe droughts occur over a period of several years and the trees have not been able to replenish their carbon storage this mechanism can also explain the multiple year period associated with tree mortality. This mechanism has been shown to be the main cause of tree death in a recent modelling study (Brolsma *et al.*, 2010). Because respiration is strongly linked to temperature increases, the predicted rise in temperatures can increase the depletion of trees internal carbon storage in future years, leading to unexpected tree death even during moderate droughts.

Under present conditions the direct and indirect effects of climate change favor tree growth because the effects of water availability are offset by temperature increases that extend the growing length season and CO_2 fertilization. Locally however, net primary productivity is reduced as a result of lowered photosynthetic rates whereas higher temperatures are associated with increased drought. It is suggested in research by Easterling and Apps (2005) that plant growth may benefit more from CO_2 enrichment in drought conditions than in wet soil because photosynthesis would be operating in a more sensitive region of the CO_2 response curve especially in C4 photosynthesis. Results from this and other experimental studies have shown that it is no longer realistic to examine the effects of climate change on plants without also accounting for the direct effects of rising atmospheric CO_2 at the same time. However, it has to be kept in mind that the responses to elevated CO_2 remain difficult to extrapolate from isolated plants grown in artificial conditions to actual conditions and on larger scales. Although at present the global forests are acting as a net sink of atmospheric carbon, this is not always the case on local scales. There is a growing consensus that the average carbon storage response in forests is not sustainable, and will decline or disappear as global change continues (Easterling and Apps, 2005).

2.4. Carbon allocation and water resources

The distribution of energy and carbon for tree growth varies during its entire lifetime and between seasons. Patterns of allocation between leaves, branches, stem and roots vary with species and growth stages. For example, in trees, different parts act as sinks at different stages of their growth. In deciduous trees every year, top growth is usually accomplished first, followed by radial expansion of the stem. The availability of nutrients, in particular, nitrogen, also affects the distribution of allocated carbon. For example, in nutrient-poor environments, plants allocate more resources to roots in order to reduce nutrient deficiency (Hattenschwiler and Korner, 1998), while in nutrient-rich environments, more resources are allocated to stem and leaves. Various studies suggest that trees are able to store carbon from the previous year that can be used for leaf and root development in the next growing season. It is not known whether an allocation mechanism similar to that of nutrient deficiency is in place for tree adaptation to soil moisture deficits.

Soil moisture is first depleted in the top layer of the soil under the influence of incoming radiation and water extraction by shallow roots. The deeper layers of the soil remain moist and deep soil moisture can be replenished by interaction with the ground water. Capillary rise of water pulled up from the ground water level into the unsaturated zone by the pores in the soil can serve as a source of soil moisture under drought. The depth of the ground water table and the soil characteristics influence the height to which this process can play a role. Vincke and Thiry (2008) conclude in a recent study that ground water table is a relevant source for water uptake by Scots pine under the assumption that daily transpiration was corresponding to water uptake. During the drought period in June, the water table contributed to 98.5% of the water uptake by vegetation, through its contribution to the capillary rise above the water table. From May to November, the contribution of the water table to forest transpiration reached 61%. They conclude that water table depth is probably the most important factor determining the water table contribution to water uptake through roots. However, ground water can only be a significant contribution to water uptake by trees if the roots of trees are in place at sufficient

depth. Simulations made with a recent tree model developed by Zhu *et al.* (2009) for constant water table depths found that increasing the water table depth from 2 to 3 m resulted in a 74% reduction in transpiration. For simulations with water tables between 2 and 2,5 m, more than 90% of the transpired water originated from groundwater (Zhu *et al.*, 2009). The large reduction in transpiration that was found in the model study indicates that water level was reduced below the depth of the tree roots, resulting in a water shortage that was previously extracted from the ground water.

Droughts are usually measured as a soil moisture deficit, which is often called agricultural drought opposed to climatic drought which is classified as a period of below average rainfall. While soil moisture deficit in the top meter of the soil is relevant for vegetation with shallow roots, changes in water table depth seem to be at least equally important for trees. Changes in ground water under changing climate conditions are hard to predict and are usually profoundly influenced by nearby human activity, such as the extraction of drinking water, changes in irrigation regime, upstream changes in water use or the partitioning of runoff. In semi-arid, arid and Mediterranean zones the groundwater is found at such great depths that direct uptake and evaporation of groundwater through vegetation does not play a role in the water balance of these areas.

Furthermore the predicted effects from climate change can induce a shift in vegetation that can cause a large loss of carbon in a ecosystem. Trees can store much more carbon as their biomass is much larger than that of low vegetation such as shrubs, herbs and grasses, thus forest die-back or a vegetation shift can have a significant effect on carbon storage. Harte *et al.* (2006) found in a combination of model simulations and observational studies of a recent wide-scale drought that the drought induced substantial terrestrial ecosystem carbon loss. They argue that the loss of carbon in the first five years of the experiment was caused by a decline in carbon inputs from vegetation community production, a consequence of two distinct effects of soil drying: a direct physiological drought-stress response to decreased soil moisture, and an indirect effect of the shift in species composition, from forest to shrubs. This local shift in vegetation does not have to be the effect of a soil moisture deficit, but could also be induced by a shift in the water table depth. It has to be taken into account that the death of trees could have been the result of a decrease in ground water for example, and the loss of shading from the tree overstory could be the cause of the measured drought.

Temporary reduction in soil moisture and drops in ground water level can be buffered by the available water in the stem that has been stored there during periods of abundance to be able to continue photosynthesis, thus it seems that, below a specific soil moisture threshold, the trees pull out water from their stem for use in transpiration (Kobayashi and Tanaka, 2001). This could be important for trees in general and in particular for those located in Mediterranean areas (Hernandez-Santana *et al.*, 2008) in order to cope with the summer deficit. This water decrease is the result of the incomplete daily recovery of the stem water content during the growing season. In this study a decline in stem water content occurred in the daytime, especially in the morning, and there was a recovery after sunset. However, stem water content often did not recover completely to the level of the previous night if there was soil water deficit. This means that a net reduction of water stored in the stem continued during the observation period. During times of high evaporative demand, the tree stem serves as a water storage system. It is possible that the deployment of stem water storage system is to buffer stem xylem potentials during periods of high transpiration and to contribute to leaf survival during extended periods of low soil water availability (Kobayashi and Tanaka, 2001).

2.5. Drought adaptation strategies and root distribution

Several mechanisms and adaptation strategies have been proposed for tree development under drought. The ones that will be investigated further during this research project are reducing water loss by transpiration or increasing the water uptake by increasing fine root mass at depth. Reducing water loss can be accomplished by closing the stomata of leaves to prevent transpiration. This measure however, stops the ability of the tree to gain carbon and energy during photosynthesis. Additionally, closing the stomata and reducing respiration will drastically increase the temperature of the leaves, as they are no longer cooled by evaporation, which can lead to leaf death. Dead leaves and dry leaves turn brown or yellow. This can be observed by remote sensing techniques that can be used to assess the health of

forests, for example with the normalized difference vegetation index (NDVI). High NDVI values (0.6-0.8) are observed when forest is present, these values decrease as leaves change in colour and reflect more light in the visible spectrum. In cases of prolonged drought the discoloured leaves will die completely and fall of the tree. Shedding leaves is a more common phenomenon in deciduous trees, but has also been observed in evergreen trees under conditions of extreme drought. Vincke and Thiry (2008) for example observed a loss of needles in a evergreen pine trees just after a June drought period of 5% of the total leaf area index (LAI), defined as the leaf area per unit soil area. The observed loss of needles could indicate an adjustment to dry conditions.

Several studies (e.g. Zhu *et at.*, 2009; Hernandez-Santana *et al.*, 2008) find the highest concentration of roots in the top half of the soil. A deeper root system however, enables transpiration rates to be maintained throughout the summer when the trees are subject to drought. In summer months the top layers of the soil are depleted from moisture by evaporation and transpiration of vegetation with shallow roots, such as herbaceous and shrub species. The trees are faced with a progressive decrease in soil moisture and will use up the water reserve and progressively absorb water from deeper layers. To be able to extract water from the deeper layers of the soil, the tree needs to have fine root mass in place or allocate additional carbon to its roots to form fine root mass at a depth where water is still available. Fine roots are those parts of the roots that are capable of water uptake (usually taken smaller than 10 or 5 mm in diameter), as opposed to structural roots that give support and anchor the tree. It has also been suggested that vegetation characteristics, such as the fine root biomass, depend more on the location of the corresponding trees, their interactions and competition with nearby vegetation (Wälder and Wälder, 2008), than on species and environmental conditions. Thus, it seems that many different aspects influence the distribution of roots and the water uptake capacity of trees.

Also, seasonal fluctuations of fine roots occur in relation with soil moisture (Vanguelova *et al.*, 2005) and roots might develop deeper during the season. As far as root water uptake is concerned, fine roots are especially sensitive to water shortage in early summer and root growth may be inhibited even before the first leaves grow. It has also been observed that fine tree roots die almost immediately in local dry areas (Vanguelova *et al.*, 2005). In the same study, the decrease in fine root biomass was significantly greater in the organic and top mineral layer (up to 30 cm) than in the deeper soil. In other terms, even if very few roots are present at the deepest wet horizons, still they can significantly contribute to water uptake. However, the root distribution is not necessarily correlated with root water uptake (Vincke and Thiry, 2008).

2.6. Trade-off strategies to be investigated

Due to the many processes and feedbacks involved in the climate system, the interaction between vegetation and local hydrology is very complex. This non-linearity is captured by increasingly complex scientific eco-hydrological models that try to make reliable simulations of the effects of climate change. There are still feedback mechanisms and processes that are not adequately included in these models that can potentially result in unexpected model behaviour. But there are also feedback processes in the environment itself that can suddenly make a system change from one state to another or cause an existing ecosystem to collapse (tipping points). Cox *et al.* (2000) for example report acceleration of global warming due to carbon-cycle feedbacks in a coupled vegetation-climate model. They find that that under a 'business as usual' scenario, the terrestrial biosphere acts as an overall carbon sink until about 2050, but turns into a source thereafter. The reduction in terrestrial carbon from around 2050 onward is associated with a loss of soil carbon as a result of higher respiration rates. The projected increases in temperature will increase both the rates of plant respiration, soil microorganism respiration and photosynthesis. This signifies the importance of our understanding of terrestrial ecosystems in response to changes in climate.

In this research project it will be investigated whether trees are capable of extracting water from deeper down the soil and experience a smaller loss of carbon than predicted by a model that does not include the relocation of fine root mass. Evaporation observations of forests in the Netherlands during periods of regular drought show that trees are able to evaporate almost at full potential, while surrounding crops and grasses show an evaporation

reduction (Schuurmans, 2008). The additional soil moisture that could be accessed through additional root repositioning would allow trees to maintain high values of photosynthesis and transpiration. Although in some areas it has been shown that trees directly utilize ground water as a source for moisture (e.g. Vincke and Thiry, 2008) this will not be taken into account in the model as there is no such contribution in the Mediterranean climate and German site where the model simulations will be done. During drought there are two potential strategies a tree could follow to reduce the adverse effects of water deficiency, namely reducing LAI or utilizing deeper soil water.

The leaves of a tree will exceed the maximum temperature they can cope with when transpiration is not taking place anymore. The evaporation of moisture from the leaves at the same time cools the leaves and hereby keeps the temperature below the critical level that makes biological processes stopping. The loss of water is necessary both for the trees internal water and nutrient flows as well as photosynthesis. For a tree to totally stop transpiration it would have to close its stomata completely, allowing no more gas exchange necessary for the uptake of CO_2 needed in photosynthesis. Reducing LAI is a way to reduce the water demand and maintenance costs, however this consequently reduces the potential carbon gain that a tree can have through photosynthesis. Therefore there is a trade-off between reducing maintenance costs by shedding leaves or keeping transpiration rates high. The mechanism that is proposed here to maintain water uptake is the relocation of roots from soil layers with deficit moisture to deeper layers where moisture is still present. In addition to this, trees are forced to reduce LAI when severe droughts occur to reduce water loss and maintenance costs. Leuzinger *et al.* (2005) found that during the extreme drought in the summer of 2003 daily peak values of sap flow decreased to only about half of the early summer maxima in *Fagus sylvatica L*. Whereas *Acer campestre* and *Tilia platyphyllos* were more affected and *Quercus petraea* less. The less severe decrease in sap flow rate could potentially be attributed to the relocation of roots to layers where soil moisture was still present. The evaluation of this mechanism will be done by optimizing the Net Carbon Profit (NCP), calculated as the remainder of energy (i.e. carbon) gained by photosynthesis minus the respiration costs of maintaining leaves, roots and woody tissue. Thus a tree will maximize its NCP by the optimal choice of the following trade-off strategies: (1) keeping assimilation going by replacing fine root mass and extracting water from deeper down the profile or (2) decreasing maintenance respiration by decreasing leave area. This will be evaluated by comparing the measured and carbon and water fluxes at two different sites, one in Germany and one in France.

3. From theory to practice: Model considerations

Models have increasingly been used to make predictions on future climate and climate sensitivities. Depending on the models purpose and complexity, choices have to be made whether or not to include specific processes and on their mathematical representation. Many models are based on physical and empirical relationships from original research whose validity has been proven in many applications. Hydrological parameters or processes and vegetative processes like photosynthesis, transpiration, respiration and allocation are the basics that have to be included in a model to simulate drought and tree growth. These processes and the most common ways of modelling them will be explained in this chapter, to bridge the gap from theory to practice, before the chosen model representation and equations are explained in the next chapter. First, a more general introduction to eco-hydrological models and their role in relation to General Circulation Models will be given.

3.1. Coupling carbon and water processes

To model the interaction between soil moisture and tree growth, a model that simulates photosynthesis and evapotranspiration has to be coupled to a hydrological model that calculates the water availability. Traditionally, there have been two types of models: hydrological and ecological models. Ecological models that simulate canopy photosynthesis and plant growth have simple hydrologic components, while estimates of actual evapotranspiration in hydrological models are obtained by scaling potential evaporation using empirical functions of soil moisture and/or vegetation. To improve the model representation and predictions, both types of models can be coupled to provide dynamic values of parameters calculated by the other model instead of using empirical relationships. The primary purpose of coupling a vegetation module with a hydrologic model is to provide it with dynamic values of LAI (Arora, 2002). The LAI values in the ecological model are commonly estimated on the basis of the amount of carbon present in the leaf biomass. In the hydrologic model the LAI affects transpiration, interception, and evaporation from the canopy leaves. The relationship between photosynthesis and stomatal conductance may additionally be used to couple vegetation with the hydrologic model. In this case, photosynthesis is used to estimate stomatal conductance, which, in turn, can be used to estimate transpiration. The hydrological model affects the vegetation module via soil moisture. For example, a reduction in soil moisture (due to reduced precipitation) decreases or inhibits photosynthesis. If the coupling between photosynthesis and stomatal conductance is explicitly modelled, this in turn reduces stomatal conductance, which acts to prevent further soil moisture reduction. The two primary variables that are exchanged between the vegetation and the hydrological model are thus LAI and soil moisture. The partitioning between hydrological processes is strongly affected by LAI. Photosynthesis, respiration and allocation in turn are strongly related to soil moisture and other environmental conditions, including temperature, precipitation, humidity and light availability. These relations make vegetation a dynamic component that should be modelled separately in hydrological models. At least LAI and stomatal conductance should be coupled to find evapotranspiration; this has been done in an increasing number of models as the importance of vegetation on the global climate and hydrology has become more evident.

3.2. Vegetation representation

Large scale General Circulation Models (GCMs) have only recently started to include a dynamic vegetation component and previously ignored the direct effects on vegetation changes on the carbon cycle and climate. Vegetation was usually prescribed as a boundary condition using a static map with vegetation cover, in which often only a separation between over- and understory vegetation was made, or a map with vegetation classes based on plant functional types and calculated off-line. Atmospheric GCMs have been used to predict weather and climate variability originally and have later been coupled to ocean and land components. Land Surface Schemes (LSS) or Soil Vegetation Atmosphere Transfer (SVAT) schemes are used to estimate the fluxes of energy, carbon and water between vegetation, land, ocean and atmosphere. In most current SVAT schemes the seasonal evolution of LAI is prescribed and the

effect of atmospheric CO_2 concentration on stomatal conductance is not taken into account (Arora, 2002). Still these models are used by almost all scientific agencies to make large scale predictions. The direct coupling between vegetation and the environment mostly influences atmospheric moisture, through evaporation, and is therefore especially important for short term weather forecasts and less so for long-term climate modelling. In the fourth assessment report (AR4), the IPCC estimates the potential future climate change using fifteen GCM simulations for different scenarios. Each scenario represents different mixes of changes in population, economic output, land use, energy use and technology, among others, but can be generally characterized by maximum atmospheric CO_2 concentrations. These SRES scenarios were developed by the IPCC for the third assessment report (TAR) and run from 2001 to 2100, and are based on choices between economical or ecological and regional or global development. In the calculations for the AR4 the GCM runs were provided with offline calculations that include changes in vegetation, but are not a full dynamic component as there is no direct feedback, through LAI or soil moisture for example, onto vegetation growth.

The SRES scenarios are needed as boundary conditions for GCMs to perform climate simulations. The predictions of increased large scale droughts in the future, for example, originate from these models and scenarios. Sheffield and Wood (2008) have analysed changes in drought occurrence using soil moisture data for the SRES and pre-industrial control scenarios for eight coupled atmosphere-ocean GCMs that participated in the IPCC AR4. Comparison with observations indicate that the models do reasonably well at replicating best estimates of twentieth century, large scale drought occurrence, although the frequency of long-term (more than 12-month duration) droughts are over-estimated. The conclusion of the latest IPCC report (IPCC, 2007) was that "In a warmer future climate, most atmosphere–ocean GCMs project increased summer dryness and winter wetness in most parts of the northern middle and high latitudes. Summer dryness indicates a greater risk of drought." However, the detection of statistically significant changes in climate data depends on the strength of the signal against the background of natural variability (noise). Whether the changes in drought occurrence are statistically significant is dependent on the region, drought characteristics and scenario. Although the predicted drought occurrence is increasing globally and in many regions, it is generally not statistically different for the different regions. Wang (2005) for example uses a majority index to assess the similarity in climate predictions between models, his results show that no model stays within the majority across all continents. Overall, changes in the extremes of primary climate variables may be easier to detect than changes in their means, such as global mean surface air temperature and precipitation. Changes in annual and seasonal means of other terrestrial hydrologic variables, such as evaporation and soil moisture, are essentially undetectable within the twenty-first century (Sheffield and Wood, 2008). The stiffness in their results could be the result of the inclusion of static vegetation, as the absence of dynamic vegetation in SVAT schemes implies that the effect of climate variability in modifying physiological characteristics of vegetation is not taken into account. Too little or too much precipitation, for example, is assumed to make no difference in plant productivity and resulting LAI. However, it is well known that precipitation, along with temperature, and soil moisture determines photosynthesis and plant productivity. A dynamic value of LAI would result in more variable values of evaporation and soil moisture.

3.3. Vegetation Optimality Modelling

A promising alternative to the conventional, statistical correlation-based eco-hydrological models, are models based on optimality (Schymanski, 2007). The assumption that the self-organization of biological systems is governed by some principles of optimal adaptation is not new in biological thinking, but has only recently been used to construct quantitative models and test their predictions (Sutherland, 2005). Optimality-based models have the advantage that they do not rely on observed correlations as model input, but aim at predicting the correlations themselves, hereby reducing the need for site-specific calibration. Schymanski *et al.* (2007; 2008b) have demonstrated that the principle of vegetation optimality provides an attractive alternative to using site-specific calibration measurements for estimating vegetation properties, transpiration fluxes, and CO_2 assimilation.

Models based on optimality need to have at least two elements:

- An objective function that guides the optimization (e.g. maximization of photosynthesis, maximization of water use or minimization of "stress")
- Adjustable levers or 'degrees of freedom' that can be adjusted by the system (e.g. stomatal conductivity, canopy cover, rooting depth)

Optimality principles have also been used in eco-physiology, for example to make predictions of gas exchange at leaf scale. Cowan and Farquhar (1977) assumed a priori that plants would optimize stomatal conductivity dynamically in order to maximize total photosynthesis for a given amount of transpiration. A major innovation in the concept of optimality modelling however is the maximization of the 'Net Carbon Profit' as objective function (Schymanski *et al.*, 2007), as opposed to for example the maximization of water use, photosynthesis, Net Primary Production, or the minimization of 'stress'. The Net Carbon Profit (NCP) is defined as the difference between carbon assimilated by photosynthesis and carbon spent on maintenance of the organs involved in its uptake and can be seen as the 'biological fitness' of a plant. The choice of the objective function in optimality modelling has been subject to considerable debate, questioning whether the underlying plant optimization strategy had been found. The principle of vegetation optimality provides a new way to analyze and understand vegetation dynamics and structure for given soil and environmental conditions. Eco-hydrological optimality models are suited for the prediction of long-term averages, while the eco-physiological concept is suited for the prediction of short-term dynamics. Predictions of the year-to-year variability of transpiration at canopy or catchment scale have not until recently been investigated with optimality models (Schymanski *et al.*, 2008a; Schymanski *et al.*, 2009). Under expected climate change there is high potential for vegetation optimality models to predict the response of vegetation and the functioning of ecosystems.

The model that will be used in this research project is an optimality-based eco-hydrological model that will have dynamic values of LAI and couples water and carbon fluxes. The choice for an optimality model allows for evaluation of the vegetations energy gain or fitness in addition to simulating the traditional processes. The model will be driven by atmospheric forcing under assumed water and heat balances. To weigh the maintenance cost of keeping and creating fine root mass at depth against the benefit of shedding leaves under water stress, dynamic values of LAI, soil moisture and stomatal conductance will be used. Groundwater will not be taken into account as the model is intended for tree species that suffer from a persistent lack of water and are not able to reach the groundwater table and evaporate from this source, i.e. trees in topographically high places in humid climates or trees in climates where groundwater reservoirs are depleted in summer, like in the Mediterranean climate. Therefore, capillary rise of groundwater into the root zone is neglected.

The model is based on the model by Schymanski (2007) rewritten for Matlab by Dekker *et al.* (2009). While some components, like canopy interception and the degree-day method to estimate the phenological development, were taken from Daly *et al.* (2004) as modified by Brolsma *et al.* (2010). The model will be run on a half hourly basis using input data from local flux tower eddy-correlation measurements. The hydrological processes that need to be calculated at every timestep are interception, infiltration, percolation and evaporation. Soil moisture is determined by these processes together with transpiration, which in turn influences the stomatal conductance and assimilation rate. Tree respiration depends on the temperature and LAI. Under drought, stressed trees will resort to reducing LAI and/or creating additional fine root mass to keep assimilation going. The model will simulate an adult tree, with a simple initial root distribution and soil moisture content, during the growing season and assess the influence of potential droughts over a single year. There are several ways of modelling these processes and calculating parameter values. The most important ones will be explained in the remainder of this chapter. Their inclusion and way of representation that has been chosen for the model will be highlighted here and described in detail in chapter 4.

3.4. Photosynthesis

Photosynthesis can be modelled using different approaches and formulations. The three most common ways are: (1) a biochemical approach, (2) a light use efficiency approach, or (3) simpler carbon assimilation approaches. For this research, the carbon assimilation will be

based on stomatal CO_2 conductance and the carboxylation capacity of the leaf. The carboxylation capacity of the leaves is calculated using a biochemical approach that can be limited by light, rubisco and electron transport and is influenced by the temperature of the leaves.

The canopy is usually approximated as a single big leaf. In these models, photosynthesis is modelled for a leaf at the top of the canopy and then is scaled up for the whole canopy. The central assumption that is made when scaling up for the entire canopy is that the photosynthetic properties of leaves, including leaf nitrogen content, acclimate fully to the prevailing light conditions within a canopy so that the photosynthetic capacity is proportional to the time-integrated absorbed radiation, normalized with respect to photosynthetic capacity and absorbed radiation, at some reference point, typically at the top of the canopy (Kull and Jarvis, 1995). Respiration estimated at the top of the canopy can similarly be scaled to obtain the total canopy values.

In a multilayer model, the canopy is divided into horizontal layers of foliage, where all leaves are assumed to be randomly distributed and horizontal. Each layer of horizontal leaves can be further subdivided into sunlit and shaded fractions. The sunlit fraction receives beam (or "direct") and diffuse light, while the shaded fraction only receives diffuse light. For simplicity, it is assumed that reflectance and scattering of beam light by the foliage is negligible. Multi layer canopies try to explicitly take into account the radiation distribution and turbulent exchange within the vegetation to simulate the detailed behaviour of the stomata on individual leaves. These models have become the fundamental tools to study stomatal behaviour, and the exchange of CO2 and H2O between vegetation and the atmosphere.

3.4.1. Biochemical approach

The biochemical approach is based on the complex biological reactions that take place inside of plants. Photosynthesis is limited by light, enzyme kinematics, especially the enzyme Rubisco, electron transport and the capacity to transport and utilize photosynthetic products. The simplest approach is to assume that the assimilation rate is the minimum of functions that estimate the maximum obtainable photosynthesis from light, electron capacity and utilization of photosynthetic products. The minimum of these functions will express the most limiting factor for photosynthesis at that moment and determine the maximal assimilation rate. This is the original approach of Farquhar *et al. (1980)* which is still widely used.

3.4.2. Light-Use Efficiency Approach

The light-use efficiency (LUE) is defined as the ratio between the net carbon assimilation rate and the photosynthetically active radiation absorbed by the canopy (APAR). LUE has been measured for many different plant species and has been found to be fairly constant within vegetation classes when plants are unstressed and nitrogen is optimally distributed. The linear relationship between carbon uptake and intercepted light implies that LUE can be used to construct photosynthesis models that require fewer equations, parameters and groundbased measurements than leaf parameterizations. LUE models are also well suited for application over large geographical regions since APAR can be estimated by remote sensing reasonably accurately. LUE is high variability over daily and shorter time steps however and an empirical function is commonly used to calculate the accumulative effect of water, nutrient and temperature stress. For C3 plants, which include trees, LUE is a function of both temperature and atmospheric CO_2 and the LUE is therefore not suited to use in transient climate simulations.

3.4.3. Carbon Assimilation Approach

The carbon assimilation approach uses a prescribed or constant maximum assimilation rate. Models using the carbon assimilation approach express canopy-level photosynthesis as a function of this maximum assimilation rate and a series of environmental dependencies with values generally varying between 0 and 1, which imply the effects of the environmental factor on photosynthesis as being severely limiting and not limiting at all, respectively. The functions

usually used depend on PAR, LAI, stomatal conductance, atmospheric CO_2 concentration and nitrogen availability. The carbon assimilation approach is largely empirical and requires calibration parameters that can introduce significant uncertainty into the model when the measured values are scaled up for larger areas.

3.4.4. Soil moisture deficit

However, the photosynthesis formulations mentioned above do not take into account the effect of soil water stress on stomata closure directly, and this is parameterized separately. Models may choose to decrease photosynthetic rate in response to soil water stress, by reducing stomatal conductance or reducing the maximum non-stressed photosynthetic rate using an empirical soil moisture stress function. Reducing stomatal conductance can be modelled in response to air vapor pressure deficit, when relative humidity falls below a threshold, or using empirical relationships. Reduction of stomatal conductance or photosynthetic rate in response to soil moisture stress implicitly models the effect of precipitation deficit and drought. Assimilation is limited by the inflow of CO_2 into the leaves through stomatal conductance and transpiration by the outflow of water through the stomata. Additionally, hydraulic failure, extreme leaf temperatures and other damaging processes can take place when water is limiting. Schymanski (2007) hypothesises: *"A reduction in water content of living tissues by 10% from the saturated value is reversible, while further reduction in water content may lead to permanent cell damage."* In this research any reduction below 90% of the saturated water content leads to reduced LAI and transpiration.

3.5. Transpiration

The coupling between photosynthesis and transpiration is expressed via stomatal conductance. Since the opening of stomata is related to how much CO_2 is fixed by the plants, the photosynthetic rate can be used to determine stomatal conductance, which in turn, can be used to estimate transpiration. Stomatal conductance is often parameterized using formulations of the Jarvis (1976) type that express stomatal conductance (gs) as a function of maximum stomatal conductance (gmax) and a series of environmental dependences (with values between 0 and 1) whose effects are assumed to be multiplicative, similar to the carbon assimilation approach for photosynthesis. The environmental dependencies are functions of incoming solar radiation, vapor pressure deficit, soil or leaf water potential, and temperature. Net photosynthesis and stomatal conductance both depend on the internal CO_2 pressure in the leaves and the equations must be solved iteratively. In this model the stomatal conductance will be directly linked to the soil moisture instead of soil water potential by a reduction function that decreases for low moisture content. Transpiration is determined as in Schymanski (2007) using the slope of the curve between transpiration and photosynthesis, which is determined by the atmospheric vapour deficit, as well as irradiance and canopy properties of the electron transport capacity. The shape of the curve changes drastically during the day, as both photosynthesis and transpiration depend on stomatal conductivity, but while photosynthesis has an upper limit determined by the electron transport capacity, transpiration increases indefinitely with increasing stomatal conductivity.

3.6. Respiration

Autotrophic plant respiration consists of growth and maintenance components. Respiration rates are required to estimate the net primary productivity (NPP), the difference between photosynthesis and respiration. Models based on the LUE approach that estimate NPP directly need not estimate respiration separately. Since growth respiration is related to the total growth of plants, it is usually expressed as a fraction of NPP. Total maintenance respiration is the sum of respiration from leaves, sapwood (including branches, stem and roots) and fine root mass. Sometimes a distinction is made between above and below ground respiration as the temperature differences can be large and respiration is strongly dependent on temperature. In this research a separation will be made into the following respiration components: leaf respiration, foliage turnover cost, root respiration and vascular system respiration. However,

the proportion of respiration for growth and maintenance is not constant and primarily depends on the age of plants (Arora, 2002), but this will not be taken into account.

3.6.1. Maintenance respiration

Leaf maintenance respiration can be expressed as a function of the maximum catalytic capacity of Rubisco, as a function of nitrogen content, or using a Q10 function. A Q10 function represents an exponential increase in some quantity with an increase in temperature. For example, a Q10 value of 2.0 implies a doubling of respiration rate with a 10 fold increase in temperature. Stem and root maintenance respiration is usually parameterized as a function of specified respiration rates at a reference temperature, an amount of live carbon present in these components, and a temperature response function similar to Q10 (Arora, 2002).

3.6.2. Whole Plant Respiration

In most models, growth respiration is expressed as a constant fraction of NPP, while maintenance respiration is estimated separately for different plant components. Cannell and Thornley (2000) argue that it is not possible to clearly distinguish between growth and maintenance respiration components, although it might be useful for some purposes. They propose a more mechanistic approach, which requires several empirical relations to be measured more exactly and put the remaining processes into one parameter that has to be calibrated. Also they warn against overestimation of maintenance costs, because there is some retrieval of energy and substrates from senescing tissues in mature plants.

3.7. Carbon allocation

Allocation of the carbon that is gained during photosynthesis can be parameterized on the basis of (1) fixed allocation fractions, (2) allometric relationships, and (3) maximization of LAI. Most models do not explicitly take into account the variation in allometric patterns according to the growth stages in a plant's life. The allocation patterns of plants are often assumed to achieve maximum growth; they are the result of natural selection and are best suited for the environments in which they grow according to the vegetation optimality hypothesis. The amount of carbon allocated to the leaves determines the biomass of the leaves and the LAI. Allocation to leaves is also linked to their phenology. Phenology describes the response of the leaves to seasonal and climatic changes to the environment. The timing of bud burst, senescence (leaf maturity or browning), and leaf abscission (leaf fall), which are functions of the environmental conditions and vegetation types, is described by leaf phenology. For vegetation types that are characterized by leaf onset and offset, no allocation is made to leaves after leaf abscission until the environmental conditions are favourable again for bud burst. Also, leaf onset and leaf offset times can be partitioned into stages of shooting, growth, shedding and dormancy. Or models may choose to prescribe the leaf onset and offset dates on the basis of observations rather than modelling the phenology.

Models that allocate carbon resources may make the distinction between leaves, sapwood and fine root mass depending on the complexity of the model. Allometric relationships that can be used are for example: (1) the relationship between tree breast height diameter and the amount of woody carbon, (2) proportionality between foliage and sapwood area, and (3) the fixed ratio between foliage and fine root carbon. The third category of allocation explicitly calculates allocation patterns to maximize growth or LAI (Arora, 2002). The problem of estimating leaf area can be regarded as an optimization problem in which the benefits of increasing leaf area in terms of light interception are traded off against the costs in terms of transpiration. An implicit assumption made in this approach is that the vegetation and the climate are both in equilibrium with each other. This approach is therefore not suitable for transient climate change simulations. This model will not be used to simulate growth and run over longer time periods. Thus allocation will not be modelled explicitly, but rather as an optimization of LAI and fine root mass. An initial LAI and Root Area Index (RAI) will be used, based on allometric relationships. During the simulation however, the trees 'choice' between creating additional fine root mass and reducing LAI under soil moisture stress will determine

these ratios.

3.8. Hydrology

The modelled soil moisture is the result of a local hydrologic balance. Precipitation that is not intercepted and evaporated from the leaves, replenishes the soil moisture. Water is removed through root uptake by the tree and percolation to deeper soil layers. Local soil characteristics determine the hydraulic conductivity which can be related to soil moisture using a soil water retention curve. Other meteorological conditions like air temperature, global radiation, relative humidity, vapour pressure deficit and wind speed are taken from nearby flux tower measurements and influence the partitioning between these processes. Opposed to the method utilized by Schymanski (2007), precipitation interception will be calculated based on total LAI and evaporation will be based on the reference potential evapotranspiration calculated according to the FAO Guidelines. This includes the recommendation by Allen et al. (1998) to replace the originally preferred Penman Equation by the Penman-Montheith Equation (Monteith, 1965) to calculate the reference potential evaporation. Precipitation is averaged on a daily basis and assumed to fall at a constant rate throughout the given time interval.

4. Model description

Whereas the previous two chapters were more concerned with the theoretical background and processes underlying the parts of the hydrological cycle and vegetation that are part of the model, this chapter focuses on the actual representation and formulation in the model. First the equations for the processes that influence the carbon cycle, both uptake and respiration are shown. The second part of the chapter focuses on the hydrological processes and soil representation. The models initialization and input parameters will be given in chapter 5.

4.1. Carbon dynamics

The developed vegetation model, coded in the Matlab programming language, is a point model that could potentially be used as a component in a spatially distributed model. It is run on a half hourly basis, compliant with the available measurements from CarboEuropeIP. First a description of the carbon balance of the modelled vegetation will be given, after that the hydrology will be discussed in relation to the water balance of the soil. Next the model's initialisation, dynamical variables and parameter calibration will be discussed. Finally the possibilities for model validation are explored.

4.1.1. Carbon assimilation

The canopy was modelled as a series of layers with horizontal leaves that were randomly distributed in each layer, with a leaf area (LA) of 0.1 per layer. Each layer was further subdivided into a sunlit and shaded fraction, where the sunlit fraction receives direct and diffuse light, while the shaded fraction only receives diffuse light. The intensity of diffuse light in each layer ($I_d(i)$, where i denotes the layer) was calculated using Eqn 1. The sunlit fraction ($I_{sun}(i)$) [mol quanta m^{-2} s^{-1}], receives both direct (I_b) [mol quanta m^{-2} s^{-1}] and diffuse light (I_d) [mol quanta m^{-2} s^{-1}] and was calculated using Eqn 2. The sunlit leaf area in each layer (LA_{sun}) was then calculated using Eqn 3. The proportion of leaf area in the shade ($LA_{shade}(i)$) was then simply the remaining portion of leaf area (Eqn 4). These equations are based on the assumption that each foliage layer is composed of randomly distributed horizontal leaves, and hence, diverges from the common approach assuming certain leaf angle distributions. For the derivation of the equations, see appendix A.2.1.2 in (Schymanski, 2007).

$$I_d(i) = I_{dtop} \times (1 - LA)^{(i-1)} \quad (1)$$

$$I_{sun}(i) = I_b + I_d(i) \quad (2)$$

$$LA_{sun}(i) = LA \times (1 - LA)^{(i-1)} \quad (3)$$

$$LA_{shade}(i) = LA - LA_{sun}(i) \quad (4)$$

The process of photosynthesis was subdivided into two steps: light processing (generation of electron transport) and CO2 uptake. The modelled electron transport rate per leaf area (J) [mol m^{-2} s^{-1}] as a function of photosynthetically active irradiance (I_a) [mol quanta m^{-2} s^{-1}] and biochemical electron transport capacity (J_{max}) [mol m^{-2} s^{-1}] is summarized in Eqn 5 and its components will be described thereafter.

(5)

4.1.2. Electron transport

The rate of electron transport achieved in any layer of the canopy per unit of ground area is given as the electron transport rate achieved by shaded leaves ($J_{shade}(i)$) plus the electron transport rate achieved by sunlit leaves in the layer ($J_{sun}(i)$). $J_{shade}(i)$ and $J_{sun}(i)$ were found as follows in equation 6 and 7 respectively:

(6)

(7)

where α = 0.3, a parameter set by common practice (Schymanski, 2007 p.20).

For the temperature dependence of J_{max}, Schymanski (2007) was followed and Equation 18 in Medlyn *et al.* (2002) was used, which was normalized for Ta = 298 K. With this function J_{max} can be written as a function of the photosynthetic electron transport capacity per leaf area at 25°C (J_{max25}), the optimum temperature for electron transport (T_{opt}) and air temperature (T_a):

$$\frac{J_{max}(i)}{J_{max25}(i)} = \frac{e^{\frac{H_a(T_a-298)}{298R_{mol}T_a}}\left(\left(-1+e^{\frac{H_a(T_{opt}-298)}{298R_{mol}T_{Opt}}}\right)H_a+H_d\right)}{\left(-1+e^{\frac{H_d(T_a-T_{Opt}}{298R_{mol}T_aT_{Opt}}}\right)H_a+H_d} \quad (8)$$

where T_a is the air temperature in Kelvin, R_{mol} is the molar gas constant [=8.314 J mol^{-1} K^{-1}], T_{opt} [K] is the mean daytime temperature on site during the period of interest, while H_d and H_a are parameters from empirical curves (Medlyn *et al.*, 2002) that determine the slope of the function above and below T_{opt}. H_a and H_d are site dependent parameters (table 1).

The total electron transport rate (JA), could finally be found by summing all J(i) and multiplying by the fraction of vegetated cover (MA) [-]:

$$JA = MA \times \sum_{i=1}^{n} J(i) \quad (9)$$

where n denotes the total number of foliage layers in the canopy. Note that J(i) is given per unit vegetated ground area, while JA is given per unit total ground area. In contrast, $J_{max}(i)$ is given per unit leaf area in layer i.

4.1.3. Gas exchange

While the canopy light environment was described using a multi-layer sun–shade approach, the gas exchange was calculated using a big leaf approach. Specifically, the equations and variables, originally defined for the leaf scale (Farquhar *et al.*, 1980) were now formulated at the canopy scale. It was assumed that, to a good approximation, carboxylation is predominantly light limited in a canopy. A calculation of the likely error because of neglecting the enzyme Rubisco (ribulose 1·5-bisphosphate carboxylase) as a limitation of carboxylation in the model is given in Appendix 2.2 in Schymanski (2007). Rubisco limitation could indirectly be caused by nutrient limitation as insufficient elements are available to form the necessary enzymes.

The rate of CO_2 exchange between the inside of the leaf and the atmosphere (A_g) [mol CO_2 m^{-2} ground area s^{-1}] is formulated in Eqn 10, where G_s is the stomatal conductivity [mol m^{-2} ground area s^{-1}] while C_l and C_a [both in mol CO_2 mol^{-1} air] are the mole fractions of CO_2 inside the leaf and in the atmosphere, respectively (Cowan and Farquhar, 1977). Inside the leaf, leaf respiration (R_l) [mol m^{-2} ground area s^{-1}] replenishes some of the CO2 consumed by Ac, so that at steady state, only the difference between A_c and R_l has to be balanced by A_g. This is expressed in Eqn 11. A_g was finally found as equation 12 (Schymanski, 2007):

$$A_g = G_s(C_a - C_1) \quad (10)$$

$$A_g = A_c - R_l \quad (11)$$

$$A_g = \frac{1}{8}\left(4C_aG_s + 8\Gamma G_s + JA - 4R_l - \sqrt{(-4C_aG_s + 8\Gamma G_s + JA - 4R_l)^2 + 16G_s(8C_aG_s + JA + 8R_l)\Gamma} \right) \quad (12)$$

where Γ* is the CO_2-compensation point, which is only dependent on temperature. For the temperature dependence of Γ* the empirical relationship established by Bernacchi *et al.* (2001), as reformulated in Medlyn *et al.* (2002) was used. After converting to molar units and under the assumption that leaf temperature is the same as air temperature, independent of the position in the canopy, this becomes:

$$\Gamma_* = 0.00004275\, e^{\frac{126.946\,(T_a - 298)}{R_{mol}\,T_a}} \quad (13)$$

4.1.4. Leaf respiration

The rate of CO_2 exchange across the stomata per ground area (A_g) in this formulation accounts for leaf respiration as well as CO_2 assimilation. CO_2 uptake is positive if there is a sufficiently large electron transport rate (JA) and stomatal conductivity (G_s), and negative if there is no electron transport, e.g. at night.

Leaf respiration (R_l) was modelled as a function of total electron transport capacity for the canopy, J_{maxtot} [mol m^{-2} s^{-1}]:

$$R_l = \frac{cR_l J_{max\,tot}(t)(C_a - \Gamma)}{4(c_{RL} + 1)(C_a + 2\times\Gamma)} \quad (14)$$

where c_{RL} is an unknown proportionality constant that is tuned to match the observed data unlike Schymanski (2007) where c_{RL} has a fixed value of 0.07.

J_{maxtot} can be found by summing all $J_{max}(i)$ and multiplying by the fraction of vegetated cover (MA) and leaf area (LA).

$$J_{max\,tot} = LA \times MA \times \sum_{i=1}^{n} J_{max}(i) \quad (15)$$

4.1.5. Stomatal conductance

Transpiration (E_t) was modelled as a diffusive process, similar to the CO_2 uptake of plants through their stomata. The different diffusivities of CO_2 and H_2O vapour were taken into account by multiplying the stomatal conductance for CO_2 (G_s) by a constant factor a, which was set to 1.6, following Cowan and Farquhar (1977). This is shown in Eqn 16, where W_l and W_a are the mole fractions of water vapour inside and outside the leaf, respectively. Assuming that the air inside the leaf is at 100% relative humidity, the term (W_l - W_a) is approximated by dividing the measured atmospheric Vapour Pressure Deficit (VPD) by the air pressure, becoming the molar vapour deficit (D_v) [mol mol^{-1}]:

$$E_t = aG_s(W_l - W_a) \approx aG_sD_v \quad (16)$$

Water loss by evapotranspiration (E_t) and the rate of photosynthesis (A_g) are linked by stomatal conductance, such that any increase in CO_2 uptake rate under given atmospheric conditions and foliage properties has the inevitable consequence of increased water loss through the stomata. This relationship between E_t and A_g can be expressed by combining

Equations 16 and 12 to obtain:

$$E_t = \frac{a A_g D_v G_s (4A_g - J_A + 4R_l)}{C_a(4A_g - J_A + 4R_l) + (8A_g + J_A + 8R_l)\Gamma_*} \quad (17)$$

Both A_g and E_t depend on stomatal conductance (G_s), but while A_g has an upper limit determined by JA, E_t increases indefinitely with increasing stomatal conductance. The slope of the curve (λ) between A_g and E_t at any value of A_g is thus determined by D_v and JA, the latter of which is determined by solar irradiance (I_a) and canopy properties.

According to Cowan and Farquhar (1977), for any given amount of total water available for transpiration in a period of time, a leaf can achieve a maximum in CO_2 uptake if it adjusts G_s in such a way that λ is maintained at a constant value. The variables ce and me are unitless empirical parameters that define the functional shape of the relationship between λ (the slope of the curve between A_g and E_t) and h. Because λ is dependent on the available soil moisture within the rooting zone, the following explicit relationship (equation 18) between λ and soil water pressure head (h_i) is used.

$$\lambda = ce\left(\sum_{i=1}^{irp} h_i\right)^{me} \quad (18)$$

To optimise G_s, λ was held constant and used to compute the instantaneous rates of E_t as a function of λ with Eqn 20. Afterwards the stomatal conductance, G_s, could be inferred from E_t as follows with Eqn 19:

$$G_s = \frac{E_t}{a \times D_v} \quad (19)$$

$$E_t = \frac{aD_v(C_a(J_A - 4R_l) - 4(J_A + 2R_l)\Gamma_*)}{4(C_a + 2\Gamma_*)^2} + \frac{\sqrt{3}\sqrt{aD_v J_A \Gamma_*(\lambda C_a - 2aD_v + 2\lambda\Gamma_*)^2(\lambda C_a - aD_v + 2\lambda\Gamma_*)(C_a(J_A - 4R_l) - (J_A + 8R_l)\Gamma_*)}}{4(C_a + 2\Gamma_*)^2(\lambda C_a - aD_v + 2\lambda\Gamma_*)} \quad (20)$$

And finally the CO_2 uptake (A_g) could then be found using G_s in Eqn 12.

4.1.6. Carbon respiration

Carbon is lost from a plant in the form of CO_2 as a result of respiratory processes. These are often divided into above- and belowground processes or split into the different components. Soil respiration generally includes the decay of soil organic matter and root respiration. Because of its inhomogeneous and variable nature no general models and equations exist for soil respiration and it is often based on specific empirical formulas taken from measurements. Above ground respiration includes respiration from woody tissues and leaves. Respiration can also be divided into the following different components: root- and foliage turnover cost and root-, leaf- and vascular system respiration. In this research project both above- and belowground respiration are taken into account separately when calculating the net CO_2 flux to compare with the FLUXNET data and the separation into the different components is used when calculating the internal carbon profit of the tree.

4.1.6.1. Belowground Respiration

Soil respiration is commonly measured as the release of CO_2 at the soil surface and can be seen as a result of decomposition of organic matter in the soil combined with respiration by plant roots. The rate of microbial decomposition depends on the amount of organic matter in the soil as well as soil temperature and moisture, while root respiration responds to soil

temperature, moisture and nutrient availability in the soil. The non-linear feedbacks in soil respiration components, make measured soil respiration vary seasonally and in response to rapid changes in soil moisture and soil temperature. A recent study by Moyano *et al.* (Moyano *et al.*, 2008) for example found a direct connection between photosynthesis a couple days earlier and root derived carbon respiration fluxes. The model is based on empirical formulations that were derived from measurements taken on site in Hainich and Puechabon respectively.

Soe and Buchmann (2005) conducted soil respiration measurements at the study site in Hainich National Park in 2000 and 2001. Soil temperature alone explained between 68 and 95% of the temporal variation in soil respiration. An empirical exponential formula was fitted to the data, which included soil temperature (Ts) and soil moisture content (θ), the explanatory value of the model was R^2=0.84. Equation 21 was used to model soil respiration (R_s) [µmol CO_2 m^{-2} s^{-1}]. The empirical relation found by Soe and Buchmann (2005) was adjusted to match observed data by Kutsch *et al.* (2010), who found the mean total soil respiration in 2000-2007 to be 876 g C m^{-2} y^{-1}. The exponential size constants and relationship of the model were retained, but the equation was multiplied by 0.7 instead of 0.31. This number was inferred from soil moisture and soil temperature in an equilibrium situation to give a total yearly soil respiration flux of 879 g C m^{-2} y^{-1}. This following formulation is used for the model runs in the Hainich area:

$$R_s = 0.7e^{0.13T_s}e^{0.02\theta} \quad (21)$$

Where θ=su*E, the water saturation degree times the porosity of the soil.

For the Puecabon area, a different empirical relationship was used, derived by Joffre *et al.* (2003) who monitored soil CO_2 efflux monthly during 1999 and 2001 and conducted experimental water treatments in 1999 in Puéchabon State Forest. Respiration was modelled with different formulas and models parameters were estimated using a non-linear regression procedure. The model where the rate constant of temperature is a linear function of soil moisture had the highest explanatory value (r2=0.68) and is used to calculate soil respiration (Rs) [µmol CO_2 m^{-2} s^{-1}] for the Puechabon site.

$$R_s = R_{s,ref} \cdot f(\theta) \cdot e^{((b\,f(\theta)+c)(T-Tref)/10)} \quad (22)$$

with T = soil temperature at 15-cm depth (°C), Rs,ref being the respiration under standard conditions (at Tref and nonlimiting soil moisture). f(θ) was expressed as the percentage of soil water content compared to field capacity:

$$f(\theta) = \frac{\theta}{\theta_{fc}} \quad (23)$$

with θ current soil water content and θfc soil water content at field capacity, that is θ measured after a large rain event and two draining days or calculated at a matrix potential of -2m.

4.1.6.2. Above-Ground Respiration

Total above-ground woody-tissue respiration (R_w) [µmol CO_2 m^{-2} s^{-1}] is estimated by a Q10 relationship:

$$R_w = R_{w25}\, Q_{10,w}^{(T_w - T_r)/10} \quad (24)$$

where R_{w25} is the wood respiration at reference temperature (T_r=25 °C), $Q_{10,w}$ is the proportional increase in R_w with 10 K increase in wood temperature (T_w). To estimate T_w (Cernusak *et al.*, 2006) used the observations that the daily mid-range stem temperature at their study site in Northern Territory (Australia) was linearly correlated with daily mid-range air temperature and that the daily temperature amplitudes of stems and air were similar, which lead to the following formulation:

$$T_w = 1.11\, T_a - 1.36 \quad (25)$$

$Q_{10,w}$ was given by Cernusak *et al.* (2006) as 1.92 for all species, and the value of $R_{w,25}$ ($R_{w,25}$ = 0.606) [µmol CO_2 m^{-2} s^{-1}] was fitted by Schymanski (2007) to match the observed annual

woody-tissue respiration of 297 g C m^{-2} measured by Cernusak *et al.* (2006). Unfortunately, no relationships that simulate above-ground respiration in climate and ecosystems more similar to the study sites used in this research project were found in the literature.

4.1.7. Net Carbon Profit

The Net Carbon Profit (NCP) is defined as the difference between carbon acquired by photosynthesis and carbon spent on maintenance of the organs involved in CO_2 uptake. This definition allows attributing generic costs in terms of NCP to plant organs like leaves or roots, so that unrealistically high values for leaf area or root abundance are avoided (Schymanski, 2007). NCP basically only refers to the energy that is available to the plants for increasing their biological fitness.

NCP was thus found as the difference between the CO_2 uptake and the maintenance costs:

$$NCP = \sum_{t_{start}}^{t_{end}} \left[A_g(t) - R_{ft}(t) - R_v(t) - R_r(t) \right] \Delta t \tag{26}$$

where R_{ft}, R_v and R_r are the foliage turnover costs and maintenance costs of the vascular and root systems respectively. Leaf respiration is accounted for in the formulation of A_g.

4.1.7.1. Foliage Turnover Costs

Wright *et al.* (2004) compiled an extensive database of leaf properties (GLOPNET), which is available online. The database contains "leaf dry mass per area" (LMA) and "leaf life span" (LL) for a global range of plant species, which were used to obtain an estimate of the costs involved in the maintenance of a certain leaf area. Assuming a construction cost equivalent to 2 g CO_2 per g leaf dry matter (Givnish, 2002), the foliage turnover costs (Rft) [mol carbon s^{-1} m^{-2} ground area] were formulated as:

$$cR_{ft} = \frac{\left(\frac{2 \cdot LMA}{LL} \right)}{mmCO_2} \tag{27}$$

$$R_{ft} = cR_{ft} \cdot LAI \tag{28}$$

where mmCO2 is the molecular mass of CO_2 [=44 g mol^{-1}] and leaf area index (LAI) [m^2 m^{-2}] was found as the number of leaf layers (m) multiplied by the fraction of vegetated cover (MA) [-] by the leaf area per layer (LA):

$$LAI = MA \cdot m \cdot LA \tag{29}$$

4.1.7.2. Root respiration

In the absence of a general relationship in literature between root maintenance costs and their water uptake capacity, Schymanski (2007) was followed, who used published measurements on citrus roots, for which observations of both respiration rates and hydraulic properties were available. Assuming cylindrical roots, root respiration (R_r) [mol m^{-2} s^{-1}] is formulated as a function of root radius (rr) and root surface area (SAr) for a single soil layer:

$$R_r = c_{Rr} \left(\frac{r_r}{2} S_{Ar} \right) \tag{30}$$

where c_{Rr} = 0.0017 mol s^{-1} m^{-3} and r_r = 0.3x10^{-3} m.

4.1.7.3. Vascular system respiration

Water that is taken up by fine roots needs to be transported to leaves where it is transpired. The vascular system required for this transport is most obvious in the stems and branches of

trees. A relationship between size and carbon costs of the vascular system could not be derived from the literature. Therefore, the simple assumption that the carbon costs related to the maintenance of the vascular system are a linear function of rooting depth and the vegetated area of the vegetation has been made:

$$R_v = c_{rv} M_A y_r \quad (31)$$

where y_r is the depth of the roots, c_{rv} is an unknown proportionality constant, which was set to an arbitrary value of $1.2*10^{-6}$ that lead to realistic model results in Schymanski (2007).

4.2. Water Balance

The hydrological processes described earlier in this report were also 'translated' into equations to be implemented in the model. The canopy water demand has to be met by root water uptake in the soil. Precipitation infiltrating into the ground refills the soil moisture compartment, which is depleted by percolation, evaporation and transpiration by different types of vegetation. Rainfall infiltration is limited by the hydraulic conductivity of the soil and replenishes top layer soil moisture. Any excess water is removed from the model, which reflects runoff in the field. The separation between a saturated and unsaturated soil and surface area fraction used in Schymanski (2007) was not retained for this research project. Reference evaporation was used to determine actual rainfall interception and soil evaporation. To parameterise the soil water equations, values of the parameters saturated hydraulic conductivity (K_{sat}), residual water content (θ_r), saturated water content (θ_s) and the empirical van Genuchten parameters (αvG and mvG) had to be obtained from soil physical measurements, or "typical" values for the prevalent soil type obtained from literature can be used, which has been done for this research project.

4.2.1. Soil representation

The soil was divided into n layers of equal thickness. A homogeneous soil profile and type is assumed because there is no good information about the soil profile at the site and to evaluate the model without unnecessarily complicated information. Unsaturated hydraulic conductivity (K_{unsat}) and matrix potential (h) in each layer are considered to be functions of soil properties and water saturation degree (su), but there are many other, mainly empirical, formulations of these functions in literature. The empirical formulations by Brooks and Corey (1966) and Van Genuchten (1980) are among the most widely used for modelling.

Observed soil moisture (θ) in the top 10 cm of soil was converted to units of relative saturation (su) using Equation 32, where θ_s was replaced by the maximum observed soil moisture at the different sites, while θ_r and the van Genuchten parameters were estimated according to (Schaap *et al.*, 1998) for the site specific soil type.

$$s_u = \frac{\theta - \theta_r}{\theta_s - \theta_r} \tag{32}$$

The matric suction head, h(i) [m], was defined as positive and increasing with decreasing soil saturation, using the van Genuchten parameters:

$$h(i) = \frac{1}{avG}\left(su(i)^{\frac{-1}{mvG}} - 1 \right)^{\frac{1}{nvG}} \tag{33}$$

where avG [m-1], nvG [-] and mvG [-] are the empirical van Genuchten soil properties and su(i) [-] is the water saturation degree (range 0-1). nvG and mvG are assumed to follow the relation:

$$m_{vG} = 1 - \frac{1}{n_{vG}} \tag{34}$$

The hydraulic conductivity, $K_{unsat}(i)$ [m s^{-1}], was also found as a function of the water saturation degree, su(i):

$$K_{unsat}(i) = K_{sat} \times \sqrt{su(i)} \times \left(1 - \left(1 - su(i)^{1/mvG}\right)^{mvG}\right)^2 \quad (35)$$

where K_{sat} [m s^{-1}] is the saturated hydraulic conductivity and is considered constant for a given soil layer.

4.2.2. Interception

Precipitation is intercepted by vegetation before infiltrating into the ground; the total interception capacity is based on the total LAI of the canopy present. For this research project the assumption that precipitation falls at a constant rate throughout the given time interval is made. Part of the precipitation (P) that reaches the top of the canopy falls on the soil directly as direct throughfall, while part of the precipitation is intercepted depending on the fraction of vegetated cover. On a daily timestep the assumption is made that as long as the interception capacity of the canopy is not exceeded and the open water evaporation for a day is not exceeded all water is intercepted. Leading to the following formulation of interception:

$$I = EI = \min(MA \cdot Eo, LAI \cdot Icap, MA \cdot P) \quad (36)$$

where I [mm day^{-1}] is interception, EI [mm day^{-1}] is evaporation of interception, Eo [mm day^{-1}] is open water evaporation that is calculated using the Penman-Monteith equation (Monteith, 1965) applied to open water and Icap [mm] is the maximum interception capacity.

4.2.3. Soil evaporation

Soil evaporation was based on the reference potential evapotranspiration ET_0 [mm d^{-1}] that was calculated according to the FAO Guidelines. Allen *et al.* (1998) recommended replacing the originally preferred Penman Equation by the Penman-Montheith Equation (Montheith, 1965) to calculate the reference potential evaporation. Through the inclusion of the canopy resistance, the Penman-Montheith Equation performs relatively accurate and consistent in both arid and humid climates whereas the Penman Equation was shown to overestimate the evapotranspiration frequently. In this model the following version of the Penman-Montheith Equation was used:

$$ET_0 = \frac{\delta(R_n - G) + \rho_a c_p \dfrac{(e_s - e_a)}{r_a}}{\lambda_v\left(\delta + \gamma\left(1 + \dfrac{r_s}{r_a}\right)\right)} \quad (37)$$

where e_s is the saturation vapour pressure, e_a is the actual vapour pressure, both in [Pa], δ is the slope of the function of the saturation vapour pressure versus the air temperature [Pa $°C^{-1}$], γ is the psychometric constant [Pa $°C^{-1}$], ρ_a is the density of air [1.205 kg m^{-3}], c_p is the specific heat capacity of air [0.24 cal g^{-1} $°C^{-1}$], R_n is the net incoming radiation and G the ground flux, both in [W m^{-2}], λ_v is the latent heat of vaporization [J kg^{-1}], and r_s and r_a are the surface and aerodynamic resistance respectively [s m^{-1}].

The ground flux in equation 37 was neglected, assuming no heat exchange between soil and air over longer periods. Of the variables of Equation 37, ρ_a and c_p are constants and vapour pressure, net radiation is taken from the CarboEurope flux measurements on site. All other variables had to be calculated. The saturated vapour pressure was calculated from the average daily temperature under the underlying assumption of the isothermal conditions of the Penman Equation (Allen et al., 1998):

$$e_s = 611 \cdot \exp\left(\frac{17.27 + \overline{T}}{\overline{T} + 237.3}\right) \quad (38)$$

The slope of the saturation vapour pressure versus the air temperature (δ) and the

psychrometric constant (γ) were calculated as (Allen *et al.*, 1998):

$$\delta = \frac{4098 \cdot e_s}{(T + 237.3)^2} \quad (39)$$

$$\gamma = \frac{c_p \cdot P}{\varepsilon \lambda_v} \quad (40)$$

where Pa is the atmospheric pressure [= 1013 hPa], e is the ratio of the molecular weight of water vapour and dry air [=0.622 -].

The psychometric constant is not constant as both the latent heat of vaporization and the atmospheric pressure vary with the air temperature and the elevation respectively. Allen *et al.* (1998) ignore the variation in λ_v with T but this relationship is maintained here as:

$$\lambda_v = 2.501 \cdot 10^6 - 2370T \quad (41)$$

The effectiveness by which heat and vapour can be exchanged with the atmosphere depend on the vertical transport capacity of turbulent air, as expressed by the friction velocity of the eddies. Allen *et al.* (1998) estimate the diffusivity as the product of the friction velocity for the momentum transfer and the heat and vapour transfer:

$$r_a = \frac{\ln\left(\frac{z_m - z_D}{z_{0m}}\right)\ln\left(\frac{z_h - z_D}{z_{0h}}\right)}{k^2 \overline{u}_z} \quad (42)$$

where z_m and z_h are respectively the heights at which the wind speed and temperature/vapour pressure are measured, z_D is the zero plane displacement height, z_0 stands for the roughness length, k is the Karman constant [=0.41 -] and $\overline{u_z}$ is the wind speed measured at height z_m.

Not specified so far are those variables that are dependent on the surface conditions being the surface resistance, r_s, and the vegetation height, z_{veg}. As a reference surface Allen *et al.* (1998) proposed hypothetical grass cover on the ground that this crop is well studied. This reference surface is defined unambiguously as *"a hypothetical reference crop with an assumed crop height of 0.12 m, a fixed surface resistance of 70 s m^{-1} and an albedo of 0.23".* The zero plane displacement height is assumed at 2/3 of the vegetation height and the heights of the measurements 2m above the top of the vegetation.

Soil evaporation in the top layer (Esu) [mol m-2 s^{-1}] was assumed to be a function of reference potential evapotranspiration ET_0, the canopy gap fraction and hydraulic conductivity in the top layer, and modelled as:

$$Esu = \exp^{-kJ \cdot LAI} \; ETo \frac{Kunsat}{Ksat} \quad (43)$$

The water flux flowing out of every layer (Q(i)) [m s^{-1}] was calculated with the unsaturated hydraulic conductivity (K_{unsat}) [m s^{-1}] and the Darcy equation depending on the matrix potential (h) [m]:

$$Q(i) = 0.5 \cdot Kunsat(i)\left(\frac{h(i)}{dz} + 1\right) \quad (44)$$

The change in soil moisture was calculated as the sum of all moisture fluxes into and out of a soil layer minus the root water uptake flux (Qr) [m s^{-1}] for every time step (dt) [1800 s]:

$$\Delta su(i) = \Delta t \frac{Q(i) + Qin(i) - Qr(i)}{E \cdot dz} \quad (45)$$

4.2.4. Root Water Uptake

Root water uptake was modelled following Schymanski (2007) using an electrical circuit

analogy, where radial root resistivity and soil resistivity are in series in each soil sub-layer (Hunt et al. 1991). Water uptake per unit root surface area in a soil layer ($J_r(i)$) [m s^{-1}] was thus written as:

(46)

where Ω_r [s] is root resistivity to water uptake per unit root surface area (assumed to have the same value in all soil layers), and $\Omega_s(i)$ [s] is the resistivity to water flow towards the roots in the soil. The driving force for water uptake by roots is the difference between the matrix potential (h(i)) [m] and the forces holding the water in the roots ($h_r(i)$) [m]. Defining $SA_r(i)$ as the root surface area per m2 ground area in layer i, root water uptake rate in layer i is formulated as:

(47)

Ωs was formulated as a function of unsaturated hydraulic conductivity ($K_{unsat}(i)$) [m s^{-1}], root radius (r_r) [m] and root surface area density in soil layer i ($SA_{dr}(i)$) [m^2 m^{-3}]:

(48)

The suction head inside the roots is often considered to be linked to the suction head in leaves, which is caused by adhesive forces and is driven by transpiration. Thus, water transport from the soil to the leaves could happen passively, without the expenditure of energy other than the maintenance of the plant tissues involved. In Schymanski (2007) Appendix A.3.3.2, a model to quantify the forces involved in such a passive process was developed. The model is based on measurements of tissue balance pressure (Pb, the pressure that has to be applied in order to force water out of the tissue) as a function of tissue water content (Mq):

$$P_b = (M_{qx} - M_q)\left\{\frac{750\,M_d}{(M_d + M_{qx})^2} + \frac{1}{M_{qx}}\right\} \quad (49)$$

where Pb is the tissue balance pressure in bars, Mqx and Mq are the potential and actual amount of water stored in plant tissues per unit catchment area respectively, and Md is the total mass of dry matter associated with living tissues per unit catchment area. Pb can only increase until Mq reaches a value of 0.9 Mqx, because any further decrease in water content is assumed to lead to tissue damage (Schymanski, 2007). The amount of water stored in the plant tissue is expected to change on a diurnal scale, affected by water loss through stomata and water uptake by the roots. This diurnal cycle in stored water is often expressed in the swelling and shrinking of tree trunks.

In order to use the balance pressure in plant organs above ground to drive passive water uptake by roots, P_b was translated into the root suction head ($h_r(i)$) by taking into account the hydrostatic head difference between roots and trunks:

(50)

where $h_h(i)$ [m] is the hydrostatic head difference between the soil surface and the depth of layer i, while c_{Pbm} [=10.2 m bar^{-1}] is a conversion coefficient to convert from units of Pb [bar] to units of $h_r(i)$ [m]. A water storage capacity (M_{qx}) of a large tree can act as a buffer for meeting peak foliage water demands in case it exceeds root water uptake rates during the day.

The rate of change in M_q can be written as a function of root water uptake and transpiration rate:

(51)

where $Q_r(i)$ is the water uptake rate by tree roots in soil layer i and irp is the deepest soil layer accessed by tree roots. The deepest soil layer accessed by tree roots (irp) [-], was found with the depth of the roots (y_r) [m]. Et(t) is calculated by Eqn 20 and used in Eqn 51 to find the change in water storage in the tree. The tissue balance pressure (given by Eqn 49) depends on

the difference between potential and actual water storage and is needed to calculate h_r (Eqn 50). The root suction head is finally used in Eqn 47, together with the current soil water potential and resistivities, to calculate the actual root water uptake flux in every layer where roots are present.

5. Practical work: Methods

This chapter gives an overview of the methods and data that were used during this research project. First some background information is given on the availability and shortcomings of the data that is utilized. The next paragraph gives information on the specific sites for which the model was calibrated. Paragraph 3 deals with the site specific input parameters and choice for the initialization of the root distribution and soil moisture content. While paragraphs 4 and 5 explain the off-line parameter optimization and the dynamic optimization by the model itself during the runs, for which the results will be shown in the next chapter. The final section explores some potential strategies for model validation by comparison with NDVI and tree ring data or other model output.

5.1. Data

The model was run using half-hourly Eddy covariance measurement data made available by the CARBOEUROFLUX programme, a programme sponsored by the European Commission to improve our understanding on magnitude, location, temporal behaviour and causes of the carbon source/sink strengths of terrestrial ecosystems. These data are freely available for the public and scientific community from the CarboEurope Integrated Project (IP) Ecosystem Component Database (at http://www.carboeurope.org/).

The methodology for ecosystem exchanges of carbon and energy is based on the Eddy covariance theory. The flux stations measure the net flux of carbon entering or leaving the ecosystem. This is the flux which, if summed annually, provides the estimate of Net Ecosystem Exchange (NEE), and thus provides a direct measurement of the annual ecosystem carbon source/sink strength. The collected data is quality controlled, corrected for frequency losses and sensor separation and, when needed, corrected for night-time fluxes with the same procedures. There are different methods that separate Net Ecosystem Exchange (NEE) into its major components, Gross Ecosystem Production (GEP) and ecosystem respiration (R_{eco}). The proposed standard method by Reichstein *et al.* (2005) uses the friction velocity as a criterion to discriminate between low and well mixed periods, this is generally known as the u_* correction. As an alternative to the u_* filter, estimated relationships between R_{eco} and temperature have also been proposed (Leuning *et al.*, 2008).

The original (level 1) data published by CarboEuropeIP have been gapfilled and partitioned according to the methods proposed in Reichstein *et al.* (2005). The same authors have shown that the temperature sensitivity of R_{eco}, derived from long-term (annual) data sets, does not reflect the short-term temperature sensitivity that is effective when extrapolating from night- to daytime. Although the model developed for this research project is not validated using separate R_{eco} and GEP values, a short explanation of the separation process and other measurement problems are given here, based on research by Reichstein *et al.* (2005) and Papale *et al.* (2006).

The separation between GEP and R_{eco} and the extrapolation of respiration from night to day are based on the temperature derived from long-term data sets. In some ecosystems, this application of a long-term temperature sensitivity leads to a systematic overestimation of ecosystem respiration from half-hourly to annual time-scales. The overestimation of respiration can reach >25% for an annual budget and consequently affects estimates of GEP (Reichstein *et al.*, 2005). On the other hand, in summer passive (Mediterranean) ecosystems, the long-term temperature sensitivity is lower than the short-term temperature sensitivity. This can result in underestimation of annual sums of respiration. During periods with low turbulence and limited air mixing, eddy covariance measurements systematically underestimate the ecosystem respiration in Mediterranean ecosystems and overestimate it in moderate ecosystems. The most probable cause of error is the presence of small scale movements associated with drainage flows or land breezes that take place in low turbulence conditions and create a decoupling between the soil surface and canopy top (Papale *et al.*, 2006). The flux problems during the night because of the low wind speeds are by-passed by discarding the data corresponding to low mixed periods and replacing them with data from periods above the u_* threshold. However, whether a reliable short-term relationship between R_{eco} and temperature can be

found, depends on the noisiness of the eddy data and the range of temperatures encompassed during the observation period (Reichstein *et al.*, 2005). These and other problems have led people to question the reliability and usability of fluxnet data, fortunately there are many other examples to be found in the literature were the use of these data has led to significant increases in knowledge and understanding of processes at the ecosystem scale and the fluxnet network sites are still being expanded.

The data available from CarboEuropeIP has been checked and treated in different ways. Not all datasets are available for every year and site, thus both level 3 and level 4 data have been used in this research project. The level 2 data are the half hourly, not gapfilled or filtered data as provided by the site staff, that has been quality checked. Level 3 data are obtained from the level 2 products, data are quality checked using standardized techniques and NEE is calculated. Data are not changed but descriptive variables ('flags') are added. Finally, the level 4 data are obtained from the level 3 products, the data are u_* filtered, gap-filled using different methods and partitioned. Datasets are also aggregated from daily to monthly. Flags with information regarding quality of the original and gapfilled data are added.

The following half-hourly (level 4) data were used as input for the model:
air temperature (Ta) [°C]
global radiation (Rg) [W m^{-2}]
latent heat flux (lE) [W m^{-2}]
Net Ecosystem Exchange (NEE) [umol CO_2 m^{-2} s^{-1}] filled using the Marginal Distribution Sampling method (Reichstein et al. 2005)
precipitation (Precip) [mm]
sensible heat flux (H) [W m^{-2}]
soil temperature (Ts) [°C]
Soil Water Content (SWC) [%vol]
Vapour Pressure Deficit (VPD) [hPa]

Photosynthetically Active Radiation (PAR, I_a) was assumed to be 50% of the global radiation and multiplied by a factor 4.57E-6 to convert to units of [mol quanta m^{-2} s^{-1}]. The percentage of diffuse solar irradiance reaching the canopy was approximated as explained in appendix 2.3 in Schymanski (2007) using the geographical location of the site.

Additional to the level 4 data, the net radiation (Rn) [W m^{-2}] and horizontal wind speed (WS) [m s^{-1}] were used from the level 3 data for the calculation of reference evapotranspiration. Since these data were not gap filled, this was done before the model runs by substituting data from the 24 hours before for any missing half-hourly data. The optimal temperature, used in the calculation of the maximal electron transport capacity (J_{max}) was taken as the mean daytime temperature on site during the period of interest. For the calculation of reference evapotranspiration the total daily net radiation was redistributed proportionally over the daytime period, defined as the period that had positive radiation in the original measurements.

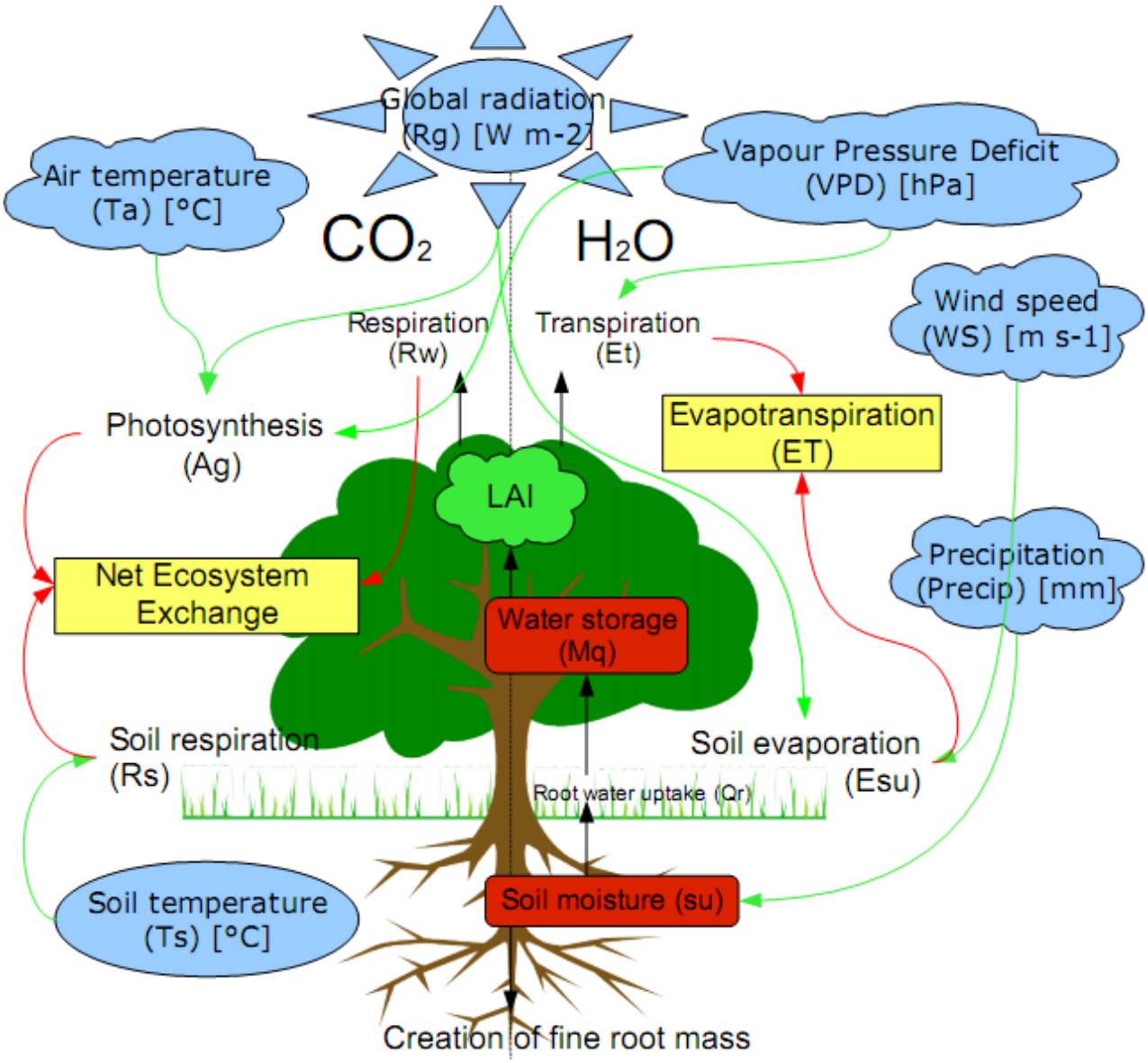

Figure 3: *A simplified schematic overview of the models input (blue) and output (yellow) parameters for the carbon (left) and the hydrological cycle (right). Green arrows indicate the use of measurements in the calculation of the processes, whereas red lines indicate the contribution of these processes to the outgoing water and carbon fluxes. The redistribution of fine root mass in layers where soil moisture is present increases the internal water storage of the tree through the root water uptake flux, thereby allowing the tree to maintain its canopy (simulated as Leaf Area Index (LAI)) under more severe drought.*

5.2. Site description

5.2.1. Hainich National Park

The Hainich forest site (DE-Hai) is one of the sites of the European CarboEurope project where continuous eddy covariance measurements are running. This mixed broadleaf deciduous forest is located within the Hainich National Park (51° 04' 45.36'' N; 10° 27' 07.20'' E; 430 m a.s.l.) in Central Germany and has mean annual values of 6.8 °C and 775 mm for air temperature and precipitation respectively.

The Hainich National Park covers an area of about 7600 ha in the Thuringia region close to the former East-West German border. It was established in 1997 to protect one of the largest broad-leafed mixed forests in central Europe. The forest has been used by the military and has been unmanaged for about 60 years. Previously the forest was managed extensively, with the result that the ages of the trees cover a wide range with a maximum of 250 years (Knohl *et al.*, 2003). The amount of woody debris on the forest floor and standing dead wood is large compared with a managed forest. Litter from trees and plants in the understory

decomposes almost completely within 1 year.

The forest is dominated by European beech (*Fagus sylvatica L.*, 65%) and codominated by ash (*Fraxinus excelsior L.*, 25%) and maple (*Acer pseudoplatanus L.* and *A. platanoides L.*, 7%). The understory vegetation is dominated by geophytes and hemichryptophytes, such as *Allium usrinum L., Anemone nemorosa L.* and *Mercurialis perennis L.* The mean canopy height is ca. 24 m. The soils are cambisols (loamy clay). The A-horizon is 5-15 cm deep, underlaid by clay and, at a depth of 40-60 cm, calcareous bedrock. The soil physical parameters for the Hainich site are estimated based on a neural network-based ROSETTA database (Schaap *et al.*, 1998). The Hainich site has been recognized as a difficult site for eddy covariance measurements as it experiences regular turbulence problems, for example in 2003 when up to 50% of daytime data had to be filtered with the highest u_* threshold (Papale *et al.*, 2006). Therefore a high uncertainty and measurement error is taken into account when comparing the measurements with the model simulations.

5.2.2. Puechabon

Puechabon (FR-Pue) consists of an evergreen broadleaf forest located in the Herault region in France (43° 44' 29" N; 03° 35' 5" E; 270 m a.s.l.). It is located 35 km NW of Montpellier and has mean annual values of 13.5 °C and 872 mm for air temperature and precipitation respectively. It has a Subtropical-Mediterranean climate and the region experiences severe droughts in summer occasionally. Rainfall occurs largely during autumn and winter with about 75% of the total occurring between September and April. Mean annual precipitation is 872 mm with a range 550–1549 mm recorded over the past 18 years.

The forest has been managed as a coppice for centuries and the last clear cut was performed in 1942. Vegetation is largely dominated by the overstory evergreen tree *Quercus ilex L.* This tree species is characterized by its sprouting ability after cutting or fire, when quickly new stems emerge from the root–shoot interface. The mean canopy height is about 5.5 m. In 2005, the density of the resprouted stems was 6885 stems ha-1, stems with diameters at breath height (DBH) < 4 cm represent 12% of the total stems, whereas stems with DBH > 10 cm represent 15% (Limousin *et al.*, 2008). Understory species compose a sparse, shrubby layer (<25% cover, <1.5m tall), including *Buxus sempervirens, Phyllirea latifolia, Pistacia terebinthus*, and *Juniperus oxycedrus*.

The forest grows on a hard Jurassic limestone formation. Soil texture does not show trends with depth between 0 and 50 cm from the surface. Clay and sand contents are, respectively, 40% and 14%. This soil is considered a silty clay loam according to the USDA texture triangle (Rambal *et al.*, 2004). The soil fills up the cracks and fractures of the limestone providing a source of water throughout the long dry summers for the deep-rooted Q. ilex. The average stone and rock content is about 75% for the top 0–50 cm and 90% for the whole profile.

5.2.3. La Peyne field work

La Peyne is part of the Puechabon region in France close to Montpellier, the area is named after the river Peyne. In the summer I spend 2 weeks in this area to see and conduct measurements of the vegetation on site. I was introduced to measurements of the soil, such as hydraulic conductivity, depth and moisture content, vegetation and other site characteristics. We 1) took infra-red and fish-eye camera pictures of under- and overstory vegetation, indentified, counted and measured diameter and height of individual trees in randomly selected plots. 2) Estimated vegetation cover and fire likelihood based on dead leaf material and understory vegetation. 3) Collected samples of tree species that were weighed and either dried of wetted to estimate biomass and interception capacity respectively. 4) Measured infiltration capacity either on site or took samples and recorded site characteristics like slope, elevation, and location.

The vegetation was primarily Q. Ilex trees which I intensively studied, including their reproductive and root system if this was possible. Roots could sometimes be seen in rock outcrops up to tens of meters below the trees, indicating the reality of deep root systems much more then was deemed possible in the Hainich area. In the previous year, tree ring samples were taken from this area during a fieldwork campaign that were counted during the

practical work of this research project to be used in further analysis, correlations with weather data and potentially model validation.

5.3. Model Initialization

The model was initialized for each run with a set root distribution and soil moisture content. Initial soil moisture was varied from field capacity to a 'spin-up' value computed at the end of the last simulation to show the effect of the onset conditions to the dynamics throughout the year. Seasonal optimisation runs were initialized with full canopy cover, while yearly runs were started without and with minimal LAI for the Hainich and Puechabon region respectively. For the runs with the hypothetical root mechanism in place the evaluation time was set at the beginning of the run.

There are several parameters in the model that are optimised in different ways. Root distribution and the maximal electron transport capacity (J_{max}) are allowed to adapt dynamically during a model run, while ce, me, c_{RI}, J_{maxtop} and phenology were optimised off-line, before the actual model runs, to minimize the error between fluxdata and model output. The parameters stated in the model description section are either constants, calculated from other parameters and some are dependent on the site. A full list of parameters used in this research project can be found in Appendix 1. The parameters that were changed for use in the different sites are explained in table 1.

Table 1: *Site specific input parameters for both the Hainich and Peyne area with their respective values, units and reference.*

Symbol	Description	Units	Hainich	Reference	Puechabon	Reference
avG	empirical van Genuchten parameter	m-1	1.27	Schaap *et al.*, 1998	1.29	Schaap *et al.*, 1998
H_a	rate of exponential increase of Jmax with temperature	J mol-1	71.38*10^3	Medlyn *et al.*, 2002	35.87*10^3	Medlyn *et al.*, 2002
H_d	rate of decrease of Jmax with temperature above Topt	J mol-1	200*10^3	Medlyn *et al.*, 2002	200*10^3	Medlyn *et al.*, 2002
Icap	maximum interception capacity	m	0.0005	Brolsma, 2010	0.00034	Vink & Oerlemans, pers. com. 2010
K_{sat}	saturated hydraulic conductivity	m s-1	8.217*10^-6	Schaap *et al.*, 1998	1.457*10^-6	Schaap *et al.*, 1998
LAI_{max}	maximum leaf area index	m2 m-2	5	Knohl *et al.*, 2003	3	Papale *et al.*, 2006
L_l	local longitude	degree	10.452	CarboEuropeIP	3.595833	CarboEuropeIP
LL	leaf life span	months	5.21	Glopnet	7.46	Glopnet
LMA	leaf dry mass per area	g m-2	2.18	Glopnet	2.29	Glopnet
nvG	empirical van Genuchten parameter	-	1.38	Schaap *et al.*, 1998	1.28	Schaap *et al.*, 1998
RAI_{max}	maximum root area index	m2 m-2	1.8*LAImax	Gansert 1994	1.8*LAImax	Espelta *et al.*, 2005
theta	geographic latitude	degree	51.0793	CarboEuropeIP	43.74139	CarboEuropeIP
θ_b	residual water content	m3 m-3	0.102	Schaap *et al.*, 1998	0.081	Schaap *et al.*, 1998
θ_s	saturated water content	m3 m-3	0.536	Schaap *et al.*, 1998	0.441	Schaap *et al.*, 1998

5.3.1. Root distribution

The maximal root area index (RAI) [m^2 root area m^{-2} ground area] was taken as 1.8 times the maximal leaf area index (LAI) based on measurements by Gansert (1994) and Espelta *et al.* (2005) for Hainich and Puechabon respectively. The initial root distribution was modeled as an exponential distribution which places 90% of the total fine root mass in the top 1 m. Soil layers with root mass lower than 0.01 were discarded. The root distribution was reset for each run and is described by equation 52:

$$SAdr(i) = \frac{RAI_{\max}}{b} e^{\frac{-dZ \cdot i}{b}} \quad (52)$$

where b=0.43 [-], $SA_{dr}(i)$ the root surface area density in soil layer i and dZ the thickness of the soil layer. The root depth is then determined by multiplying the deepest soil layer accessed by tree roots with the soil layer depth.

5.3.2. Water storage in plant tissue

The total mass of dry matter (Md) is initially equal to the potential amount of water stored in plant tissues (Mqx), assuming dry matter to be half the weight of plant tissue. Initial water storage (Mq) was assumed 0.998 times potential storage. A reduction in actual water storage of more than 90 percent of the potential water storage was dealt with in the model by reducing LAI. This is in line with the hypothesis stated by Schymanski (2007) that: *"a reduction in water content of living tissues by 10% from the saturated value is reversible, while further reduction in water content may lead to permanent cell damage"*. This hypothesis is supported by observations from Roderick and Canny (2005) and Zweifel *et al.* (2000), who showed that the linear relationship between P_b and stored water only holds for the first 10% of relative water loss. As water gets depleted past the linear stage, stem volume remains constant, while water is removed from the xylem of the stem and replaced by air, a phenomenon in plants and trees also known as hydraulic failure. Thus, in the model Mq should not fall below 0.9*Mqx (where Mqx and Mq are the potential and actual amount of water stored in plant tissues per unit catchment area respectively). The mechanism of LAI reduction in the model can only happen once during a day, although water stress below the critical value may be reached for subsequent hours and water can be lost through the roots if drought persists.

5.4. Off-line parameter calibration

The model was optimised so both carbon and water fluxes matched the measurements as close as possible. The off-line calibration is done using only the meteorological data for the months June, July and August (JJA) for Hainich and March, April and May (MAM) for Puechabon. The optimization is run for this time period until the simulated fluxes are in enough agreement with the observations. The parameters that were optimised with the stochastic optimisation algorithm are ce, me, c_{Rl} and J_{maxtop}. The variables ce and me are unitless empirical parameters that define the functional shape of the relationship between λ (the slope of the curve between A_g and E_t) and h. Because λ is dependent on the available soil moisture within the rooting zone, the following explicit relationship (equation 53) between λ and available soil water is used:

$$\lambda = ce\left(\sum_{i=1}^{irp} h_i\right)^{me} \quad (53)$$

where h_i [m] denotes the soil water pressure head of soil layer i; i = 1,…,n, irp [-] is the deepest soil layer accessed by the tree roots.

The parameters c_{Rl} and J_{maxtop} are considered to be species dependent and their values are subject to calibration. The stochastic optimization is done with the DiffeRential Evolution Adaptive Metropolis (DREAM) algorithm with the minimization between simulation and observations as optimality criteria. The DREAM algorithm that was used for optimisation of these parameters has been described in Vrugt *et al.* (2009) and Ter Braak (2006). The DREAM is a type of Markov chain Monte Carlo method and runs multiple different chains simultaneously for global exploration, and automatically tunes the scale and orientation of the proposal distribution using differential evolution. The algorithm maintains detailed balance and ergodicity and works well and efficient for a large range of problems, especially in the presence of high-dimensionality and multimodality (Vrugt *et al.*, 2009). In this research project, the algorithm is run with 10 different Markov chains and 25,000 model runs. From the DREAM optimization the parameter set with the absolute smallest error was taken and used in subsequent model runs. The parameters were allowed to vary between a range of values that

are given in table 2.

Table 2: *Parameters optimized by the DREAM algorithm and the range between which their optimal value was sought, given by the maximum and minimum values.*

	ce	me	c_{RI}	J_{maxtop}
Minimal	Log10(10)	-3.0	0.005	10
Maximal	Log10(10000)	1.0	0.15	450

Phenology which is derived from the Greek word "phaino" meaning to show or to appear, is the study of plant and animal life cycle events, which are triggered by environmental changes, especially light and temperature. In this case it is used to indicate the appearance (budburst) and fall (senescence) of leaves. Leaf flushing is usually seen as the time between budburst and the full maturation of leaves. For use in the model it is better to take the time between flushing and senescence into account than the time between budburst and senescence, because although the first leaf material is capable of photosynthesis it is unlikely to have a noticeable influence on the measured carbon and water fluxes yet. To optimize phenology, the error between measurements and model outcome was minimized by an unconstrained nonlinear optimization function. The error was weighed for the different components (water and carbon) to take the difference in measurement errors into account. The following equation was used to incorporate the relative weight of the different components:

$$Error = \frac{W_{CO_2}}{W_{CO_2} + W_{H_2O}} \sum_{i=1}^{n} \left(\frac{CO_2{}^m - CO_2{}^s}{\mathrm{M}CO_2{}^m}\right)^2 + \frac{W_{H_2O}}{W_{H_2O} + W_{CO_2}} \sum_{i=1}^{n} \left(\frac{H_2O^m - H_2O^s}{\mathrm{M}CO_2{}^m}\right)^2 \quad (54)$$

where CO_2m, H_2Om, CO_2s and H_2Os are measured and simulated CO_2 and H_2O fluxes respectively, MCO_2m and MH_2Om the mean of the measured carbon and water flux and:

$$W_{CO_2} = \frac{1}{\sigma_{CO_2}} \;\&\; W_{H_2O} = \frac{1}{\sigma_{H_2O}} \quad (55)\&(56)$$

where σ is the error in the measurements, taken as 10% of the outgoing water flux, (latent heat, lE) and 25% of the outgoing carbon flux (Net Ecosystem Exchange, NEE) measurements.

Phenology was simulated using the degree-day method, which is also applied frequently in crop timing and energy monitoring. LAI increases as leaves start to grow when an arbitrary 10 day maximum temperature sum exceeds a threshold which is varied by the optimisation function. At the end of the growing season, when the 10 day maximum temperature sum becomes lower than the second threshold, leaves start to be shed and LAI decreases. Temperature is thus seen as the only factor that determines the onset and senescence of leaves, although solar insolation, day length and other factors have also been suggested to influence leaf flushing. Research by Vitasse *et al.* (2009) for example showed that temperature better explained phenological variations than altitude whatever the variable (flushing, senescence and canopy duration) and the species. They found highly significant linear relationships between flushing dates and spring temperatures for all species (r2 = 0.57, P < 0.0001) although beech had the lowest sensitivity to temperature (-1.9 ± 0.3 days C-1). In autumn, they found a significant and strong relationship between senescence and temperature for oak and beech only, with a delay of 5.6 ± 0.6 days C-1 for beech (r2 = 0.75, P < 0.0001). For beech, the sensitivity of senescence to temperature was more than twice as high as that of flushing (Vitasse *et al.*, 2009). Thus, for senescence is seems more justified to use the temperature dependence then for leaf flushing. However, because the effect of other variables on phenology is relatively unclear the degree-day method with only temperature dependence is used in this research.

5.5. Dynamic optimality approach

The electron transport capacity (J_{max}) was optimised during the simulation to include short-term adaptation of vegetation to its environment. J_{max} has a direct impact on photosynthetic rates (A_g) and daily Net Carbon Profit (NCPd) and is allowed to change dynamically throughout the model runs following the method by Schymanski (2007): The dynamic adaptation was modelled on a daily scale, by computing NCPd for each day using the actual value and

alternative values taken as a specified increment higher and lower than the actual value. The value for J_{max25} on the subsequent day was then set to the value that would have led to the maximum NCPd on the previous day. The daily increment had to be small enough to prevent oscillation between two highly non-optimal states under stable environmental conditions and large enough to allow a quick enough adaptation to seasonal changes in environmental conditions (Schymanski, 2007). This was achieved by setting the daily increment for J_{max25} to 1% of the actual value.

The hypothetical root optimisation strategy proposed in this research project was modelled to achieve maximum NCP for the tree. The assumption that NCP is maximized by vegetation, allows formulating a single objective function accounting for both productivity and "water stress," as water stress has a quantifiable impact on carbon uptake by the reduction of stomatal conductivity (Schymanski *et al.*, 2009). The amount of days after which the achieved NCP with an adjusted root distribution is evaluated, was varied as a parameter throughout the model runs to investigate the possible differences. The amount of fine root mass and its distribution determine the possible root water uptake which has to meet the canopy water demand resulting from evapotranspiration and meteorological conditions. In periods of drought, when canopy water demand is higher than maximum root water uptake and water storage (Mq) decreases, it might be beneficial to let roots in top soil layers die off in order to create new fine root mass at depth. During the daily optimisation up to 5% of the total root mass is removed from the soil layer with the lowest water content and added to another layer that contains roots or as an extension below the deepest soil layer accessed by roots. Utilizing this mechanism could prevent Mq from dropping below the critical value of 0.9*Mqx where a tree is forced to drop leaves to prevent further water losses.

The cumulative NCP over the evaluated time period was compared for the current root distribution and each of the possible other distributions. These other distributions were created by placing the mass taken from the driest soil layer in every other soil layer connected to the current root distribution. For the options where root mass was replaced in a different layer the NCP was reduced because of the costs of creating new root mass. Additionally, the vascular tissue respiration will increase if roots are created below the current root system because this is dependent on the deepest layer accessed by tree roots. The cost of creating new fine root mass at depth is calculated by subtracting the carbon content of the replaced root mass from the final NCP calculated. Root mass was assumed to consist of CH_2O, which has a molecular mass of 40 g mol^{-1}, thus the carbon content is 12/40% of the total root mass. The distribution that results in the highest NCP after the evaluation period is then taken as the new current root distribution and at the next day the optimisation starts again.

5.6. Possibilities for model validation

At the beginning of the research project, several options for model validation were investigated. For both the sites fluxdata measurements are available that can be compared to model outcome, this will be done in the results section. In this section 1) Normalized Difference Vegetation Index, 2) Dendrology, the use of tree rings, and 3) Intermodel comparison are explained and discussed as possible ways to validate this or a similar vegetation growth model.

5.6.1. Normalized Difference Vegetation Index

For the Hainich area regular satellite images are made from which, for example Normalized Difference Vegetation Index (NDVI), measurement data can be extracted for several applications of which one is model validation. The NDVI is calculated from the visible and near-infrared light reflected by vegetation. Healthy vegetation absorbs most of the visible light that comes in and reflects a large portion of the near-infrared light. Unhealthy or sparse vegetation reflects more visible light and less near-infrared light. Unhealthy brown leaves are observed during autumn and prolonged drought and should be seen in the NDVI measurements. The numbers in figure 3 are representative of actual values, but real vegetation is much more varied.

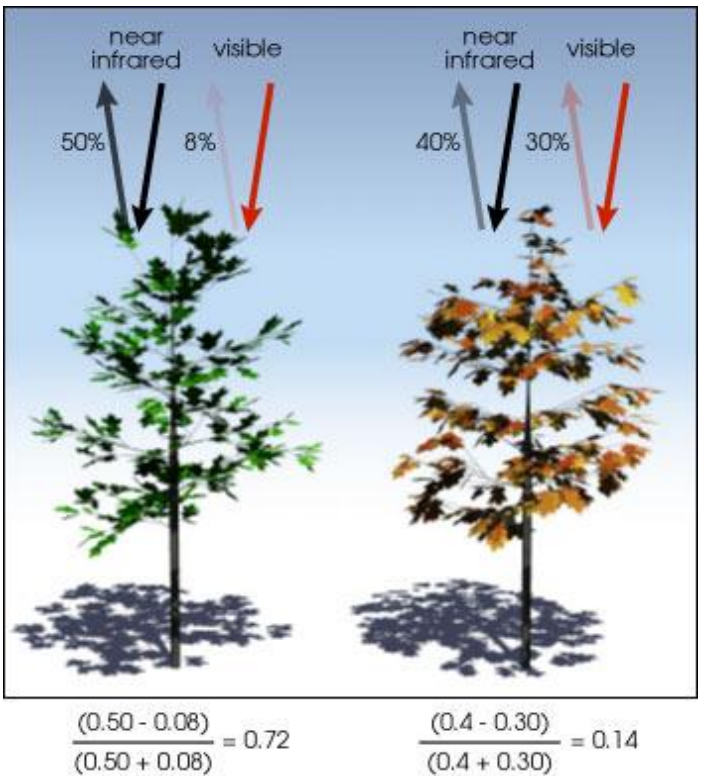

Figure 3: *NDVI calculations of healthy (left) and unhealthy (right) vegetation (Illustration by Robert Simmon).*

NDVI data were compared for the years 2003 to 2005 because the model will be run for these years. The results can be seen in figure 4 which shows no clear difference for the year 2003 assuming the sudden drops of 0.5 in all the data are measurement errors. A difference in 2003 was expected due to the extreme drought event that occurred in Europe. Ciais *et al.* (2005) for example estimate a 30 per cent reduction in gross primary productivity over Europe caused by the heat and drought in 2003. If the timing of the reduction in leaf health or brown color could have been seen, it would have been a potential validation for the model. If the timing of the models reduction in LAI would have been simultaneous with a reduction in NDVI, this would have strengthened believe in the correctness of the models water balance, water storage and vegetation dynamics. Unfortunately no such effect could be seen in the measurements and the NDVI data could not be used to validate the timing of leaf browning and LAI reduction.

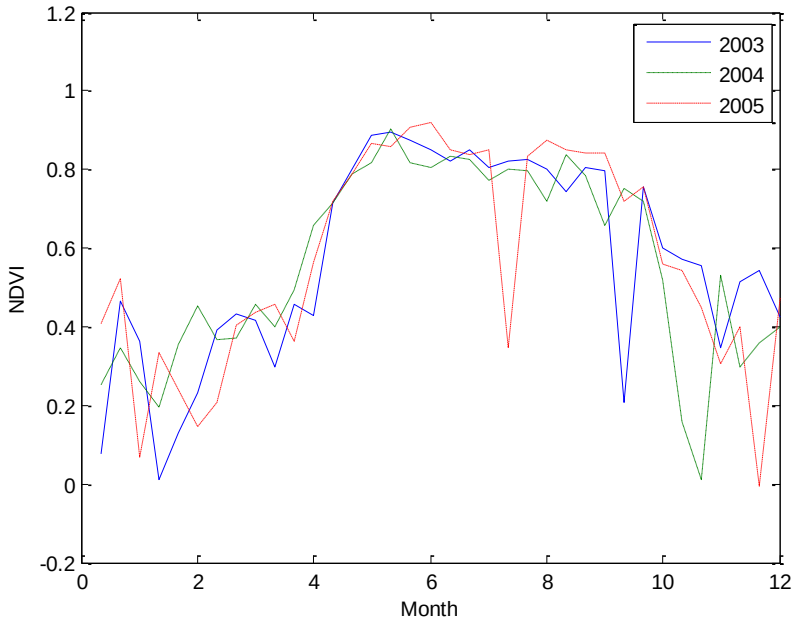

Figure 4: *Normalized Difference Vegetation Index (NDVI) for Hainich National forest extracted from the 10 day data set of the "VEGETATION" programme (W. Immerzeel, personal communication, 2009).*

5.6.2. Dendrology

Tree rings are traditionally used to estimate the age of trees. Their yearly stem growth or the diameter increment of the stem can also be used to assess the environmental conditions in which the growth took place. In *Quercus Ilex* (an evergreen Mediterranean oak species) for example, drought reduced the stem diameter increment of 53% for large trees (Ogaya *et al.*, 2003). Meteorological data and soil moisture measurements or simulations are used to estimate the annual increase in stem diameter and tree ring width. However, it has been reported that the annual variation of measured values exceed the annual variation of model simulation results of stem increments within a 5 years interval (Jochheim *et al.*, 2009). In other words, the measurements are noisier than the variability in stem growth as predicted by a simulation model. This suggests that tree ring variability may not be correlated to the meteorological forcing used in the model. However, process-based models have achieved considerable success with simulating tree-ring variability when driven by daily meteorological data (Hughes *et al.*, 2004). Drought is expected to have a stronger effect on the ring growth of large trees as they are more dependent on water availability, while photosynthesis in shorter trees and other vegetation is more limited by light. Even in low forest stands, mortality in Quercus Ilex trees was significantly ($p = 0.05$) higher under drought (Ogaya *et al.*, 2003).

In a recently published study by Van der Werf *et al.* (2007) the growth patterns of beech and oak in the Netherlands were compared focussing on the extreme drought in the summer of 2003. The results indicate that oak and beech reacted differently during the drought, as wood formation in both species ceased, but in beech it recovered after the drought. Generally there is a positive correlation between radial stem growth and precipitation. However, the two species differ in their response to weather changes during the growing season and the initial spring soil moisture conditions are relatively more important. Good starting conditions lead to the formation of a wide tree ring, even if conditions later in the growing season are unfavorable, as was the case in 2003. Good starting conditions are mainly defined by a high amount of available reserves stored at the end of the previous growing season. Unfavorable starting conditions occur, however, if the conditions during the previous growing season limited growth: the summer drought in 2003 resulted in a lower growth rate in 2004, even though weather conditions in 2004 were favorable. This can also be explained by a reduction of the trees internal carbon storage and the carbon starvation that has occurred during the previous year. The temperature effect is less consistent, but the results from this study show that the growth of both species is negatively correlated with the temperature of the previous summer (in July and August). This correlation indicates that a high summer evapotranspiration rate might reduce the amount of available reserves. Neither of the species formed an unusually small ring in 2003. The implication is that summer drought did not seriously affect the diameter growth of the oaks and beeches in The Netherlands. Yet one Europe-wide study has reported a large reduction in primary productivity in the summer of 2003 (Ciais *et al.*, 2005). This could lead to substantial problems when trying to relate meteorological variables to stem growth as daily data has an insignificant influence, compared to the conditions of the previous year. The unresponsiveness of the tree ring width to drought could potentially also be attributed to a mechanism that allows trees to maintain their evaporation by utilizing deeper water under conditions of low soil moisture. There have for example been observations that daily peak values of sap flow remained surprisingly constant over the whole drought period in the summer of 2003 in *Quercus petraea* and decreased to only about half of the early summer maxima in *Fagus sylvatica* L. (Leuzinger *et al.*, 2005).

5.6.3. Tree ring data Puechabon

For the Puechabon area the possibility existed to compare the model results with tree ring data collected in the Mediterranean *Quercus Ilex* forest surrounding the river Peyne. For this reason, rings were counted for 20 Q. Ilex trees from the region and correlated to meteorological data. The trees were sampled in the summer of 2007 and 2009 and the rings were counted using the software CDendro7.1 developed by Ed Weiss. Q. Ilex is an oak species that is relatively well adapted to drought and the dry summers of the Mediterranean climate. Still Ogaya et al. (2002) show a 55% reduction in growth rate as a response to drought for Q. ilex in a holm oak forest in NE Spain. This reduction should also be seen in radial expansion of stem diameter.

Translating NCP to stem diameter increment is cumbersome and was outside the scope of this research project. But the relative similarity of a decrease in stem growth and NCP during the drought of 2003 for example can be indicative of the correctness of the model. However, there are some factors that bring uncertainty into the tree ring results. Q. Ilex trees produce a very dense wood structure (Figure 5) in which the xylem vessels produced in spring, often used for ring counting, are hard to distinguish. Additionally, local influences like forest fires, insect outbreaks and death or clearing of nearby trees can leave marked impact on the stem growth. Furthermore, the pronounced radial rays and often inconcentric shape make it harder to accurately position the rings and determine the ring width. Finally, false rings, that look just like true rings, can be produced during a year of extreme environmental variation. Still, tree ring records can be very valuable to reconstruct past climate and are often used in research.

Figure 5: *Cross-section of a Quercus Ilex tree from the Peyne area in Southern France cut in 2008 showing the growth rings and radial rays.*

The radial expansion of tree trunks is often approximated by formula (equation 57), taking into account the different factors that have an influence on growth:

$$R_t = A_t + C_t + \delta D1_t + \delta D2_t + e_t \quad (57)$$

where R is Radial Growth, A the Aging effect, C the Climate effect, D1 the Forest internal disturbance (tree fall), D2 the Forest external disturbance (Pollution, Insects) and e any other unexplained factors. The tree ring records used in further analyses were corrected for the aging effect, but internal and external forest disturbances and other unexplained factors can potentially have a large influence on ring width next to the climate variability with which correlations are sought. The cross-section disks were counted in two directions to reduce the chance of missing rings or including false rings into the data. Rings were counted where a sharp transition in colour, density and amount of vascular vessels could be seen.

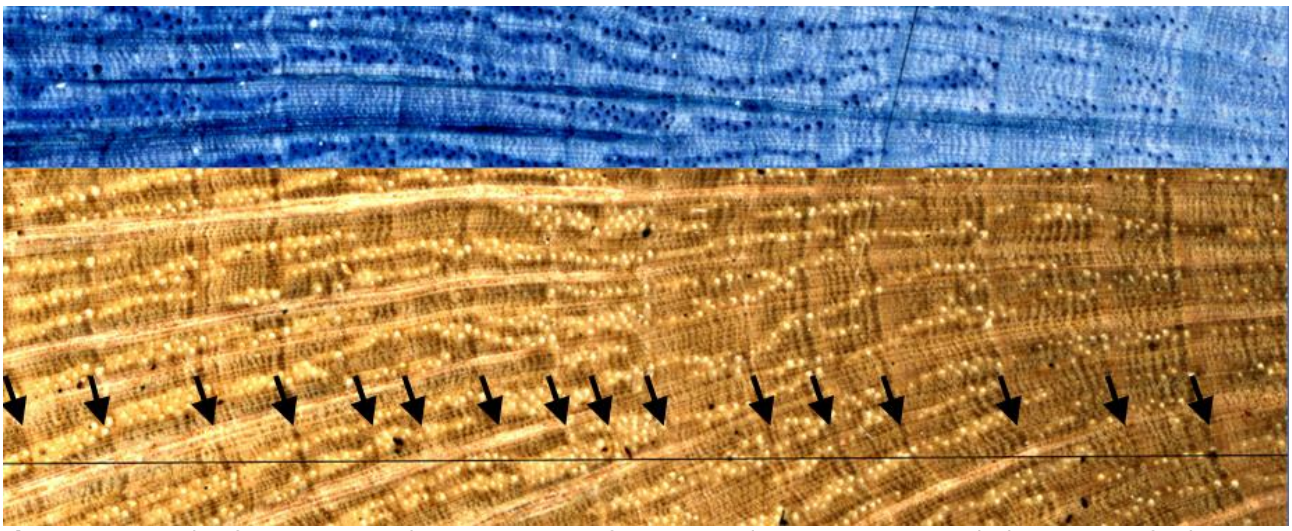

Figure 6: *Example of ring counting the cross-section of a Quercus Ilex tree; arrows mark the position of subsequent tree rings.*

The tree ring data was used to find correlations between ring width with temperature (figure 7) and precipitation (figure 8) respectively. A moderate positive correlation between ring width and temperature was found in winter, where an increase in temperature leads to an increase in ring width. This could be explained by limitation of biological processes such as enzymatic activity, nutrient uptake and photosynthesis at low temperatures, leading to growth reduction. In both summer and autumn tree ring width is moderately negatively correlated with temperatures. High temperatures can lead to leaf death when stomata are closed because insufficient moisture is available to keep transpiration going and cool the leaves. This limitation on tree growth by temperature is indirectly included in the model in the reduction of LAI when the water storage drops below the critical value. A forced reduction of leaf area limits the maximum photosynthesis that can take place when moisture is no longer limiting. Knowledge of the correlations between climatic variables and ring width can be used to compare specific model outcome to explore whether dominant processes are taken into account. Another mechanism that could explain the negative correlation is the increase of leaf (and woody tissue) respiration, reducing the total carbon gain and thus stem diameter increase.

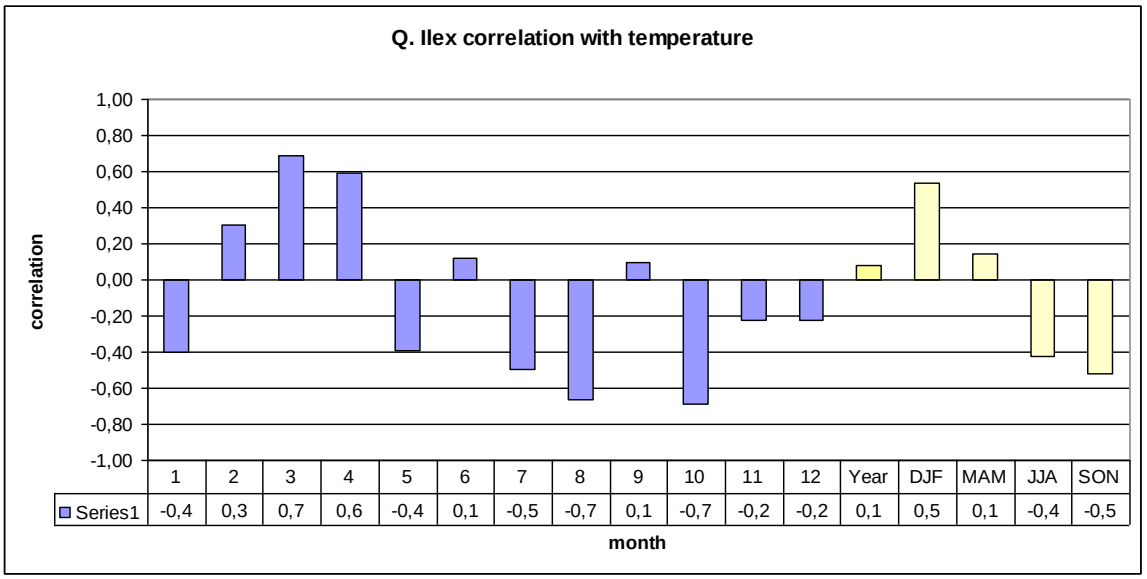

	1	2	3	4	5	6	7	8	9	10	11	12	Year	DJF	MAM	JJA	SON
Series1	-0,4	0,3	0,7	0,6	-0,4	0,1	-0,5	-0,7	0,1	-0,7	-0,2	-0,2	0,1	0,5	0,1	-0,4	-0,5

Figure 7: *Correlation of Quercus Ilex tree ring width and temperature for 2000-2008 in the Puechabon area. Blue, yellow and light yellow bars give the monthly, yearly and seasonal correlation respectively (W. Nijland, personal communication, 2010).*

For precipitation weak correlations were found in winter and spring and a strong correlation with summer precipitation was found. Apparently an increase in summer precipitation will lead to an increase in photosynthesis and radial expansion of the stem. A summer drought, such as

the 2003 event, should thus lead to a reduction in ring width and modelled NCP.

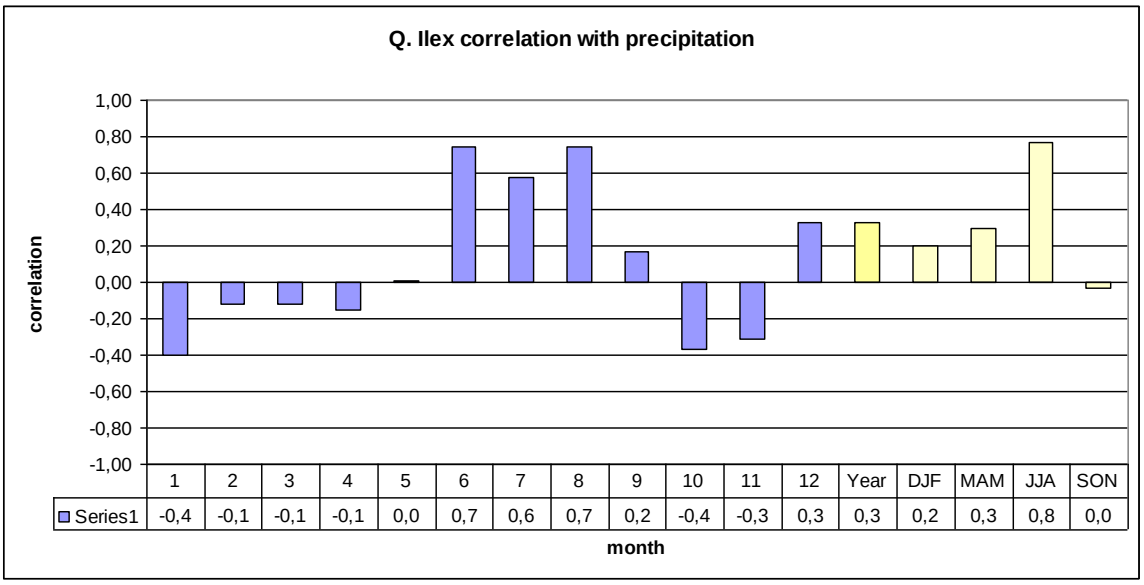

Figure 8: *Correlation of Quercus Ilex tree ring width and precipitation for 2000-2008 in the Puechabon area. Blue, yellow and light yellow bars give the monthly, yearly and seasonal correlation respectively (W. Nijland, personal communication, 2010).*

Judging the results from the correlations with precipitation and temperature, it seems likely that the extreme drought event with high temperatures in 2003 would have left an impression on tree ring width. The results (figure 9) on average show a slight reduction in ring width that continues into 2004. Caution should be taken with the results for the last two years as very few data are available (n=11). The trees that show a more pronounced reduction in radial expansion during 2003 are those growing on clay rich, stony soils on a schist bedrock (H2). This is surprising as clayey soils are be able to retain a higher moisture content than a more sandy soil such as dolomite (J2). The trees growing on limestone (E0) have on average smaller rings in 2004 than in 2003, possibly indicating that drought affects the growth in the next year as well if insufficient rain has fallen during the winter to fully replenish the trees and soil water supply.

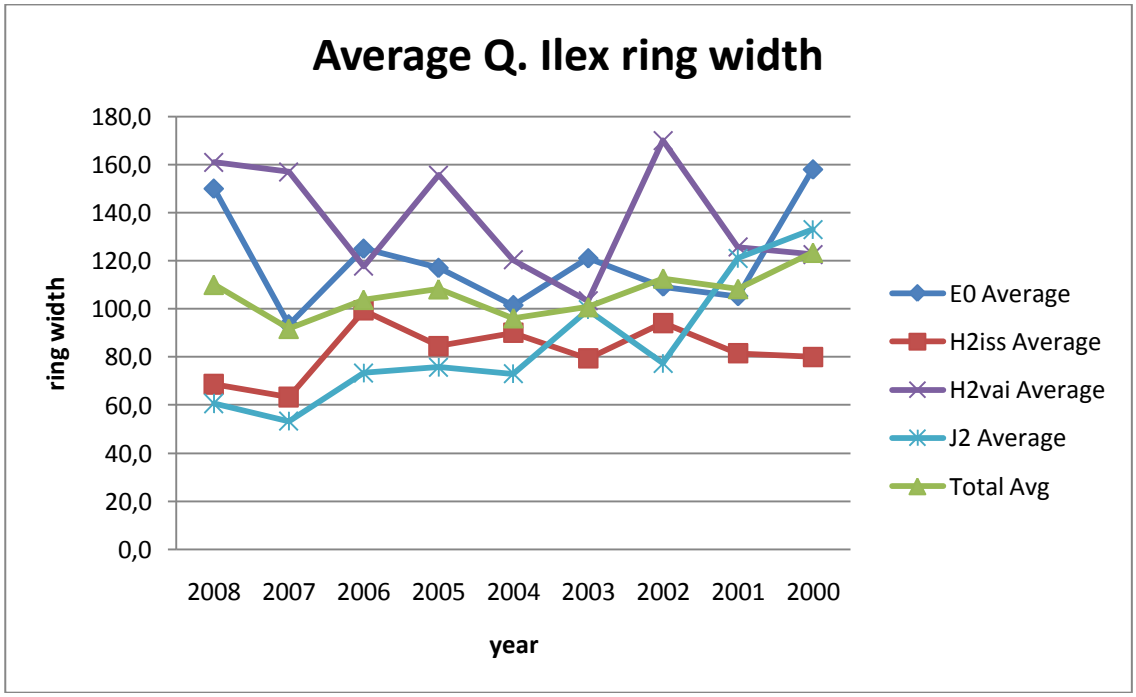

Figure 9: *Average detrended yearly ring width for Quercus Ilex trees from the Puechabon region for different soil types. J2 = Dolomite, E0 = Limestone, H2 = Schist; the additions vai and iss are indicative for the region: vai = Vailhan, east of barrage d'olivettes, iss = Foret d'issaerts, west of barrage d'olivettes.*

5.6.4. Inter-model comparison

Finally, as a validation tool, the model outcome could be compared to other eco-hydrological models that have been developed. The model by Schymanski *et al.* (2007; 2009) that has been the basis for many of the processes and formulations of the developed model, for example, is relatively easy to adjust for different sites and can be run with fluxdata or REMO regional climate model data from the Max Planck Institute for Meteorology. The latest version of this Coupled Water Balance and Vegetation Optimality Model (VOM_0.2) has also been run for both the Hainich and Puechabon (figure 10) region, but did not produce satisfying results (S. Schymanski, personal communication, 2010). The model predicts vegetation water use based on meteorological information, soils and topography only, without the need for prescribing site-specific vegetation properties or calibration against observed fluxes which has been done for some of the parameters that were used in the model that was designed during this project. The VOM model uses the Shuffled Complex Evolution (SCE-UA) global optimization algorithm to optimize vegetation properties for NCP under given environmental conditions from the meteorological input data. For the Puechabon region, the difference between modelled and measured evapotranspiration is large because ET is consistently overestimated by the model. Such as consistent overestimation of one of the fluxes could not occur in the model results for this project because the models parameters were optimized to minimize the difference between simulations and observations. The VOM_0.2 however was only optimised to maximise biological fitness with a focus on NCP.

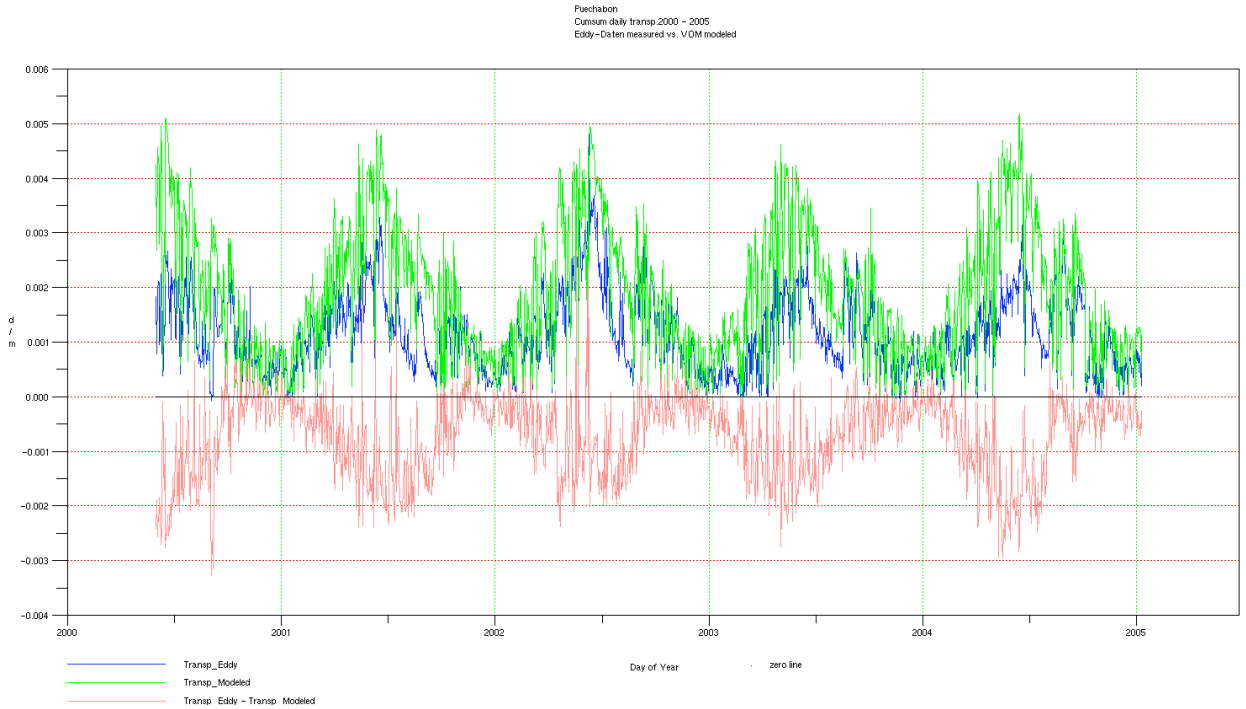

Figure 10: *Comparison of the daily Vegetation Optimality Model 0.2 (green) and evapotranspiration measurements (blue) for the Puechabon area. The red line shows the difference between model and data [m d^{-1}] (S. Schymanski, personal communication, 2010).*

6. Model development

In the following chapter the model simulations are directly with the discussion of these results as this allows for better understanding of the development of the model. Since some changes in the model were made as the simulations progressed and different critical points revealed themselves. The actual results for the model runs of the years 2003-2007 and the simulations in the year of the extreme drought (2003) with the hypothetical root mechanism in place will not be discussed until the next chapter. The current model deals with the optimization and validation of the model and discusses some adjustments that were made because the model needed to be improved after the initial results were produced.

This chapter first of all shows the results of the DREAM optimization for both the Hainich and Puechabon region for the off-line parameter calibration. Since the simulations for both regions, that are shown in paragraph 2, were not satisfying some adjustments to the model were made. These adjustments are discussed in paragraph 3, but were only incorporated for the model at the Hainich site and further simulations for the Puechabon region are omitted. Paragraph 4 shows the results for the summer months for which the model was calibrated and validates that the model simulations are in good agreement with the observations. The same paragraph discusses the dynamics of the root water uptake flux (Qr). Next, in order to simulate yearly fluxes, it was necessary to optimize the degree-day thresholds for the increase and decline of LAI. This was done in paragraph 5 which gives the models final parameter settings to be used in the subsequent runs.

6.1. DREAM optimization

The species dependent parameters c_{Rl} and J_{maxtop} and the parameters that determine the relationship between λ and h(i) were optimised off-line with the DiffeRential Evolution Adaptive Metropolis (DREAM) algorithm (Vrugt *et al.*, 2009). Optimization of some parameters is a relatively standard procedure as nearly all coupled eco-hydrological models contain parameters whose values cannot be measured directly in the field, but can only be derived through calibration against site-specific output data. However, the validity of these models outside the range of measurements for which they have been calibrated cannot be guaranteed (Schymanski *et al.*, 2008a). The model was calibrated for the summer months June, July and August (JJA) 2005 for Hainich and the spring months March, April and May (MAM) 2005 for Puechabon. The year 2005 was chosen for calibration as it presumably is an average year in the proximity of the extreme drought in 2003. The year 2004 was not used because drought can have a prolonged effect on tree growth into the next year and in some regions abnormal weather ware observed in 2004 as well. During the calibration of the parameters, LAI was kept constant at its maximum value, corresponding to observations and assumed the most profitable for this time of the year. The mechanism of decreasing LAI under drought was therefore not activated yet as LAI was assumed to be maximal in the average year of 2005 and should not show a reduction. Output of the DREAM optimization for Hainich is shown in figure 11 and 12. The strong correlation between ce and me indicates that the relationship between λ and h could be simplified using only a single calibration parameter. The parameter me has two optimal values, which are dependent on the value of ce. The optimal values of ce are close to the upper and lower limit of the range specified for the algorithm. The parameters c_{Rl} and J_{maxtop} on the contrary still fluctuate in the entire range of the parameter space and have not converged to a single optimal solution towards the end of the optimisation. This shows that there are multiple parameter sets for which the model behaves similarly and there is no single best parameter set that gives a much better fit. The chosen optimal values are now simply those from the run with the smallest absolute difference between observations and simulations.

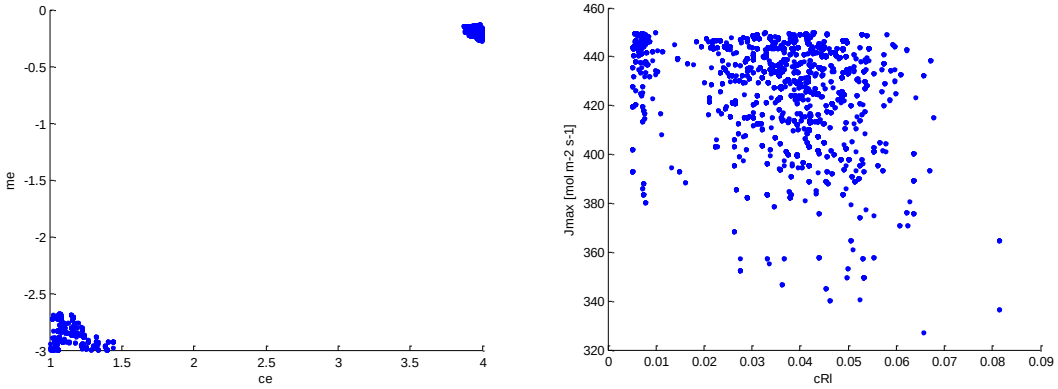

Figure 11: *Scatter plots showing the range of (left) me and ce (empirical parameters defining water use efficiency) with a Pearson correlation of r = 0.9965 and (right) c_{Rl} (leaf respiration coefficient) and J_{maxtop} (electron transport capacity at the top of the canopy) with a Pearson correlation of r = -0.2627 during the final 5000 runs of the DREAM optimization for the Hainich site.*

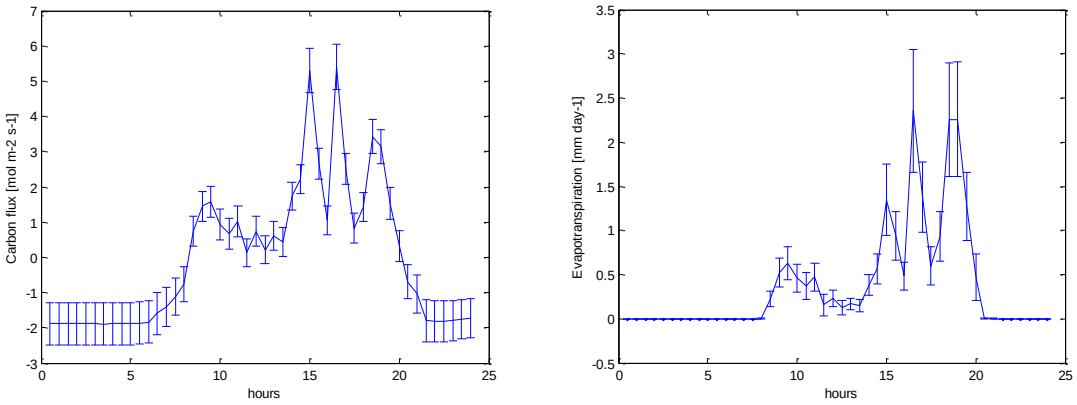

Figure 12: *Mean and standard deviation of the simulated carbon flux (left) and evapotranspiration (right) in the last 100 runs of the DREAM optimization for Hainich on 06/07/2005.*

Similar results, with a little more fluctuation in ce and less in J_{maxtop} and c_{Rl}, were found for the calibration of the model for the Puechabon site (figure 13 and 14). The scatter plot between J_{maxtop} and c_{Rl} shows more clearly that there are several values for c_{Rl} for which J_{maxtop} has a constant value of 20 mol m^{-2} s^{-1}.

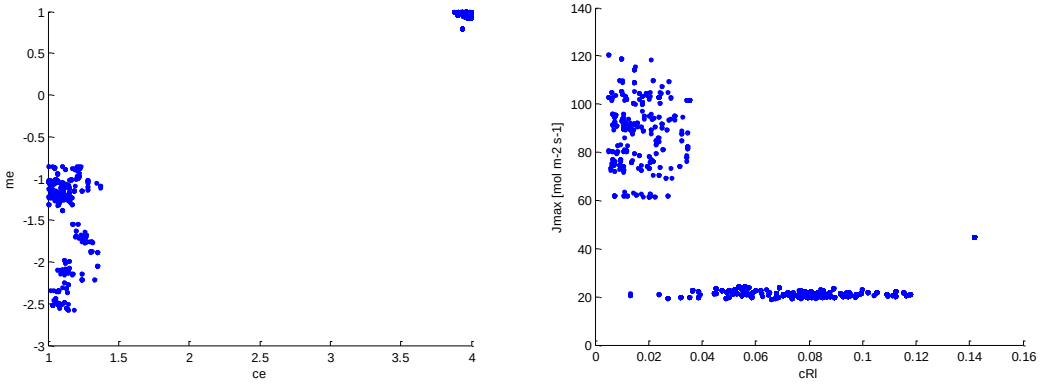

Figure 13: *Scatter plots showing the range of (left) me and ce (empirical parameters defining water use efficiency) with a Pearson correlation of r = 0.9701 and (right) c_{Rl} (leaf respiration coefficient) and J_{maxtop} (electron transport capacity at the top of the canopy) with a Pearson correlation of r = -0.3848 during the final 5000 runs of the DREAM optimization for the Puechabon site.*

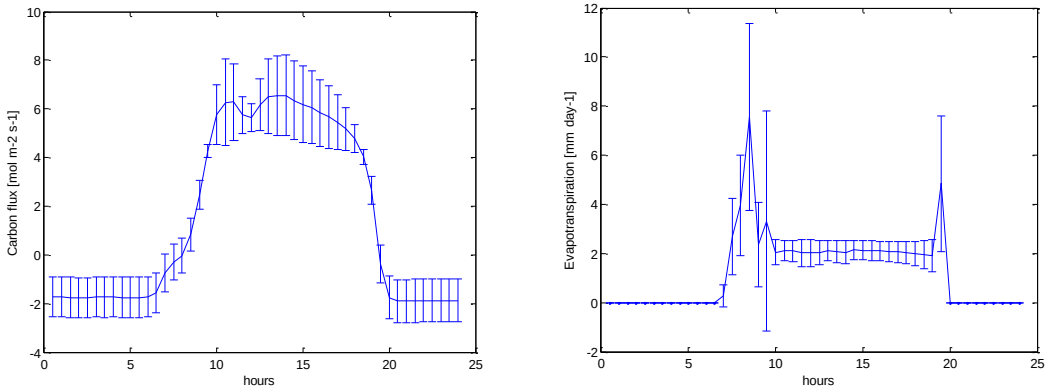

Figure 14: *Mean and standard deviation of the simulated carbon flux (left) and evapotranspiration (right) in the last 100 runs of the DREAM optimization for Puechabon on 17/04/2005.*

The simulated carbon fluxes and evaporation for Hainich and Puechabon, figure 12 and 14 respectively, are highly fluctuating during the day, but a clear distinction can be made between night- and daytime. The model results for evapotranspiration have a larger standard deviation than the modeled carbon fluxes, possibly indicating a less robust water balance simulation. The results for the different parameters from the DREAM optimization can be found in table 3 and 4 for Hainich and Puechabon respectively. The initial range of the parameters, between which they are allowed to fluctuate, is given together with the minimal and maximum values that were used in the 5000 final runs of the DREAM optimization. This is done to allow evaluation of the convergence in the parameter space utilized by the optimization algorithm during the final runs. This can be seen for both c_{Rl} and J_{maxtop} in the Hainich as well as the Puechabon site. Notice the difference in NCP between the mean and best run of the DREAM optimization. The mean is simply the average of the minimal and maximum values that were used during the final runs of the optimization, while best give the values for the run with the smallest difference between observations and simulations. The NCPmax values were selected by taking the run with the highest value for NCP from the final 100 runs of the optimization as the solution was expected to converge and the best solution to be found in one of the final runs. For the Hainich site it seems like a totally different parameter set was selected for the best run and the one with maximal NCP values, judging from the values of ce and me, which are highly correlated. In the Puechabon outcome a very small change in parameter values (between the best and maximal NCP runs for example) leads to a large difference in the model's outcome. The model thus seems to be very sensitive to the parameter setting and is not very robust.

Table 3: *Initial range and results for the last 5000 runs of the DREAM optimisation of the parameters me and ce (empirical parameters defining water use efficiency) and c_{Rl} (leaf respiration coefficient) and J_{maxtop} (electron transport capacity at the top of the canopy) for the Hainich site.*

	Initial range		**DREAM optimization**				
	Min	**Max**	**Min**	**Max**	**Mean**	**Best**	**NCPmax**
ce	1	4	1.002	4.000	3.695	4.000	1.062
me	-3.0	1.0	-2.999	-0.125	-0.475	-0.225	-2.994
c_{Rl}	0.005	0.15	0.005	0.081	0.035	0.032	0.007
J_{maxtop}	10	450	327.208	449.983	427.919	442.048	441.456
NCPtot			21.761	-80.405	23.281	10.207	24.256

Table 4: *Initial range and results for the last 5000 runs of the DREAM optimisation of the parameters me and ce (empirical parameters defining water use efficiency) and c_{Rl} (leaf respiration coefficient) and J_{maxtop} (electron transport capacity at the top of the canopy) for the Puechabon site.*

	Initial range		**DREAM optimization**				
	Min	**Max**	**Min**	**Max**	**Mean**	**Best**	**NCPmax**
ce	1	4	1.000	4.000	3.675	3.978	3.990
me	-3.0	1.0	-2.569	1.000	0.712	0.976	0.981
c_{Rl}	0.005	0.15	0.005	0.142	0.078	0.073	0.082

J_{maxtop}	10	450	19.214	120.661	30.361	20.873	20.595
NCPtot			-13.367	-67.803	-4.827	-8.891	9.439

6.2. Simulations after DREAM optimization

Next, the resulting parameter sets were used to run the model to compare the model output with actual measurement fluxes of water (H_2O) and carbon (CO_2) at both sites. These runs, shown in figure 15 and 16 for the Hainich and Puechabon site respectively, were conducted for the same period as the off-line parameter optimization to calibrate the model.

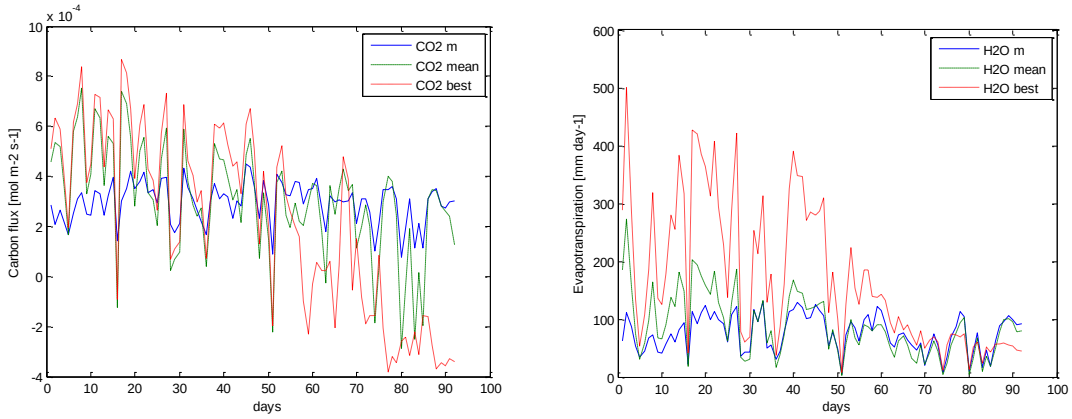

Figure 15: *Daily sum of the measured (CO_2m) and simulated carbon flux (left) and evapotranspiration (right) in the months JJA using the mean and best parameter sets from the DREAM optimization for Hainich.*

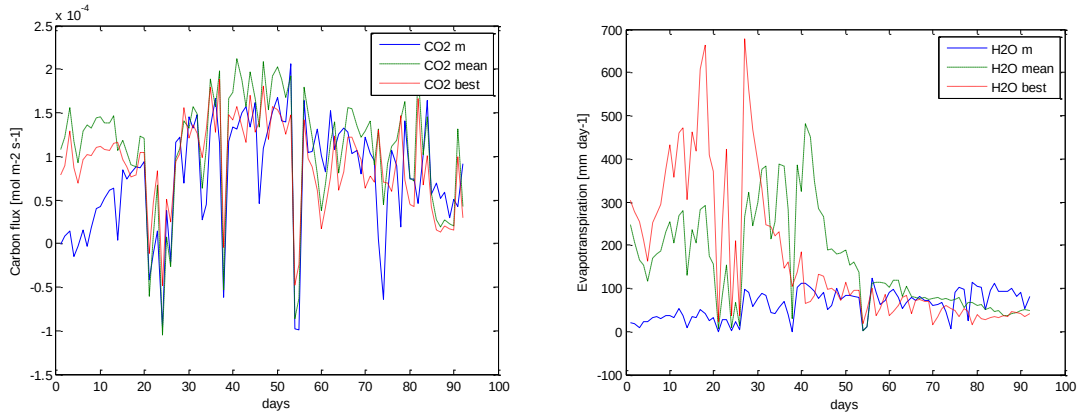

Figure 16: *Daily sum of the measured (CO_2m) and simulated carbon flux (left) and evapotranspiration (right) in the months MAM using the mean and best parameter sets from the DREAM optimization for Puechabon.*

The results do not show a good match between the simulated and measured fluxes, especially for evapotranspiration. Except for an initial mismatch between carbon flux results in Puechabon, the model adequately simulates photosynthesis and respiration. The difference in fluxes in the first 20 days could result from a natural incomplete vegetation cover in the beginning of spring where a full vegetation cover was already simulated by the model. For the Hainich site the model captures the dynamics of carbon throughout the simulation and shows peaks were these can also be seen in the measurements. Evaporation however is not captured well by the model and does not even resemble the measured dynamics for the Puechabon site. An initial difference in fluxes could be explained from the soil moisture initialization used in the model. The difference in simulations resulting from the initialization of the soil moisture content was therefore tested and the results can be seen in the model validation section. The difference between simulations due to the initial soil moisture content does not last for more than about a month and cannot explain the large differences compared to simulated values throughout the rest of the model run. Thus the models current set of equations is not able to produce realistic results. This deviation could result from missing processes, separate processes that were not coupled correctly, unrealistic parameter values or inability of some of the equations to perform well under the conditions at the chosen sites. Since it is not easy to

figure out what the causes and effects are in a multifactoral problem, the model was simplified, excluding or changing several processes. The resulting outcome was evaluated for single changes in variables/factors to pinpoint the models weaknesses.

6.3. Model adjustments

First of all, to test the robustness of the model and because of the large differences in simulated and measured evapotranspiration, the models representation of root water uptake, water storage and consequently water loss were simplified. Root water uptake was assumed to be equal to the water lost through transpiration at every time step, this is an assumption more often made in (eco)hydrological models (e.g. Vincke and Thiry, 2008) since water uptake and loss have to be equal over longer periods. Thus the original resistivities and tissue water balance pressure, used to calculate root suction head and water uptake, were omitted from the model. This also removed the need to calculate water storage and update tissue water content. Root water uptake from the different soil layer was modeled relative to the amount of fine root mass present in each of the soil layers. The model was again optimized with the DREAM algorithm to get the best fit with the measured carbon and water fluxes. The fit of the final mean fluxes (figure 17) compared to the measurement data did not improve much, but the deviation between the different runs increased a lot, because of the sensitivity of ET to meteorological parameters. The deviation between the different runs can be evaluated through the standard deviation, plotted as arrow bars, showing the range of different outcomes.

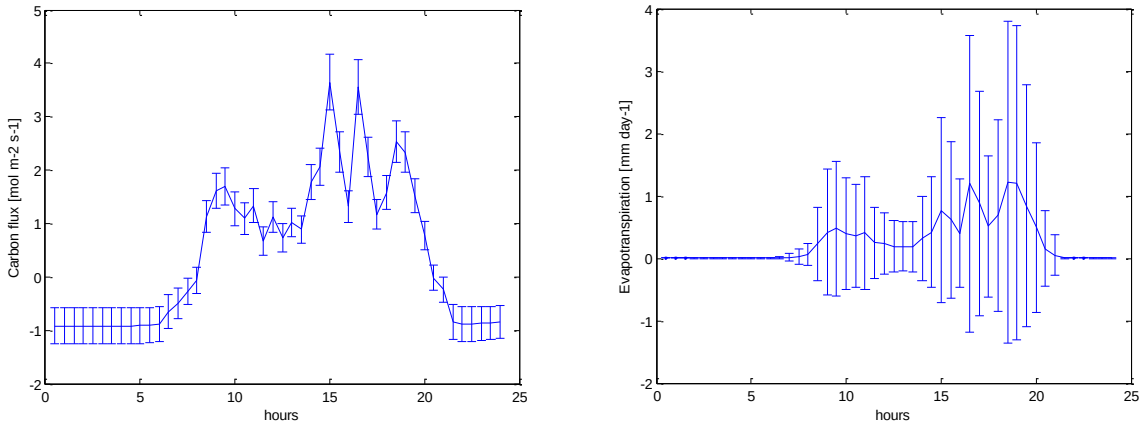

Figure 17: *Mean and standard deviation of the simulated carbon flux (left) and evapotranspiration (right) in the last 100 runs of the DREAM optimization for Hainich on 06/07/2005.*

It was expected that such a simplification and drastic change in the trees internal water circulation and storage would have a noticeable impact on the results. This was not the case however, and it neither improved the simulations nor the realism of the representation, but only lead to a larger spread in modeled evapotranspiration fluxes. The simplification was therefore not retained in consequent model runs.

Secondly, the difference between initializing the models soil moisture at field capacity compared to steady-state soil moisture was investigated to explore the influence of initializing at higher soil moisture has on the model results and the influence on carbon fluxes. The soil in the model was assumed to be homogenous, thus every soil layer had the same depth, saturated hydraulic conductivity, porosity, Van Genuchten parameters and consequently soil moisture at field capacity. Field capacity was calculated at a matrix head of h=-2m. Running the model for the summer in Hainich while using the final water saturation degree at the end of the run as the initial conditions for the subsequent run, led to a near steady-state situation in all of the modeled water fluxes. Since the dynamics of the systems were well retained under lower initial conditions , the final water saturation degree was saved and used in further JJA runs of the model. The lower initial soil moisture content is expected to be in better agreement with the natural situation where the soil moisture at any moment in time is the result of previous rainfall and continuous hydrological processes such as runoff, percolation and evaporation.

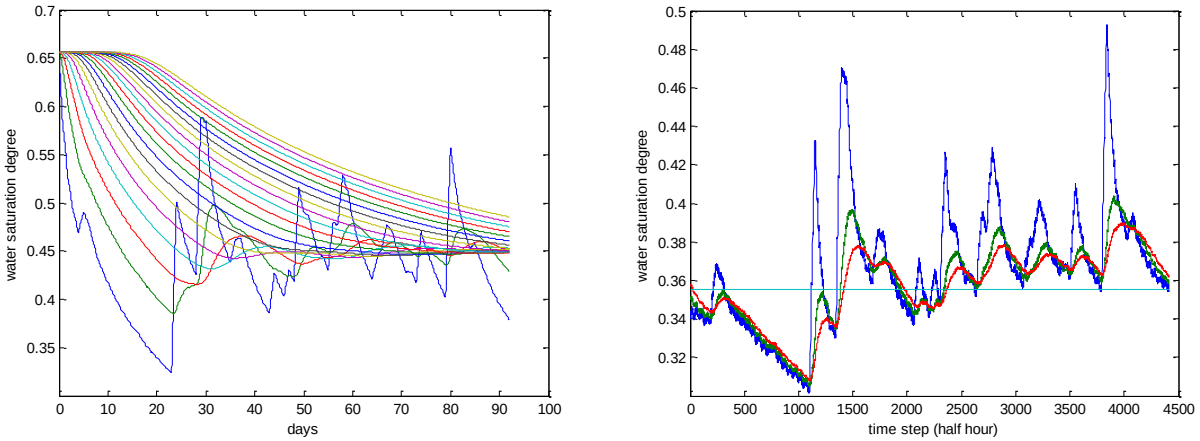

Figure 18: *Water saturation degree during JJA at the Hainich site with initial soil moisture at field capacity (left) for all 20 soil layers and in an equilibrium situation (right) for the top most 3 and deepest soil layers.*

Thirdly, the waterbalance of the model was studied to locate any missing dynamics, sources or sinks in the model. The waterbalance is closed when all water that comes into the model is either stored in the different compartments at the end of the run or has left the model, in this case either as percolation or evapotranspiration. Water enters the model in the form of precipitation (Qrain), which infiltrates into the top soil layer (Qin(1)). From the top soil layer water can either infiltrate into deeper soil layers, be evaporated or taken up by the tree roots. Water from the deepest soil layer leaves the model as it percolates to the ground water (Qout). Root water uptake by the tree (Qr) can temporarily be stored in the tree trunk but should eventually be used during photosynthesis and lost through transpiration. If the water balance is closed in the model, the incoming flux (Qrain) should be equal to the sum of the outgoing evapotranspiration (ET) and percolation fluxes. With constant LAI, as it is in the 3 month runs for optimization, the precipitation reaching the forest floor and entering the model is the same in every model run. The outgoing fluxes vary slightly over model runs, but the overall waterbalance is near zero and strengthens confidence in the modeled hydrologic dynamics.

Table 5: *Results for the final 10 runs of 100 runs with the Hainich model using the calculated soil moisture as input for the next run. Showing the balance between fluxes into and out of the model both with and without taking into account the water storage in the tree trunk.*

Run	Qin	Qout	ET	Water imbalance	Qr	Esu	ET-Esu-Qr
91	669.71	36.40	633.94	-0.09%	430.83	203.14	-0.02
92	669.71	36.39	633.90	-0.09%	430.71	203.14	0.05
93	669.71	36.37	633.86	-0.08%	430.44	203.14	0.28
94	669.71	36.33	633.86	-0.07%	428.43	203.14	2.30
95	669.71	36.29	634.06	-0.10%	429.35	203.14	1.57
96	669.71	36.25	634.16	-0.11%	428.93	203.14	2.09
97	669.71	36.21	634.30	-0.12%	429.92	203.14	1.25
98	669.71	36.17	634.34	-0.12%	431.26	203.14	-0.05
99	669.71	36.15	634.24	-0.10%	431.07	203.14	0.04
100	669.71	36.15	634.15	-0.09%	430.03	203.14	0.98

Finally, the formulation for soil evaporation (eq 43) was reformulated, to match observed water fluxes more closely, to:

$$Esu = \exp^{-kJ \cdot LAI} \cdot ETo \cdot su(1) \tag{57}$$

where su(1) refers to water saturation degree in the top layer. This formulation retains the reduction of transpiration under full canopy cover and low soil moisture conditions. Also, to improve the difference in simulated and measured water fluxes, the amount of transpiration under perceived water stress by the tree was temporarily set to 0. Since the calibration is done for the year 2005, which is an average year with enough available soil moisture, there should be no water stress perceived by the vegetation. Because the difference between simulated wa-

ter fluxes between stressed and normal conditions might have been too small, adjusting the transpiration to 0 when water stress is perceived should minimize the amount of days in the yearly model runs when this condition is fulfilled.

Here water stress is defined as the condition when Mq (actual water storage) is equal or lower than 90 percent of the potential amount of water stored in plant tissues (Mqx). A further reduction in water content may lead to cell damage under hydraulic failure, as hypothesised by Schymanski (2007). Since it is not realistic to assume that transpiration totally stops under these conditions, it is therefore not retained in the rest of the model runs as water is thought to be lost through transpiration even under conditions of extreme drought to reduce internal leaf temperature. The adjusted finalized model, taking into account the four adjustments discussed above, was taken through the optimization procedures described earlier.

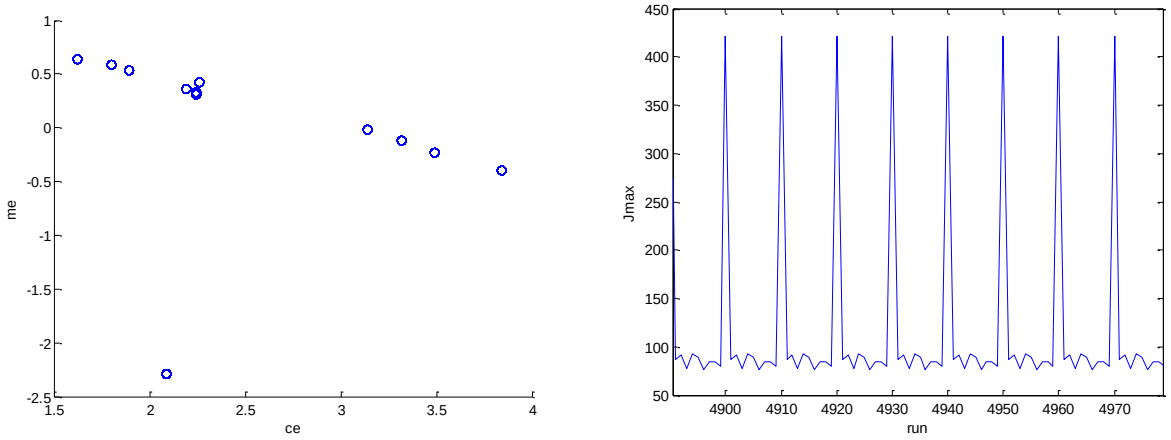

Figure 19: *Scatter plot (left) showing the range of me and ce (empirical parameters defining water use efficiency) with a Pearson correlation of r = -0.2308 and (right) the evolution of J_{maxtop} (electron transport capacity at the top of the canopy) during some of the final 5000 runs of the DREAM optimization for the Hainich site.*

The results of the latest DREAM optimization after the adjustments to the model were made, were markedly different from those in earlier versions of the model. The model no longer simulated any days where it previously experienced water stress, because the difference in transpiration was extremely high since simulated transpiration was temporarily set to 0 as explained in the forth adjustment. The exclusion of these days where the tree experienced drought resulted in much better agreement between the modelled and measured fluxes. From the evolution of J_{maxtop} over some of the final runs (figure 19) it becomes clear that the solution seems to have converged towards a low value, but 1 in every 10 runs shows a different solution where J_{maxtop} is near its maximum. These dynamics can also be seen for the other optimized parameters, ce, me and c_{RI}. The correlation coefficient between ce and me is unexpectedly low for the final 5000 runs. However, excluding the outlying points (under the condition that me<-2) results in a perfect correlation of r=1. The correlation between c_{RI} and J_{maxtop} is r = -0.4202 (not shown in the figure). The carbon and water fluxes (figure 20) did indeed improve with the latest model runs compared to the earlier model outcome, but an increase in the standard deviation can was also observed. This likely results from the observed dynamics in the parameter optimizations, giving a markedly different value 1 in every 10 runs, that results in values further from the mean.

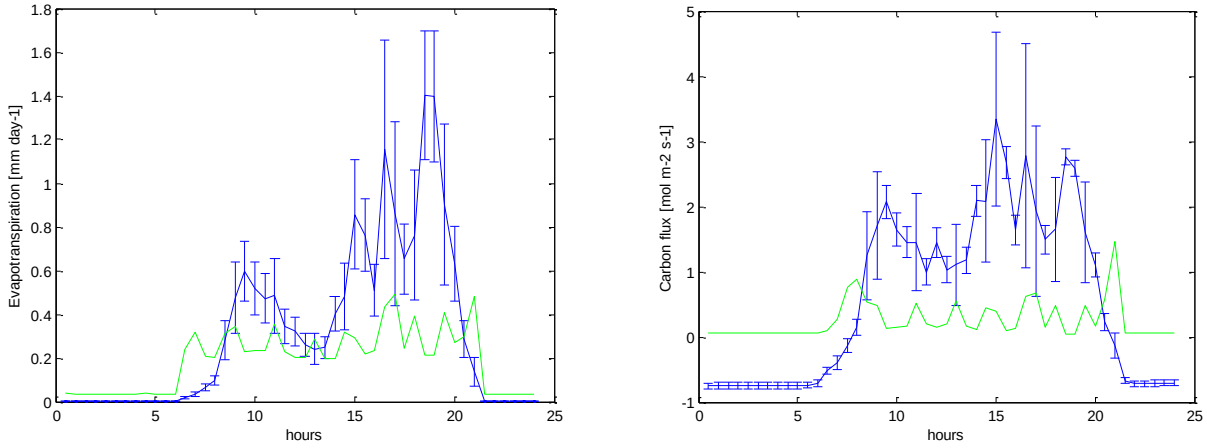

Figure 20: *Mean and standard deviation of the simulated carbon flux (left) and evapotranspiration (right) in the last 100 runs of the DREAM optimization for Hainich on 06/07/2005. Green lines show the relative deviation of the standard deviation compared to the mean.*

Overall, the results of the adjusted model showed good visual agreement and were satisfying, whereby confidence was gained in the adjustments that were made to the model. The adjustments and the resulting parameter settings from the best DREAM optimization (Table 6) were used in subsequent model runs. The total NCP in the model runs is slightly larger for the mean and the maximal NCP settings than for the best parameter settings. The reduction in difference between the two gives confidence about the calibration of the model and the justness of the given parameters, as the model seems less sensitive to the choice of parameters. Also, after the given adjustments, the model is less sensitive to small changes in parameter values and gives a more robust outcome. Unfortunately, the calculation of NCP cannot be tested or measured as it is an internal plant specific value that might not even have a biological meaning. It is only used as in indication of the plants fitness and reproductive capability.

Table 6: *Initial range and results for the last 5000 runs of the DREAM optimisation of the parameters me and ce (empirical parameters defining water use efficiency) and c_{Rl} (leaf respiration coefficient) and J_{maxtop} (electron transport capacity at the top of the canopy) for the Hainich site.*

	Initial range		DREAM optimization				
	Min	**Max**	**Min**	**Max**	**Mean**	**Best**	**NCPmax**
ce	1	4	1.62	3.84	2.43	1.62	2.26
me	-3.0	1.0	-2.29	0.64	0.00	0.64	0.42
c_{Rl}	0.005	0.15	0.01	0.02	0.01	0.01	0.01
J_{maxtop}	10	450	76.35	421.69	118.68	91.41	76.35
NCPtot			-5.39	-36.05	31.14	28.64	28.88

6.4. Model validation

The results (figure 20) for the half hourly data show very good agreement with the observed data at the Hainich flux site. Since the model was initialized during the optimization with steady-state soil moisture (su spin up) the agreements between these fluxes and the measurements is slightly better than with initial soil moisture at field capacity. The steady state soil moisture was again obtained by running the model until no change in water saturation degree could be seen between succeeding runs. Unexpected were the lower carbon fluxes that can be seen under the higher water saturation degree that is initialized in these model runs, since carbon uptake cannot be limited by available water in this situation. The calibrated model with the optimized parameters captures both the dynamics and the size of the actual carbon fluxes and will be used for subsequent runs and the degree-day optimization that will follow in the next paragraph.

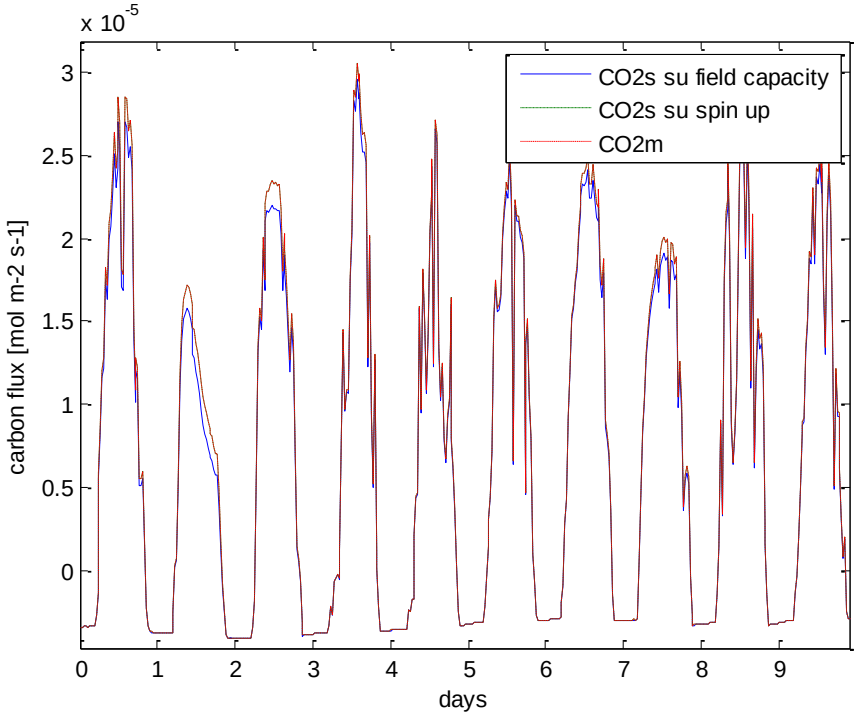

Figure 21: *Measured (CO_2m) and simulated (CO_2s) half hourly carbon fluxes of the first ten days of June after the optimization for the Hainich site in JJA.*

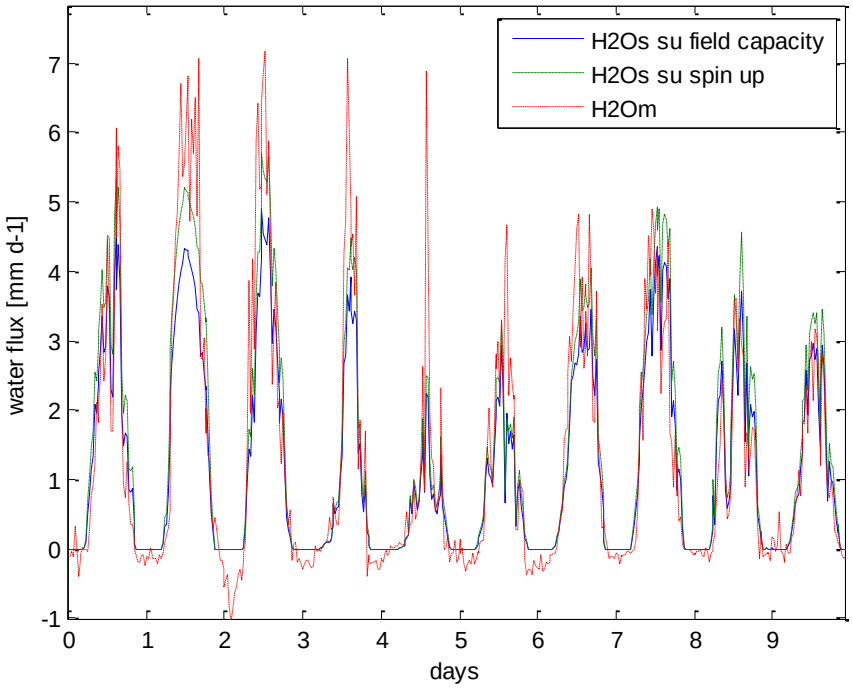

Figure 22: *Measured (H_2Om) and simulated (H_2Os) half hourly carbon fluxes of the first ten days of June after the optimization for the Hainich site in JJA.*

An important aspect of the model that is not adequately captured, is the variation of the root water uptake flux (Qr) over time (Figure 23). The dynamics of Mq and Qr only show normal behaviour from timesteps 10E3 to 13E3 and show strongly fluctuating behavior throughout the rest of the year. During most of the model runs, Qr fluctuates strongly, from unrealistically high to low values, with each time step, possibly as a result of numerical instability. Numerical instability occurs when the time step of the model is too large for the solution of some of the equations in the model. The observed dynamic of Qr also contributes to the occurrence of water stress, as the change in water storage in the tree is determined by the water uptake

through the roots and water loss through evaporation. To reduce the days of water stress, that should not have occurred during the validation period, the value of Mqx was changed to an arbitrary value of 12 that led to good observed dynamics and kept the value of Mq above the critical 90% level. The adjusted value of Mqx was kept throughout subsequent model runs.

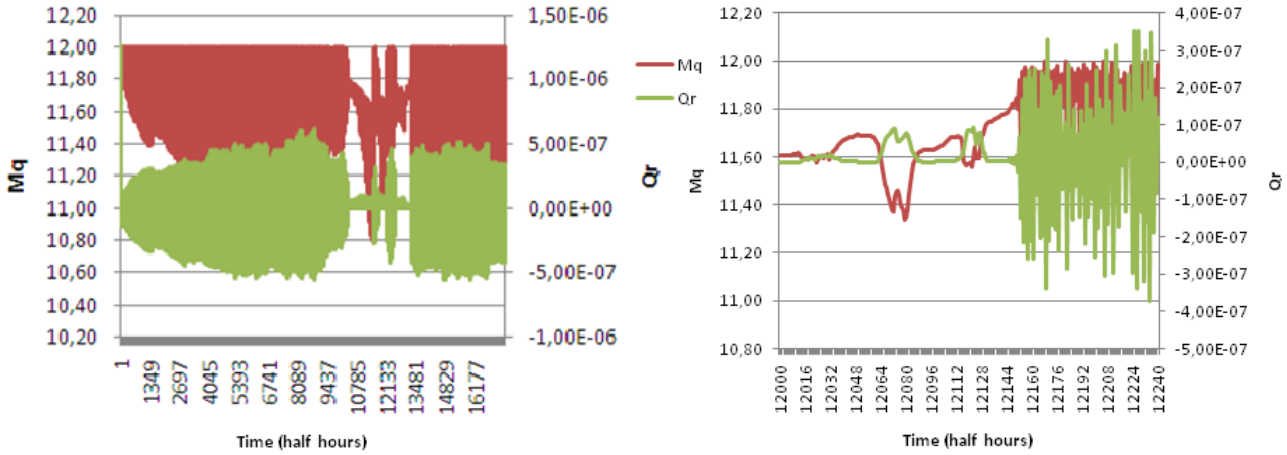

Figure 23: *Evolution of actual amount of water stored (Mq) and root water uptake flux (Qr) over time, given in half hourly model steps, simulated at the Hainich site (left) in the year 2003 and (right) for a 5 day section of the year.*

Figure 24 shows about 5 days where the of Qr were as expected, rising throughout the day as water is transported to the leaves and low values throughout the night as no photosynthesis takes place and water demand is low, because there is no sunlight and temperatures are low. On both sides of the graph the instability of Qr can be seen however. The fluctuations in Qr and Mq affected especially the water fluxes that were simulated by the model, through their influence on the tissues' water balance pressure and the in- and outgoing water fluxes. The effect on the simulated water fluxes in turn affects the evapotranspiration rate, the solution of G_s, the simulated carbon fluxes and NCP. By changing the value of Mqx (the potential amount of water stored in plant tissues per unit catchment area) and artificially keeping the water storage above the critical stress level, the resulting carbon and water fluxes were simulated reasonably well and the model could be used for further runs to explore the hypothetical root mechanism. It can be questioned whether the original value of Mqx was valid for the current site and whether it should have been changed at all. The value of Mqx was directly taken from Schymanski (2007) who used a value that was calibrated based on observations of Cernusak *et al.* (2006) in the savanna site near Howard Springs (Northern Territory, Australia). The value was estimated using the total aboveground volume of sapwood and sapwood density, using the estimate that 30% of the area was covered by trees. No such calculations were made for the Hainich site and the altered value of Mqx was based purely on the modeled dynamics.

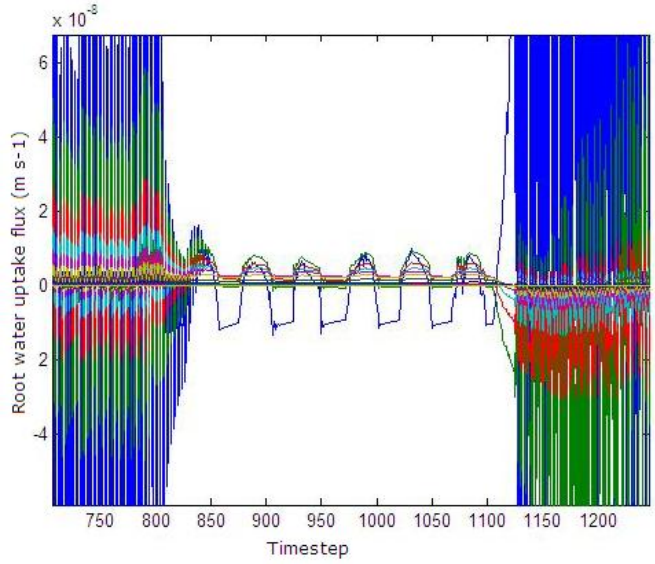

Figure 24: *Fluctuation of the root water uptake flux over time in different soil layers, depicted by the different colors where blue is the top soil layer, simulated during 2005 at the Hainich site.*

6.5. Degree-day optimization

Phenology was only based on temperature in the model and was modeled using the degree-day method. During the previous parameter calibration, the LAI was kept constant throughout the model runs as they were conducted in summer when moisture was not limiting and no reduction in LAI was to be expected. To correctly simulate water and carbon fluxes throughout the year however, it is necessary to have a mechanism that increases LAI in spring and decreases it again in fall similar to the natural local timing for the simulated species. In the model LAI increases after the 10 day maximum values exceed a certain temperature threshold that is varied during the optimization procedure. Similar to the off-line calibration, phenology is also optimized by a mathematical function that minimizes the difference between simulated and measured fluxes. The degree-day optimization was done using an unconstrained nonlinear optimization function that weighed the difference between the fluxes for the different components (water and carbon) to take the difference in measurement errors into account.

The degree-day optimization was run for the entire year 2005. Because this optimization method is very sensitive to the initial conditions of temperature thresholds, it was run several times with slightly different initial conditions, leading to a range of outcomes. Finally the outcome with the smallest error (as computed with equation 54) was chosen as the optimal solution. It was chosen to initialize the model with more realistic soil moisture rather than field capacity. To create the initial soil moisture throughout the soil (figure 25), the model was run once after which the water saturation degree was stored and used in the optimization.

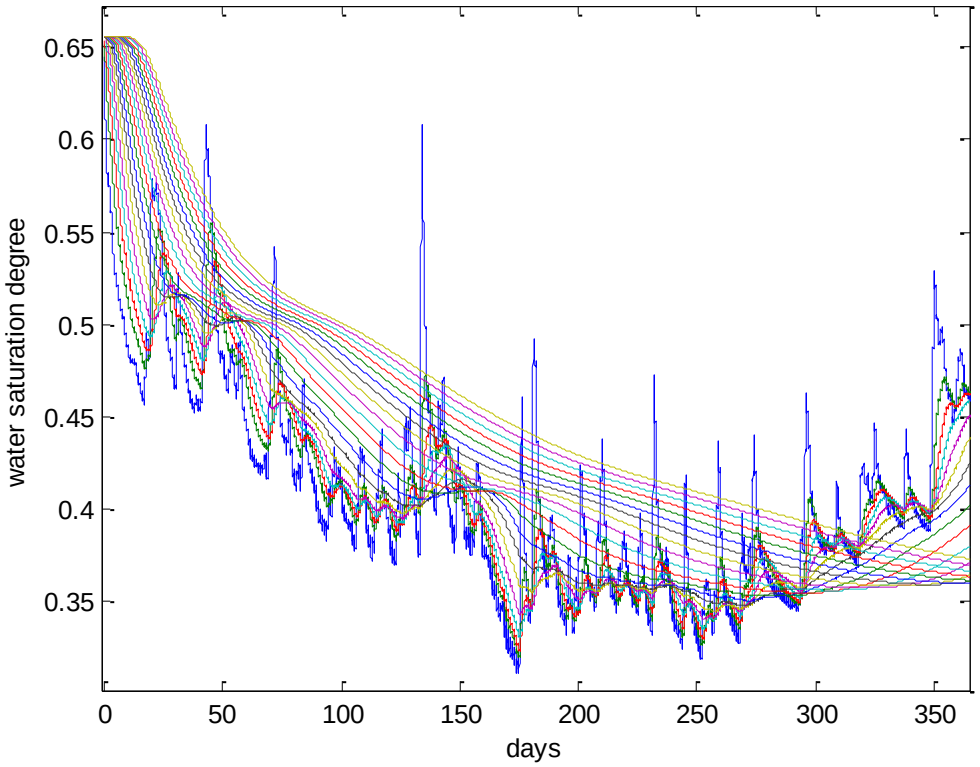

Figure 25: *Water saturation degree throughout a yearly model run in all soil layers. The greatest variation can be seen in the top layer (blue) and a gradual decrease in the deepest soil layer ("furthest away") can be seen through the year.*

In spring LAI was increased by raising the number of leaf layers in the model when the 10 day maximum temperature sum exceeded the value found by the optimisation function. It was decreased at the end of the growing season when the 10 day maximum temperature sum became smaller than the second temperature threshold and decreased LAI again. To examine the sensitivity of the degree day optimization method to the error function (Eqn 54), the optimization was both run with the weighted function and with only the carbon flux component as the optimization criteria. The results for both methods were very similar and the weighted error was nearly identical after combined and carbon only optimization. The first gave an error

of 40.3 and values for the temperature thresholds of 213.2 and 262.8, while the latter gave an error of 40.4 and values of 209.7 and 244.4. The first outcome was used in subsequent model runs to determine the start and end of LAI and the growing season, because an optimal solution was sought for both carbon and water fluxes at the same time.

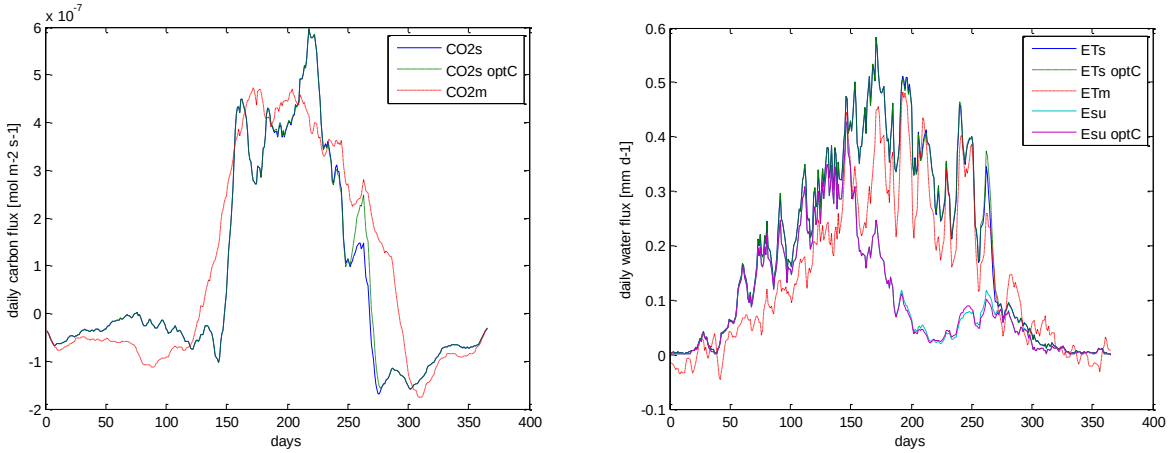

Figure 26: *30 day running mean carbon (CO_2) flux (left) and 10 day running mean water flux (right) of the measured (m) and simulated (s) carbon and water fluxes respectively with the weighted and carbon flux only (optC) error criteria for the degree-day optimization. In the water flux plot, both the soil evaporation (Esu) and evapotranspiration(ET) are shown.*

The optimized model shows differences in the fit of simulated carbon fluxes with the measurements, as the fluxes are overestimated in spring and for a short period during summer. Besides that, the increase and decrease in LAI seem more abrupt than the actual in- and decrease in carbon uptake measured by the fluxtowers. Altogether, this places doubt at the choice for the degree-day method to represent phenology and it suggests that LAI perhaps should have increased with more than one layer every day, or fewer layers should have been included in the model. The overestimation in spring can only result from an underestimation of the soil respiration, as there is no canopy present yet and outgoing fluxes are higher than the model simulates.

The dynamics in simulated water fluxes are better represented than the carbon fluxes (figure 26). The carbon plot needed to be smoothed more (30 day running mean instead of the 10 day running mean used in the water flux plots) in order to get a clear picture of the dynamics over time, because the carbon flux is much more variable from day to day and night to day. The simulated ET follows the observed water flux quite nicely in summer, but less so in spring and winter. In spring ET is too high because of an overestimation of the soil evaporation. In fall, between day of the year 275 and 300, there is a period when ET is underestimated because the degree-day threshold has been reached and LAI has decreased. The adjustment that was made in the soil evaporation (Eqn 57) is apparently not able to simulate the flux correctly, although it seemed like an improvement compared to the earlier formulation (Eqn 43). Both of the methods for example take the influence of the local climate into account that is created by the shade as the result of increasing LAI, in their exponential term. For the latter formulation both this term and the water saturation degree result in a value between 0 and 1 that should decrease the calculated reference evaporation (Eqn 37) to the appropriate amount. From the last results however, it can be seen that soil evaporation is overestimated in spring.

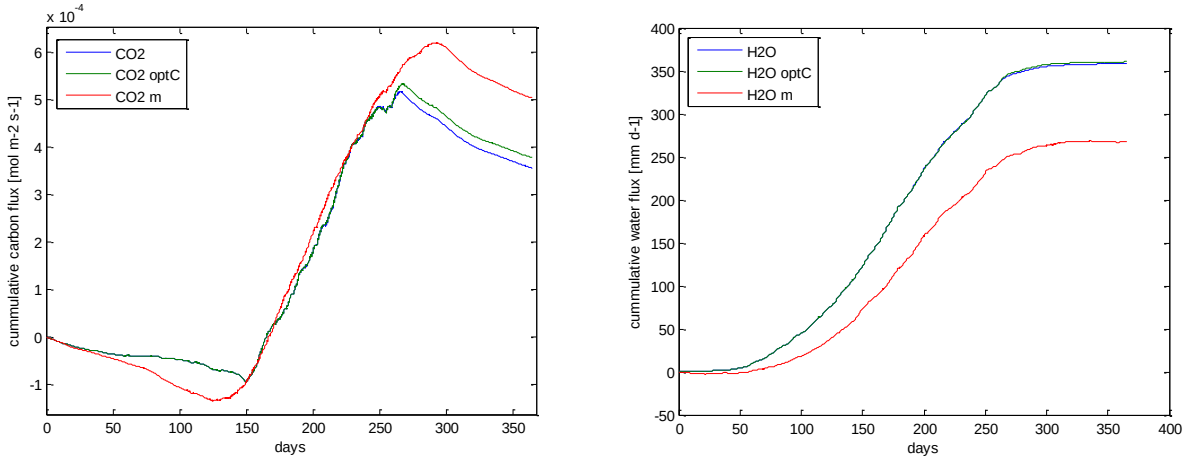

Figure 27: *Cumulative measured (m) and simulated carbon (left) and water (right) fluxes for the optimized simulations with the weighted and carbon only (optC) error function.*

In the cumulative plots (figure 27) it is easier to see the overestimation of carbon in spring and underestimation in winter. For carbon there is a slight difference between the two methods of the degree-day optimization, based on the weighed or carbon only components. The water flux however is consistently overestimated and the total error at the end of the year is about 40% of the measured water flux, in spring this is mainly due to the overestimation of soil evaporation. The daily dynamics in carbon uptake are well captured by the model, but there are several times when there is a constant under of over estimation by the model. This can for example be seen around day 275 (figure 26) when there is a steep drop in modelled carbon fluxes that does not occur in the observations until day 300. This difference probably results from the decline in LAI that is simulated too early.

To be able to simulate other years with the model, the degree-day optimization was run for the remaining years for which data were available, namely 2003-2007. The initial thresholds for the function were the optimal values found for the year 2005, although for 2004 and 2006 these had to be slightly altered to arrive at a good solution. The results of the optimization are given in table 7. Simulations for the years 2003-2007 were subsequently run with the final results of the degree-day optimization and will be described in the next chapter.

Table 7: *Final cumulative 10 day maximum degree-day temperature thresholds to determine the onset and decline of Leaf Area Index (LAI) for the years 2003-2007 at the Hainich site.*

Year	Degree-day threshold for leaf growth [°C]	Degree-day threshold for leaf decline [°C]	Error
2003	196.9	289.2	50.1
2004	181.6	248.0	58.3
2005	213.2	262.8	40.4
2006	183.7	242.8	81.3
2007	191.3	282.9	43.6
average	193.4	265.1	54.7

7. Results and Discussion

The results of the final model with its optimized parameters are given in this chapter. The calibration of the model was the final step that needed to be completed before the actual simulations that allow the investigation of the hypothetical root mechanism could be run. Simulations of soil moisture, carbon and water fluxes for the years 2003-2007 are given in the first paragraph. The second paragraph presents the results of the root optimisation strategy during the extreme drought in 2003. The chapter finishes with the remaining discussion points that led to differences in observed and simulated results and are still unresolved.

7.1. Simulations 2003-2007

The model was run for 5 consecutive years to investigate the difference in results between these years and the overall performance with the models final parameter setting that was calibrated for 2005. The summer of 2003 for example, was extremely dry all over Europe and this can be seen in the results. Figure 28 shows the dynamics of soil moisture throughout the years 2003-2007. The model was initialized with soil moisture at field capacity for each of the years and allowed to change freely throughout the year. The modelled initial dynamics are quite similar, depending on the timing and amount of rainfall based on measurement data. By summer, however, the model starts to diverge for the different years and it becomes clear that 2003 was the driest year, with water saturation degree falling and coming close to the 14% usually assumed to be fatal for vegetation. The year 2007 was the wettest year and had some heavy rain showers, this is clearly depicted in the upper soil layer water saturation dynamics (Figure 28).

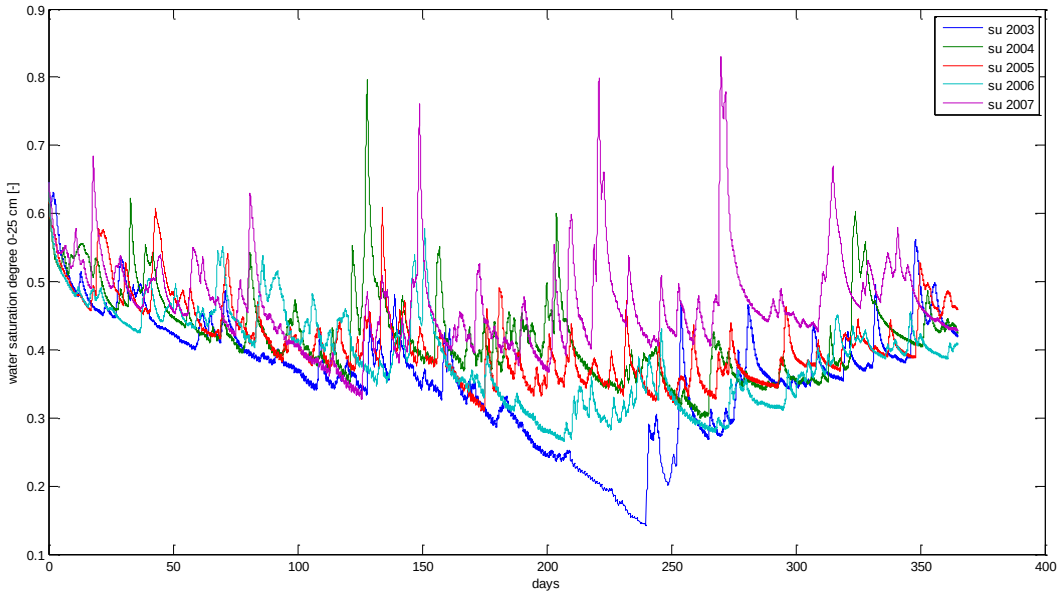

Figure 28: *Modelled water saturation degree (su) in the top layer of the soil at the Hainich site for the years 2003-2007.*

The utilization of the degree-day method to model phenology led to different timing for leaf onset and decline for each year. The modelled LAI throughout the years can be seen in figure 29. The representation of the vegetative area of the trees does not seem representative however, as the maximal cover is only reached for a few days for each of the simulations. The choice to increase the canopy layers with only 1 every day, if the degree-day threshold was exceeded, might have been too conservative as it took the tree at least fifty days to reach a full canopy cover. Since the decline in LAI was modelled in the same way, it took another fifty days to decrease LAI before the onset of winter. An improvement in simulated fluxes and the representation of vegetative cover could be expected if the number of canopy layers were increased with two per day during flushing and senescence. This would allow a full cover to be

present for a longer time during the summer months and potentially make the model less responsive to changes in the degree-day thresholds.

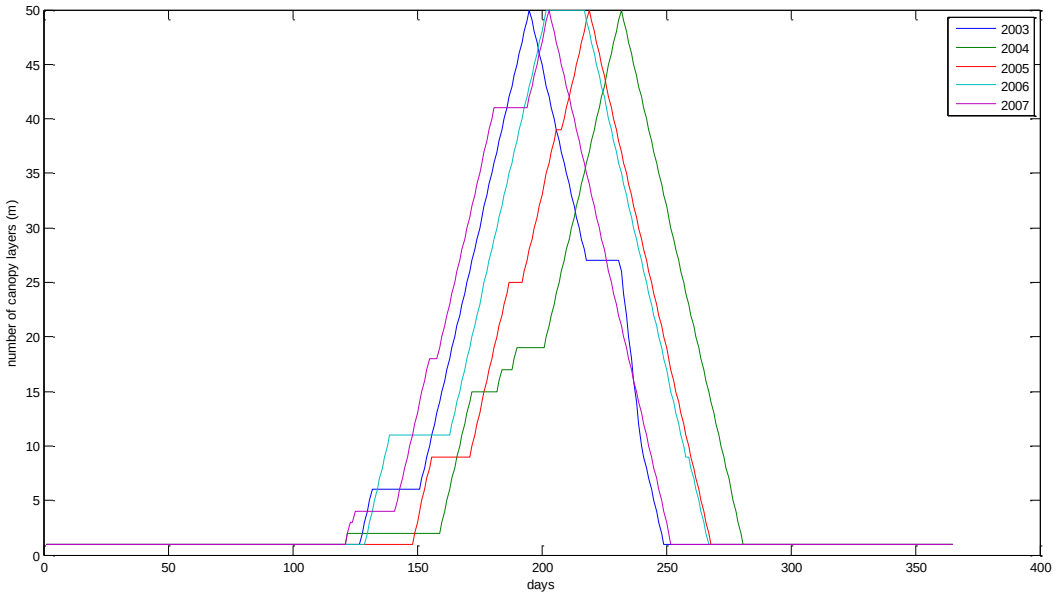

Figure 29: *Modelled Leaf Area Index (LAI) at the Hainich site for the years 2003-2007.*

To assess the fit of the model with the natural situation in the field, the observed water and carbon fluxes were substracted from the simulations for each of the years, showing the difference between model results and observations (figure 30). Striking results are the large differences between water fluxes in 2003, 2006 and 2007. Nearly all the simulations show an overestimation of the carbon flux in spring and a severe underestimation in fall. The year 2005 does on average not perform any better than other years, which shows that the off-line parameter optimization for the year 2005 had no bias to the specific conditions of this year and could be used for all years. The steep drop in carbon fluxes is caused by the delayed flushing and LAI increase in simulated the model compared to the real situation. The difference in simulated carbon fluxes in fall probably results from the degree-day method utilized, potentially in combination with the loss of leaves from the mechanism that is in place when water stress occurs. Reducing LAI is one of the strategies tested in this project that trees can use to cope with low soil moisture availability, because it reduces their maintenance cost.

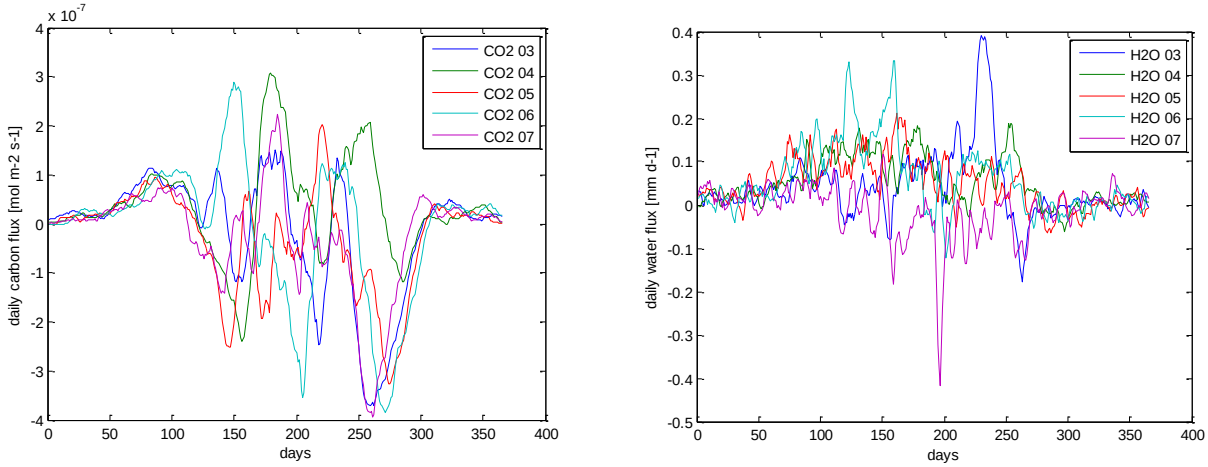

Figure 30: *Difference between simulated and observed 30 day running mean carbon (left) and 10 day running mean water (right) fluxes for the years 2003-2007 at the Hainich site.*

For each individual year the simulated and measured carbon and water fluxes can be found in figure 31. In general there seems to be an overestimation of the time of the highest LAI. The years 2003, 2004 and 2006 show a sudden drop in carbon fluxes in the middle of the summer, possibly indicating that they are experiencing water stress, although no strong reduction in

evapotranspiration can be seen. Overall, the simulated water fluxes are in better agreement with the observations than the carbon fluxes.

The high difference in observed and simulated water flux in 2003 results from the presence of vegetation at the end of summer when the expectations were a decreased vegetative cover due to the severe drought. This is clear from about day 210 onwards. During summer, transpiration is the main component of the total evapotranspiration that is measured, whereas in spring the contribution of soil evaporation (and grasses and shrubs) is higher. The carbon fluxes simulated in 2004 are higher than the observations as well and there is a pronounced difference in spring in the water flux, probably caused by the equation chosen for soil evaporation representation in the model. For 2005 the simulated carbon fluxes show a close fit to the observations but at the same time an overestimation of spring water fluxes, similar to 2004 and 2006, can be seen. The simulated carbon flux in 2006 shows a steep decrease in the middle of the year, around day 200, that cannot be easily understood or explained. In 2007 the carbon flux shows a peak that is not seen in the measurements and a drop in the middle of summer that is more pronounced in 2003, 2004 and 2006. The cause for this drop is not clear, but it could (1) result from an underestimation of LAI or (2) from an overestimation of respiratory fluxes. As could be seen in figure 29, the modelled LAI is only at its maximum level for a very short period and declines rapidly thereafter. Whereas in reality trees have their full canopy cover for a long period between spring and fall, thus the underestimation of the duration of the full LAI of a tree could explain this underestimation in the middle of summer. It does not explain however, the peak that is simulated near the end of the summer. An explanation for the decrease in simulated carbon flux only during the middle of the summer could be that respiratory fluxes are overestimated as these depend on temperature. At the start and end of summer these fluxes could be estimated well and combined with the photosynthesis result in appropriate values for the carbon flux, but if either woody tissue or soil respiration are overestimated during the high temperatures reached in the middle summer this would result in a net carbon flux that is smaller than observed.

Furthermore, in 2007, the decline of LAI can be clearly seen in fall when there is a strong underestimation of the carbon flux, similar to 2003, 2005 and 2006. The simulated water flux shows good agreement (with a correlation coefficient of r=0.8 between measured and simulated half hourly fluxes on average) with the observations in general, but some severe underestimations can be seen (see also figure 30). The water saturation degree showed high peaks during 2007 and apparently the soil evaporation cannot handle these peaks correctly. The soil evaporation must be the cause for this underestimation because there should not be a difference in the trees transpiration under increased rainfall, but there should be an increase in overall evapotranspiration. This is not simulated correctly by the model in 2007, although there is no real evidence of this in other years.

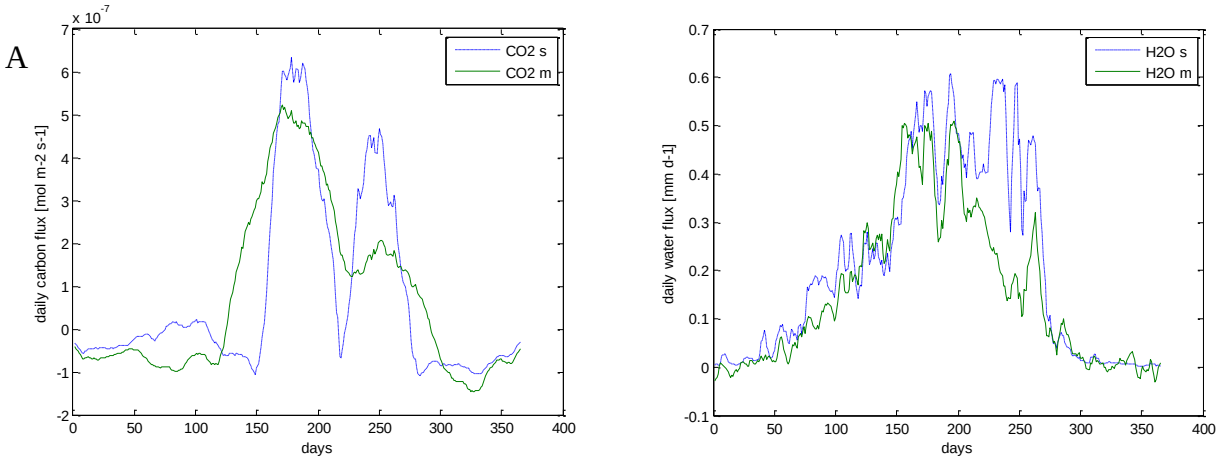

Figure 31: *Measured (m) and simulated (s) carbon and water fluxes for a 30 day running mean carbon (CO_2) flux (left) and 10 day running mean water (H_2O) flux (right) at the Hainich site for the years (A) 2003, (B) 2004, (C) 2005, (D) 2006 and (E) 2007.*

B

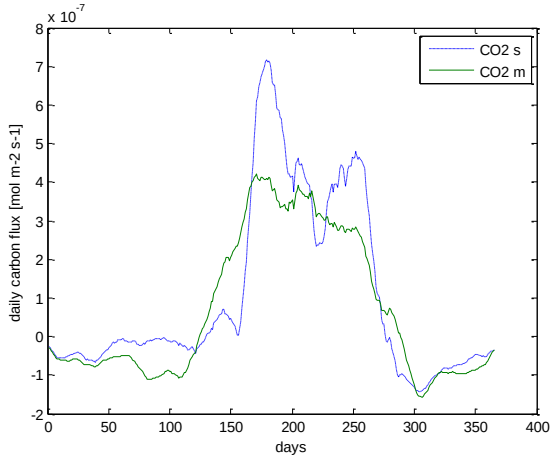
x 10^-7
CO2 s
CO2 m
daily carbon flux [mol m-2 s-1]
days

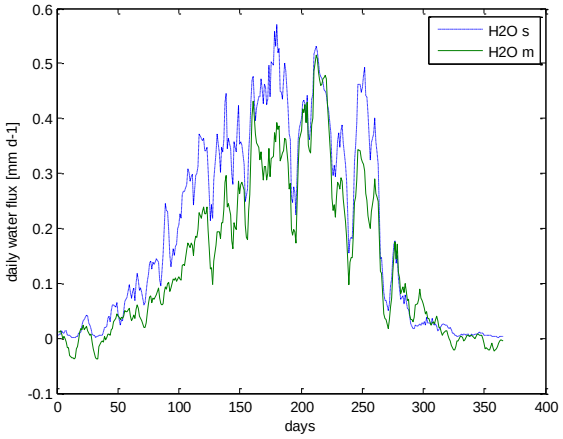
H2O s
H2O m
daily water flux [mm d-1]
days

C

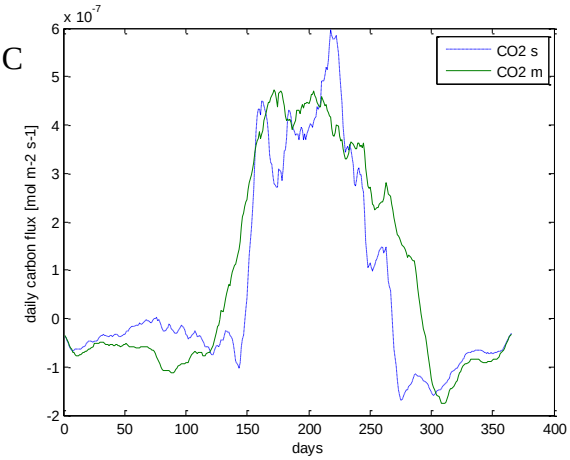
x 10^-7
CO2 s
CO2 m
daily carbon flux [mol m-2 s-1]
days

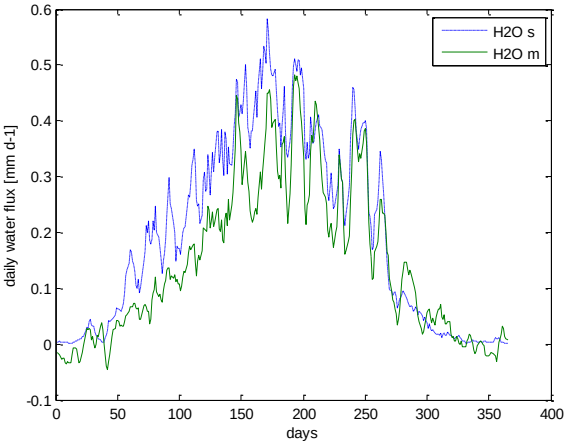
H2O s
H2O m
daily water flux [mm d-1]
days

D

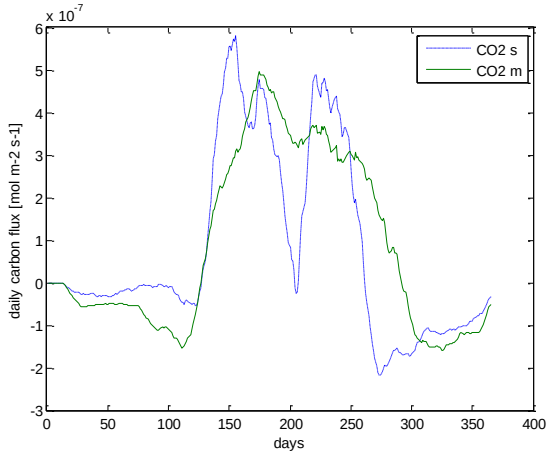
x 10^-7
CO2 s
CO2 m
daily carbon flux [mol m-2 s-1]
days

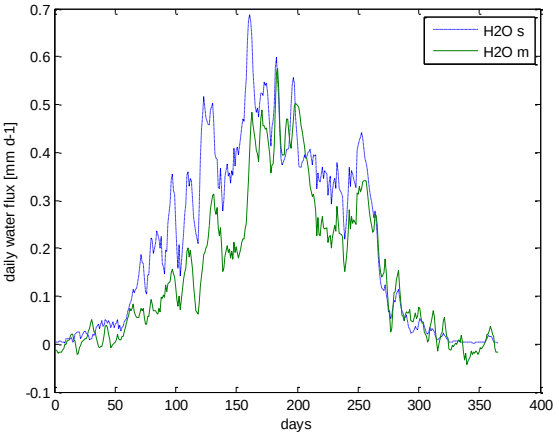
H2O s
H2O m
daily water flux [mm d-1]
days

E

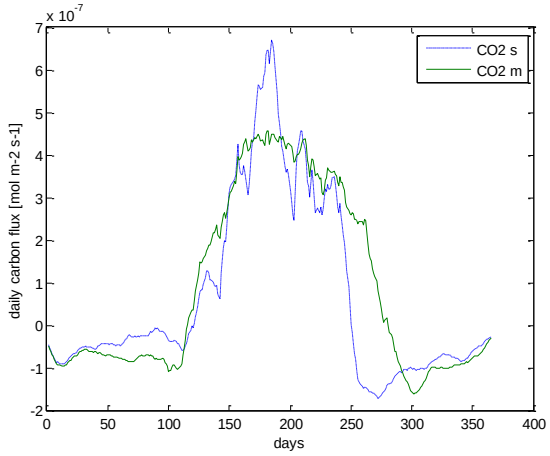
x 10^-7
CO2 s
CO2 m
daily carbon flux [mol m-2 s-1]
days

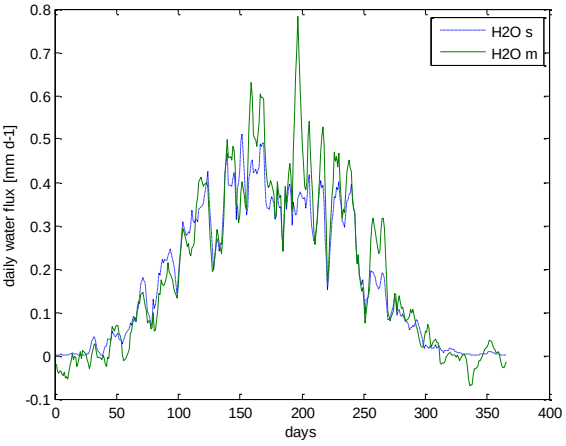
H2O s
H2O m
daily water flux [mm d-1]
days

7.2. Root optimization strategy

Finally, the model was run with the root optimization mechanism in place to investigate the hypothesis that trees will create fine root mass deeper in the soil to keep assimilation going under conditions of limiting soil moisture. The underlying assumption of the optimality approach on which the model is build, is the biological principle that vegetation maximises its 'Net Carbon Profit'. In the case of the investigated root mechanism, this means that a tree will maximize its net carbon (i.e. energy) gain by the optimal choice of the following trade-off strategies: (1) keeping assimilation going by replacing fine root mass and extracting water from deeper down the profile or (2) decreasing maintenance respiration by decreasing leave area. The NCP was evaluated after a number of days, ranging from 1 to 7, to examine the feasibility of investing in the creation of new fine root mass, allowing uptake of water from other soil layers. Hypothetically, there might be an optimum in the number of evaluation days as a new rain event could take place, restoring soil moisture in the upper layers. In this case it would not have been profitable for a tree to relocate fine root mass to a deeper soil layer.

The results for 2003 (figure 32) show that the mechanism does not take place when evaluation of NCP is done after 1 or 2 days at all and starts to make a difference after an evaluation period of at least 4 days. The models simulations of the water flux start to diverge after roots have been repositioned to deeper soil layers, allowing for higher water uptake and consequently carbon assimilation. The results show that the tree does not always relocate its fine roots to the deepest soils layers, since other layers can be equally or even more profitable. The simulated water flux increases after the hypothetical root mechanism has repositioned the roots of the trees and more water is available for transpiration.

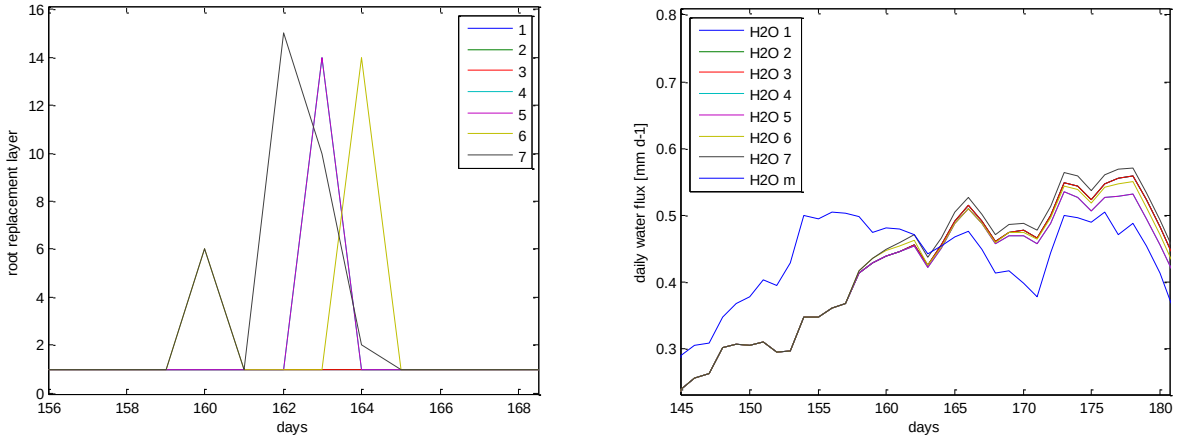

Figure 32: *Depth and day when repositioning of roots takes place and fine root mass is created for an evaluation period of 1 to 7 days (left). Daily measured (m) water flux at the Hainich site and simulated fluxes for an evaluation period of 1 to 7 days after new fine root mass has been created in deeper soil layers (right).*

From the results it can be concluded that the hypothetical root mechanism indeed takes place as apparently NCP increases when trees have access to soil moisture in deeper soil layers and carbon assimilation is not limited by water availability. Surprisingly, the root replacement only takes place after a evaluation period of more than 3 days in 2003 and is most evident after 7 days. There is very little root replacement compared to earlier model runs with the root mechanism in place before the adjustments to the model were made (not shown here). The reduction in the days that the root mechanism is effective most likely results from the adjustment of the potential water storage in the tree (Mqx) to a higher value because of the unrealistic amount of days with water stress in the model (discussed in section 6.4). The dynamics Mq are closely related to those of Qr and led to the critical value for water stress to be exceeded too often. Figure 22 and 23 showed the change of Qr over time and the unstable nature of these results. Without the change in Mqx the extreme fluctuations in Qr would have simulated 'water stress' almost every other time step. The adjustment of Mqx lead to better overall results for the yearly model simulations, but also decreased the number of days the vegetation experienced water stress when the root mechanism probably would have increased NCP.

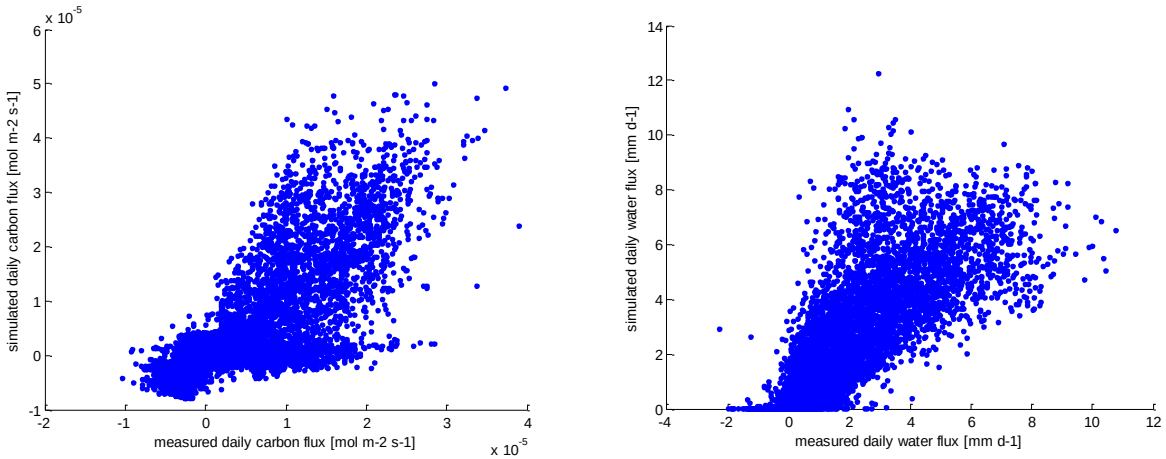

Figure 33: *Scatter plots of the measured and simulated daily carbon (left) and water (right) fluxes without the hypothetical root mechanism in place for the year 2003 at the Hainich site.*

The Pearson correlations between the simulated and observed carbon and water fluxes (figure 33 and table 8) show that there is good agreement. There are some exceptions that can best be seen in the scatter plots. For example in the water flux as the simulations are never negative, but the observations can be. This observed downward water flux could either be due to measurement errors or due to fog or dew formation or other atmospheric processes. The evapotranspiration is restricted to positive values in the model, as there is no physical interpretation of a water flux into vegetation. If the observations are correct, these negative values result from meteorological processes that were not taken into account in the model. To be able to compare the fit due to the implementation of the hypothetical root mechanism, the correlations for the different evaluation periods (indicated by the amount of days after which the cumulative NCP was evaluated) and the correlations for the simulation without the mechanism in place (column indicated by NOT in table 8) are given.

The correlations and thus fit between measured and simulated carbon fluxes is highest for the run without the root mechanism and lowest with the root mechanism in place after an evaluation period of 4 and 5 days. Because the root mechanism allows for more photosynthesis, it causes the simulated carbon fluxes to be higher, but the simulations were already higher than the measurements causing the results to lie further apart with the mechanism in place, thereby reducing the fit. The opposite is true for the correlations and thus fit between the observed and simulated water fluxes, where the correlation is lowest for the runs without the root mechanism and highest with the mechanism in place after an evaluation period of 4 and 5 days. Thus it seems that there is an optimum for the hypothetical root mechanisms evaluation period that is 4 or 5 days ahead. The same trend in the fit between simulated and observed carbon and water fluxes is detected in the Root Mean Square Error (RMSE) in table 8.

Table 8: *Evaluation of the hypothetical root mechanism in the year 2003 at the Hainich site, giving the Pearson correlations between the simulated and measured carbon (CO_2) and water (H_2O) fluxes and the Root Mean Square Error (RMSE). The correlations are given for the run without the root mechanism in place (NOT) and after an evaluation period of 1-7 days, for which the RMSE is also given.*

Hypothetical root mechanism NCP evaluation period (days)	**NOT**	**1**	**2**	**3**	**4**	**5**	**6**	**7**
Correlation coefficient (r) CO2s – CO2m	0.811	0.774	0.774	0.774	0.764	0.764	0.774	0.791
Correlation coefficient (r) H2Os – H2Om	0.858	0.862	0.862	0.862	0.867	0.867	0.863	0.863
RMSE water [*10^3 mm day^{-1}]	-	8.313	8.313	8.313	7.984	7.984	8.236	8.603
RMSE carbon [*10^{-2} mol m^{-2} s^{-1}]	-	4.210	4.210	4.210	4.214	4.214	4.201	4.293

The variation in simulated fluxes for the different evaluation periods (figure 34) is more pronounced in the daily carbon than the daily water fluxes. The carbon uptake is noticeably higher with the root optimization mechanism in place, especially after a 7 day evaluation period and the first peak in the observed carbon uptake seems to be simulated more accurately

with measurements. The overall result is that after a 4 or more day evaluation period, the hypothetical root mechanism simulates a higher NCP. However, due to the utilization of the degree-day method and LAI representation, leaf growth takes place later in the season than the observed carbon flux increases and the simulated flux decreases long before the observations decrease in fall. The peak in simulated daily water fluxes can also be attributed to the representation of vegetation in the model as transpiration is much higher from vegetation. Thus, an overestimation of the LAI will result in an overestimation of water fluxes as well, which is clearly visible in figure 34.

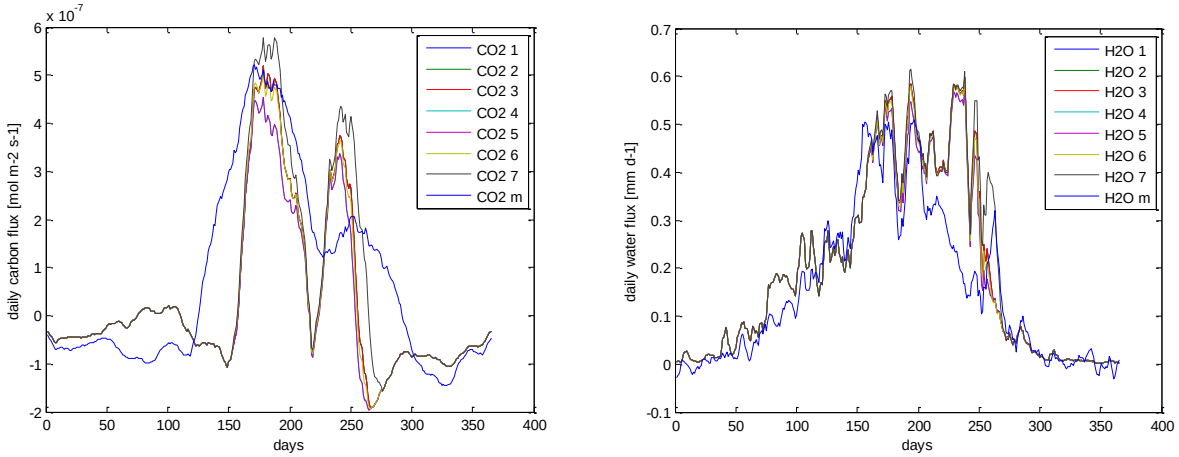

Figure 34: *30 and 10 day running mean of the simulated and measured (m) carbon (left) and water (right) fluxes respectively at the Hainich site in 2003 with the evaluation period of the hypothetical root mechanism after 1 to 7 days.*

7.3. Main discussion points

The most important adjustments that were made to the model during the course of this research project were (1) the formulation of soil evaporation and (2) the value of Mqx (the potential amount of water stored in the plans tissues). Due to difficulties to incorporate the adjustments and correctly simulate the LAI evolution of the evergreen *Quercus Ilex* trees in the Puechabon region, this site (FR-Pue) was excluded for the remainder of the project. All results discussed here are therefore based on simulations for the Hainich site (DE-Hai) only. The first adjustment to the model was made before the off-line parameter calibration was done, whereas the second one was made before the degree-day optimization. The results will be discussed in this order as well.

Soil evaporation (adjustment 1) was calculated in the final model with equation 57 instead of 43 that was previously introduced in the model description (chapter 3). Both formulations for soil evaporation take into account the influence of LAI and the difficulty to evaporate from a drier soil. The chosen representation of soil evaporation however lead to an overestimation in simulated water fluxes in spring (e.g. figure 26 for 2003). The final model, as described in chapter 4 was then calibrated for the Hainich site with two optimization procedures, the first was the DREAM algorithm during the months JJA in 2005.

The results of the off-line parameter calibration of ce, me, c_{Rl} and J_{maxtop} with the DREAM optimization greatly improved after incorporation of the adjustments, although there were some outliers for the final best solution (figure 19). When these outliers are removed the correlation of r=1 between ce and me indicates that these parameters could be combined into a single empirical parameter that has to be tuned. The sensitivity of the model to the choice of the calibrated parameters decreased after the adjustments had been made, indicating greater model robustness. This is confirmed by the simulated reduction between the modelled NCP in the run with the smallest difference between observations and simulations (the Best solution, table 6) and the run with the maximal NCP taken from the final 100 runs of the DREAM optimization.

The simulations of the calibration period (figure 21 and 22) after the DREAM optimization showed very good agreement in both the dynamics and size of the simulated fluxes compared to the observations. However, the root water uptake flux (Qr) fluctuated strongly during the simulations. The behaviour of Qr throughout the model runs (see figure 23)

is probably the result from numerical instability. Unfortunately this could not be tested as the input data were only available on the half hourly time step that the model was run with. The fluctuations in Qr and Mq affected the in- and outgoing water fluxes that were simulated by the model, through their influence on the tissues' water balance pressure. The effect on the simulated water fluxes in turn affects the evapotranspiration rate, the solution of G_s, the simulated carbon fluxes and NCP. The behaviour of the simulated water fluxes probably caused the high amount of days the tree experienced 'water stress' and led to the second adjustment in the model. Water stress was defined as the condition that the actual amount of water storage in the tree dropped below 90% of the potential amount, thus Mq<0.9*Mqx. This is based on the hypothesis stated by Schymanski (2007) that: *"a reduction in water content of living tissues by 10% from the saturated value is reversible, while further reduction in water content may lead to permanent cell damage"*.

The value of Mqx (adjustment 2) was changed from the original value used by Schymanski (2007) to a higher value that led to a reduction in the amount of days the tree experienced water stress. It can be debated whether the original value of Mqx was valid for the current site at all, because the original value of Mqx was calibrated based on observations of Cernusak *et al.* (2006) in the savanna site near Howard Springs (Northern Territory, Australia) for a different tree species and forest structure. No values more suitable for the Hainich site were found in literature, thus Mqx was changed based on the amount of days that water stress was simulated. After adjusting the value of Mqx the second optimization procedure was run with the final model for the entire year 2005.

The degree-day method that was used to simulate the phenological development of the tree was very sensitive to the initial conditions. To deal with this the optimization was started from different 10 day maximum temperature thresholds and allowed to converge freely towards the solution with the smallest error (Eqn 54). The choice to increase the canopy layers with only 1 every day, under the condition that the degree-day threshold was exceeded, might have been too conservative as it took the tree at least fifty days to reach a full canopy cover and a similar amount to decrease LAI again. Comparison of the carbon flux simulations and observations suggests that the onset of LAI was modelled too late and the decline too early, leading to an under estimation in spring and fall. Increasing the number of canopy layers added or subtracted per day during flushing and senescence could improve simulations, because this would allow the maximum LAI to be reached for a longer period during summer.

Overall, the simulations with the finalized model show good agreement with the observations, but the following points of discussion remain. The simulated carbon fluxes in 2003, 2004, 2006 and 2007 (figure 31) shows sudden drop in the middle of the year. This could be caused by (1) an underestimation of the length of the maximum LAI or (2) an overestimation of respiratory fluxes. The underestimation of LAI does not explain the peak that is simulated near the end of the summer however. An overestimation of respiration during a short (hot) period in summer could result from the dependence of respiration on temperature. Lower temperatures and therefore woody tissue and soil respiration fluxes at the beginning and end of summer combined with photosynthesis could result in appropriate values for the carbon flux, but an overestimation during the high temperatures reached in the middle summer would result in a smaller net carbon flux.

Finally, regarding to the simulations of 2003 to investigate the hypothetical root mechanism, it is important to notice that the mechanism only starts to make a difference after an evaluation period of at least 4 days (figure 32). This results from the cost-benefit trade-off between (1) keeping photosynthesis going by investing in replacement of fine root mass and extracting water from deeper down the profile or (2) decreasing maintenance respiration by decreasing leave area. The realism of the model could be improved by changing the evaluation period from days in the future to days in the past, as the tree has no knowledge about future climatic conditions, but the soil has a memory of the rain events of the previous days.

8. Conclusions

During this research project an explanation was sought for the observed difference in evapotranspiration between trees and other vegetation during periods of drought. The hypothesis that trees can create fine root mass at depth was investigated with an eco-hydrological optimality model that included this hypothetical root mechanism. The total carbon and water fluxes that were simulated for the years 2003-2007 are comparable to the observations. The simulated water saturation degree in the upper soil layer shows the expected dynamics and gives confidence in the model's accuracy and justness of the calibrated parameters. Overall, the simulated water fluxes are in better agreement with the observations than the carbon fluxes, even though there is a general overestimation of soil evaporation in spring.

For each of the simulated years, the modelled carbon flux in spring is higher than the measurements, thus the model simulates an uptake in carbon that is not observed in reality. The representation of the phenological development of the tree with the degree-day method led to further deviation between the observations and simulated fluxes. Besides the general overestimation of the carbon uptake before the onset of the vegetative period, there is an underestimation after the rapid decline of LAI. The simulated water fluxes are in general in better agreement with the observations than the carbon flux.

Simulations with the hypothetical root mechanism in place for the summer of 2003, during the extreme drought, show an increase in NCP after an evaluation period of 4 days or more. Cumulative NCP did not increase for a 1-3 day evaluation period and therefore the model did not simulate the repositioning of roots to deeper soil layers. The models simulations of the uptake of water are higher after roots have been repositioned to deeper soil layers and consequently there is an increase in carbon assimilation. The results show that the tree does not always relocate its fine roots to the deepest soils layers, since other layers can be equally or even more profitable from the NCP perspective. There is a cost-benefit trade-off between investing carbon into the creation of fine roots in a different layer and the carbon that is gained through the increase in photosynthesis that is possible due to the higher water demand that can be met. However, because the simulated fluxes depend more on the absence or presence and amount of leaf layers than the positioning of fine root mass, correlations between simulations and observations did not improve with the root mechanism in place.

The main conclusions with the hypothetical root mechanism implemented in the model are that there is indeed an increase in NCP, but there is no proof that this gives a better fit to the data, because the phenology, onset and decline of Leaf Area Index (LAI), is not simulated correctly. The model that was used during this project would benefit from (1) a better representation of the root water uptake flux. This could be accomplished through more realistic values of the water storage in the vegetative tissues and decreasing the time step in the model to reduce the experienced numerical instability. To further investigate the hypothetical root mechanism it is advised to (2) change the cost of creating new fine root mass and/or the vascular system respiration (Eqn 31). Vascular system respiration is basically unknown and is generally modelled as a linear relationship. The costs of creating fine root mass are also not measurable and were calculated as the carbon fraction of their weight. Nearly all eco-hydrological model simulations could be improved by (3) building a better phenology model. The realism of the model could further be improved by changing the evaluation period from days in the future to days in the past, as the tree has no knowledge about future climatic conditions, but the soil has a memory of the rain events of the previous days.

The hypothetical root mechanism should be further tested within models that simulate both trees and understory vegetation to distinguish between the evaporation of different vegetation types under droughts of different strengths. Especially with the foreseen increase in droughts under climate change, it is important to further investigate this mechanism to simulate atmospheric water content more realistically. The correct representation of evapotranspiration of trees could have far reaching consequences in weather and climate models in which vegetation is the link between the carbon and water cycle and plays an important role.

References

Adams, H. D., Guardiola-Claramonte, M., Barron-Gafford, G. A., Villegas, J. C., Breshears, D. D., Zou, C. B., Troch, P. A., and Huxman, T. E. (2009). "Temperature sensitivity of drought-induced tree mortality portends increased regional die-off under global-change-type drought." Proceedings of the National Academy of Sciences of the United States of America, 106(17), 7063-7066.

Allen, R. G., Pereira, L. S., Raes, D., and Smith, M. (1998). Crop evapotranspiration - Guidelines for computing crop water requirements. Food and Agriculture Organization of the United Nations, Rome.

Arora, V. (2002). "Modeling vegetation as a dynamic component in soil-vegetation-atmosphere transfer schemes and hydrological models." Reviews of Geophysics, 40(2).

Bala, G., Caldeira, K., Wickett, M., Phillips, T. J., Lobell, D. B., Delire, C., and Mirin, A. (2007). "Combined climate and carbon-cycle effects of large-scale deforestation." Proceedings of the National Academy of Sciences of the United States of America, 104(16), 6550-6555.

Beringer, J., Chapin, F. S., Thompson, C. C., and McGuire, A. D. (2005). "Surface energy exchanges along a tundra-forest transition and feedbacks to climate." Agricultural and Forest Meteorology, 131(3-4), 143-161.

Bernacchi, C. J., Singsaas, E. L., Pimentel, C., Portis, A. R., and Long, S. P. (2001). "Improved temperature response functions for models of Rubisco-limited photosynthesis." Plant Cell and Environment, 24(2), 253-259.

Brolsma, R. J., Karssenberg, D., and Bierkens, M. F. P. (2010). "Vegetation competition model for water and light limitation. I: Model description, one-dimensional competition and the influence of groundwater." Ecological Modelling, 221(10), 1348-1363.

Brooks, R. H., and Corey, A. T. (1966). "Properties of porous media affecting fluid flow." Irrigation and Drainage Division - American Society of Civil Engineers, 2, 61-88.

Cannell, M. G. R., and Thornley, J. H. M. (2000). "Modelling the components of plant respiration: Some guiding principles." Annals of Botany, 85(1), 45-54.

Cernusak, L. A., Hutley, L. B., Beringer, J., and Tapper, N. J. (2006). "Stem and leaf gas exchange and their responses to fire in a north Australian tropical savanna." Plant Cell and Environment, 29(4), 632-646.

Ciais, P., Reichstein, M., Viovy, N., Granier, A., Ogee, J., Allard, V., Aubinet, M., Buchmann, N., Bernhofer, C., Carrara, A., Chevallier, F., De Noblet, N., Friend, A. D., Friedlingstein, P., Grunwald, T., Heinesch, B., Keronen, P., Knohl, A., Krinner, G., Loustau, D., Manca, G., Matteucci, G., Miglietta, F., Ourcival, J. M., Papale, D., Pilegaard, K., Rambal, S., Seufert, G., Soussana, J. F., Sanz, M. J., Schulze, E. D., Vesala, T., and Valentini, R. (2005). "Europe-wide reduction in primary productivity caused by the heat and drought in 2003." Nature, 437(7058), 529-533.

Cowan, I. R., and Farquhar, G. D. (1977). "Stomatal Behaviour and Environment." Advances in Botanical Research, 4, 117-228.

Cox, P. M., Betts, R. A., Jones, C. D., Spall, S. A., and Totterdell, I. J. (2000). "Acceleration of global warming due to carbon-cycle feedbacks in a coupled climate model." Nature, 408(6809), 184-187.

Daly, E., Porporato, A., and Rodriguez-Iturbe, I. (2004). "Coupled dynamics of photosynthesis, transpiration, and soil water balance. Part I: Upscaling from hourly to daily level." Journal of Hydrometeorology, 5(3), 546-558.

De Swaef, T., Steppe, K., and Lemeur, R. (2009). "Determining reference values for stem water potential and maximum daily trunk shrinkage in young apple trees based on plant responses to water deficit." Agricultural Water Management, 96(4), 541-550.

Dekker, S. C., Elkington, R. J., and Vrugt, J. A. (2009). "Significant Variation in Vegetation Characteristics and Dynamics: from Ecohydrological Optimality of Net Carbon Profit"Plant, Cell & Environment. City: Utrecht University: Utrecht, pp. 49.

Dekker, S. C., Rietkerk, M., and Bierkens, M. F. P. (2007). "Coupling microscale vegetation-soil water and macroscale vegetation-precipitation feedbacks in semiarid ecosystems." Global Change Biology, 13(3), 671-678.

Easterling, W., and Apps, M. (2005). "Assessing the consequences of climate change for food and forest resources: A view from the IPCC." Climatic Change, 70(1-2), 165-189.

Espelta, J. M., Cortes, P., Mangiron, M., and Retana, J. (2005). "Differences in biomass partitioning, leaf nitrogen content, and water use efficiency (delta C-13) result in similar performance of seedlings of two Mediterranean oaks with contrasting leaf habit." Ecoscience, 12(4), 447-454.
Eugster, W., Rouse, W. R., Pielke, R. A., McFadden, J. P., Baldocchi, D. D., Kittel, T. G. F., Chapin, F. S., Liston, G. E., Vidale, P. L., Vaganov, E., and Chambers, S. (2000). "Land-atmosphere energy exchange in Arctic tundra and boreal forest: available data and feedbacks to climate." Global Change Biology, 6, 84-115.
Farquhar, G. D., Caemmerer, S. V., and Berry, J. A. (1980). "A biochemical-model of photosynthetic co2 assimilation in leaves of c-3 species." Planta, 149(1), 78-90.
Ferrell, G. T. (1996). The influence of insect pests and pathogens on Sierra Forests. In: Sierra Nevada Ecosystem Project: Final report to congress, vol. II, Assessments and Scientific Basis for Management Options. Centers for Water and Wildland Resources.
Gallardo, M., Jackson, L. E., Schulbach, K., Snyder, R. L., Thompson, R. B., and Wyland, L. J. (1996). "Production and water use in lettuces under variable water supply." Irrigation Science, 16(2), 125-137.
Gansert, D. (1994). "Root respiration and its importance for the carbon balance of beech saplings (fagus-sylvatica l) in a montane beech forest." Plant and Soil, 167(1), 109-119.
Givnish, T. J. (2002). "Adaptive significance of evergreen vs. deciduous leaves: Solving the triple paradox." Silva Fennica, 36(3), 703-743.
Guarin, A., and Taylor, A. H. (2005). "Drought triggered tree mortality in mixed conifer forests in Yosemite National Park, California, USA." Forest Ecology and Management, 218(1-3), 229-244.
Harte, J., Saleska, S., and Shih, T. (2006). "Shifts in plant dominance control carbon-cycle responses to experimental warming and widespread drought." Environmental Research Letters, 1(1).
Hattenschwiler, S., and Korner, C. (1998). "Biomass allocation and canopy development in spruce model ecosystems under elevated CO2 and increased N deposition." Oecologia, 113(1), 104-114.
Hernandez-Santana, V., Martinez-Fernandez, J., and Moran, C. (2008). "Estimation of tree water stress from stem and soil water monitoring with time-domain reflectometry in two small forested basins in Spain." Hydrological Processes, 22(14), 2493-2501.
Hughes, M. K., Swetnam, T. W., and Diaz, H. F. (2004). "Tree Rings and Climate: Sharpening the Focus." Eos, Transactions, American Geophysical Union, 85(32).
IPCC (2007). Climate Change 2007: The Physical Science Basis. Cambridge, United Kingdom and New York, NY, USA.
Jarvis, P. G. (1976). "Interpretation of variations in leaf water potential and stomatal conductance found in canopies in field." Philosophical Transactions of the Royal Society of London Series B-Biological Sciences, 273(927), 593-610.
Jochheim, H., Puhlmann, M., Beese, F., Berthold, D., Einert, P., Kallweit, R., Konopatzky, A., Meesenburg, H., Meiwes, K.-J., Raspe, S., Schulte-Bisping, H., and Schulz, C. (2009). "Modelling the carbon budget of intensive forest monitoring sites in Germany using the simulation model BIOME-BGC." IForest, 2, 7-10.
Joffre, R., Ourcival, J. M., Rambal, S., and Rocheteau, A. (2003). "The key-role of topsoil moisture on CO2 efflux from a Mediterranean Quercus ilex forest." Annals of Forest Science, 60(6), 519-526.
Knohl, A., Schulze, E. D., Kolle, O., and Buchmann, N. (2003). "Large carbon uptake by an unmanaged 250-year-old deciduous forest in Central Germany." Agricultural and Forest Meteorology, 118(3-4), 151-167.
Kobayashi, Y., and Tanaka, T. (2001). "Water flow and hydraulic characteristics of Japanese red pine and oak trees." Hydrological Processes, 15(10), 1731-1750.
Kruijt, B., Witte, J. P. M., Jacobs, C. M. J., and Kroon, T. (2008). "Effects of rising atmospheric CO2 on evapotranspiration and soil moisture: A practical approach for the Netherlands." Journal of Hydrology, 349(3-4), 257-267.
Kull, O., and Jarvis, P. G. (1995). "The role of nitrogen in a simple scheme to scale-up photosynthesis from leaf to canopy." Plant Cell and Environment, 18(10), 1174-1182.
Kutsch, W. L., Persson, T., Schrumpf, M., Moyano, F. E., Mund, M., Andersson, S., and Schulze, E. D. (2010). "Heterotrophic soil respiration and soil carbon dynamics in the

deciduous Hainich forest obtained by three approaches." Biogeochemistry.
Lauenroth, W. K., and Bradford, J. B. (2006). "Ecohydrology and the partitioning AET between transpiration and evaporation in a semiarid steppe." Ecosystems, 9(5), 756-767.
Leuning, R., Zegelin, S. J., Jones, K., Keith, H., and Hughes, D. (2008). "Measurement of horizontal and vertical advectlion of CO2 within a forest canopy." Agricultural and Forest Meteorology, 148(11), 1777-1797.
Leuzinger, S., Zotz, G., Asshoff, R., and Korner, C. (2005). "Responses of deciduous forest trees to severe drought in Central Europe." Tree Physiology, 25(6), 641-650.
Limousin, J. M., Rambal, S., Ourcival, J. M., and Joffre, R. (2008). "Modelling rainfall interception in a Mediterranean Quercus ilex ecosystem: Lesson from a throughfall exclusion experiment." Journal of Hydrology, 357(1-2), 57-66.
Medlyn, B. E., Dreyer, E., Ellsworth, D., Forstreuter, M., Harley, P. C., Kirschbaum, M. U. F., Le Roux, X., Montpied, P., Strassemeyer, J., Walcroft, A., Wang, K., and Loustau, D. (2002). "Temperature response of parameters of a biochemically based model of photosynthesis. II. A review of experimental data." Plant Cell and Environment, 25(9), 1167-1179.
Medrano, H., Flexas, J., and Galmes, J. (2009). "Variability in water use efficiency at the leaf level among Mediterranean plants with different growth forms." Plant and Soil, 317(1-2), 17-29.
Monteith, J. L. (1965). "Evaporation and environment." Symp Soc Exp Biol, 19, 205-34.
Moyano, F. E., Kutsch, W. L., and Rebmann, C. (2008). "Soil respiration fluxes in relation to photosynthetic activity in broad-leaf and needle-leaf forest stands." Agricultural and Forest Meteorology, 148(1), 135-143.
Ogaya, R., Penuelas, J., Martinez-Vilalta, J., and Mangiron, M. (2003). "Effect of drought on diameter increment of Quercus ilex, Phillyrea latifolia, and Arbutus unedo in a holm oak forest of NE Spain." Forest Ecology and Management, 180(1-3), 175-184.
Papale, D., Reichstein, M., Aubinet, M., Canfora, E., Bernhofer, C., Kutsch, W., Longdoz, B., Rambal, S., Valentini, R., Vesala, T., and Yakir, D. (2006). "Towards a standardized processing of Net Ecosystem Exchange measured with eddy covariance technique: algorithms and uncertainty estimation." Biogeosciences, 3(4), 571-583.
Rambal, S., Joffre, R., Ourcival, J. M., Cavender-Bares, J., and Rocheteau, A. (2004). "The growth respiration component in eddy CO2 flux from a Quercus ilex mediterranean forest." Global Change Biology, 10(9), 1460-1469.
Reichstein, M., Falge, E., Baldocchi, D., Papale, D., Aubinet, M., Berbigier, P., Bernhofer, C., Buchmann, N., Gilmanov, T., Granier, A., Grunwald, T., Havrankova, K., Ilvesniemi, H., Janous, D., Knohl, A., Laurila, T., Lohila, A., Loustau, D., Matteucci, G., Meyers, T., Miglietta, F., Ourcival, J. M., Pumpanen, J., Rambal, S., Rotenberg, E., Sanz, M., Tenhunen, J., Seufert, G., Vaccari, F., Vesala, T., Yakir, D., and Valentini, R. (2005). "On the separation of net ecosystem exchange into assimilation and ecosystem respiration: review and improved algorithm." Global Change Biology, 11(9), 1424-1439.
Requardt, A., Schuck, A., and Köhl, M. (2009). "Means of combating forest dieback - EU support for maintaining forest health and vitality." IForest, 2, 38-42.
Roderick, M. L., and Canny, M. J. (2005). "A mechanical interpretation of pressure chamber measurements - what does the strength of the squeeze tell us?" Plant Physiology and Biochemistry, 43(4), 323-336.
Schaap, M. G., Leij, F. J., and van Genuchten, M. T. (1998). "Neural network analysis for hierarchical prediction of soil hydraulic properties." Soil Science Society of America Journal, 62(4), 847-855.
Schuurmans, J. M. (2008). Hydrological now- and forecasting : Integration of operationally available remotely sensed and forecasted hydrometeorological variables into distributed hydrological models, Utrecht University, Utrecht
Schwinning, S., Sala, O. E., Loik, M. E., and Ehleringer, J. R. (2004). "Thresholds, memory, and seasonality: understanding pulse dynamics in arid/semi-arid ecosystems." Oecologia, 141(2), 191-193.
Schymanski, S. J. (2007). Transpiration as the Leak in the Carbon Factory: A Model of Self-Optimising Vegetation University of Western Australia, Perth.
Schymanski, S. J., Roderick, M. L., Sivapalan, M., Hutley, L. B., and Beringer, J. (2007). "A test of the optimality approach to modelling canopy properties and CO2 uptake by natural vegetation." Plant Cell and Environment, 30, 1586-1598.

Schymanski, S. J., Roderick, M. L., Sivapalan, M., Hutley, L. B., and Beringer, J. (2008a). "A canopy-scale test of the optimal water-use hypothesis." Plant Cell and Environment, 31(1), 97-111.
Schymanski, S. J., Sivapalan, M., Roderick, M. L., Beringer, J., and Hutley, L. B. (2008b). "An optimality-based model of the coupled soil moisture and root dynamics." Hydrology and Earth System Sciences, 12(3), 913-932.
Schymanski, S. J., Sivapalan, M., Roderick, M. L., Hutley, L. B., and Beringer, J. (2009). "An optimality-based model of the dynamic feedbacks between natural vegetation and the water balance." Water Resources Research, 45.
Sheffield, J., and Wood, E. F. (2008). "Projected changes in drought occurrence under future global warming from multi-model, multi-scenario, IPCC AR4 simulations." Climate Dynamics, 31(1), 79-105.
Soe, A. R. B., and Buchmann, N. (2005). "Spatial and temporal variations in soil respiration in relation to stand structure and soil parameters in an unmanaged beech forest." Tree Physiology, 25(11), 1427-1436.
Sutherland, W. J. (2005). "The best solution." Nature, 435(7042), 569-569.
Ter Braak, C. J. F. (2006). "A Markov Chain Monte Carlo version of the genetic algorithm differential evolution: easy Bayesian computing for real parameter spaces." Statistics and Computing, 16(3), 239-249.
Tubiello, F. N., and Ewert, F. (2002). "Simulating the effects of elevated CO2 on crops: approaches and applications for climate change." European Journal of Agronomy, 18(1-2), 57-74.
Van der Werf, G. W., Sass-Klaassen, U. G. W., and Mohren, G. M. J. (2007). "The impact of the 2003 summer drought on the intra-annual growth pattern of beech (Fagus sylvatica L.) and oak (Quercus robur L.) on a dry site in the Netherlands." Dendrochronologia, 25, 103-112.
Van Genuchten, M. T. (1980). "A closed form equation for predicting the hydraulic condutivity of unsaturaed soils." Soil Science Society of America Journal, 44(5), 892-898.
Vanguelova, E. I., Nortcliff, S., Moffat, A. J., and Kennedy, F. (2005). "Morphology, biomass and nutrient status of fine roots of Scots pine (Pinus sylvestris) as influenced by seasonal fluctuations in soil moisture and soil solution chemistry." Plant and Soil, 270(1-2), 233-247.
Verkaik, E., Moraal, L. G., and Nabuurs, G. J. M. M. (2009). Potential impacts of climate change on Dutch forests; Mapping the risks. Alterra.
Vincke, C., and Thiry, Y. (2008). "Water table is a relevant source for water uptake by a Scots pine (Pinus sylvestris L.) stand: Evidences from continuous evapotranspiration and water table monitoring." Agricultural and Forest Meteorology, 148(10), 1419-1432.
Vitasse, Y., Porte, A. J., Kremer, A., Michalet, R., and Delzon, S. (2009). "Responses of canopy duration to temperature changes in four temperate tree species: relative contributions of spring and autumn leaf phenology." Oecologia (Berlin), 161(1), 187-198.
Vrugt, J. A., ter Braak, C. J. F., Diks, C. G. H., Robinson, B. A., Hyman, J. M., and Higdon, D. (2009). "Accelerating Markov Chain Monte Carlo Simulation by Differential Evolution with Self-Adaptive Randomized Subspace Sampling." International Journal of Nonlinear Sciences and Numerical Simulation, 10(3), 273-290.
Wälder, O., and Wälder, K. (2008). "Modeling the fine root biomass dispersion using a special influence function." IForest, 1, 141-144.
Wang, G. L. (2005). "Agricultural drought in a future climate: results from 15 global climate models participating in the IPCC 4th assessment." Climate Dynamics, 25(7-8), 739-753.
Welp, L. R., Randerson, J. T., and Liu, H. P. (2007). "The sensitivity of carbon fluxes to spring warming and summer drought depends on plant functional type in boreal forest ecosystems." Agricultural and Forest Meteorology, 147(3-4), 172-185.
Woodward, F. I., Smith, T. M., and Emanuel, W. R. (1995). "A global land primary productivity and phytogeography model." Global Biogeochemical Cycles, 9(4), 471–490.
Wright, I. J., Reich, P. B., Westoby, M., Ackerly, D. D., Baruch, Z., Bongers, F., Cavender-Bares, J., Chapin, T., Cornelissen, J. H. C., Diemer, M., Flexas, J., Garnier, E., Groom, P. K., Gulias, J., Hikosaka, K., Lamont, B. B., Lee, T., Lee, W., Lusk, C., Midgley, J. J., Navas, M. L., Niinemets, U., Oleksyn, J., Osada, N., Poorter, H., Poot, P., Prior, L., Pyankov, V. I., Roumet, C., Thomas, S. C., Tjoelker, M. G., Veneklaas, E. J., and Villar,

R. (2004). "The worldwide leaf economics spectrum." Nature, 428(6985), 821-827.
Yadav, S. K., and Singh, D. P. (1981). "Effect of irrigation and antitranspirants on evapotranspiration, water use efficiency and moisture extraction patterns of barley." Irrigation Science, 2(3), 177-184.
Zhu, Y. H., Ren, L. L., Skaggs, T. H., Lu, H. S., Yu, Z. B., Wu, Y. Q., and Fang, X. Q. (2009). "Simulation of Populus euphratica root uptake of groundwater in an arid woodland of the Ejina Basin, China." Hydrological Processes, 23(17), 2460-2469.
Zweifel, R., Item, H., and Hasler, R. (2000). "Stem radius changes and their relation to stored water in stems of young Norway spruce trees." Trees-Structure and Function, 15(1), 50-57.

On line resources

CarboEuropeIP: http://gaia.agraria.unitus.it/DATABASE/carboeuropeip/site.aspx
Last accessed 14/03/2010

Appendix 1: List of input parameters

List of all the parameters used in this study. Addition (i) to a symbol denotes reference to the respective soil layer i where i=1,...,n and (m) denotes the respective vegetative leaf layer.

Symbol	Description	Units	Value	Reference	Puechabon	Reference
a	Molecular diffusion coefficient of CO2 in air, relative to that for water vapour	-	1.6			
A_g	CO2 uptake rate per unit ground area	mol m-2 s-1				
alp	parameter set by common practice	-	0.3	Schymanski 2007		
avG	empirical van Genuchten parameter	m-1	1.27	Schaap et al, 1998	1.29	Schaap et al, 1998
Ca	Mole fraction of CO2 in the air	mol mol-1				
Ce	parameter that define the shape of the relationship between λ and h(i)	-	variable			
C_l	Mole fraction of CO2 in a leaf	mol mol-1				
c_p	specific heat capacity of air	cal g-1 degree-1	0.24			
c_{Pbm}	conversion coefficient to convert from bar to m	m bar-1	10.2			
c_{Rl}	Leaf respiration coefficient	-	variable			
c_{Rr}	root respiration coefficient	mol m-3 s-1	0.0017			
c_{rv}	vascular respiration coefficient	mol m-3 s-1	1.2*10^-6			
dt	time step	s	1800			
Dv	molar atmospheric vapour deficit	mol mol-1				
dZ	soil layer depth	m	0.25			
e	ratio of the molecular weight of water vapour and dry air	-	0.622			
E	porosity of the soil	m3 m-3				
e_a	actual vapour pressure	Pa				
EI	evaporation of interception	mm d-1				
Eo	open water evaporation	mm d-1				
e_s	saturation vapour pressure	Pa				
Esu	Soil evaporation in the top layer	mol m-2 s-1				
E_t	transpiration rate per unit ground area	mm d-1				
E_{To}	reference potential evapotranspiration	mm d-1				
G_s	stomatal conductivity per unit ground area	mol m-2 s-1				
h(i)	matrix potential	m				
H_a	Rate of exponential increase of Jmax with temperature	J mol-1	71.38*10^3	Medlyn et al, 2002	35.87*10^3	Medlyn et al, 2002
H_d	Rate of decrease of Jmax with temperature above Topt	J mol-1	200*10^3	Medlyn et al, 2002	200*10^3	Medlyn et al, 2002
h_h(i)	hydrostatic head difference between the soil surface and the depth of layer i	m				
h_r(i)	Root suction head in layer i	m				
I	interception	mm d-1				
I_a	photosynthetically active irradiance	mol quanta m-2 s-1				
I_b(m)	intensity of direct light	mol quanta m-2 s-1				
Icap	maximum interception capacity	m	0.0005	Brolsma 2010	0.00034	Vink & Oerlemans, pers. com. 2010
I_d(m)	intensity of diffuse light	mol quanta m-2 s-1				

Symbol	Description	Units	Value	Reference	Puechabon	Reference
irp	deepest soil layer accessed by tree roots	-				
I_{sun}(m)	sunlit fraction	mol quanta m-2 s-1				
J	electron transport rate per leaf area	mol m-2 s-1				
JA	total electron transport rate per unit ground area	mol m-2 s-1				
J_{max}	biochemical electron transport capacity	mol m-2 s-1				
J_{max25}	Photosynthetic electron transport capacity per leaf	mol m-2 s-1				
J_{maxtot}	total electron transport capacity for the canopy	mol m-2 s-1				
J_{maxtop}	total electron transport capacity at the top of the canopy	mol m-2 s-1				
J_r(i)	Water uptake per unit root surface area	m s-1				
J_{shade}(m)	electron transport rate achieved by shaded leaves	mol m-2 s-1				
J_{sun}(m)	electron transport rate achieved by sunlit leaves	mol m-2 s-1				
k	Karman constant	-	0.41			
kJ	light extinction co-efficient	-	0.5	(Woodward *et al.*, 1995)		
K_{sat}	saturated hydraulic conductivity	m s-1	8.217*10^-6	Schaap et al, 1998	1.4571*10^-6	Schaap et al, 1998
K_{unsat}	Unsaturated hydraulic conductivity	m s-1				
LA	leaf area	m2 m-2	0.1			
LAI	leaf area index	m2 m-2				
LAI_{max}	maximum leaf area index	m2 m-2	5	Knohl et al, 2003	3	Papale et al 2006
LambdaE	latent heat of vaporisation	J kg-1	2.45*10^6			
LAshade	shaded leaf area	m2 m-2				
LAsun	sunlit leaf area	m2 m-2				
Ll	local longitude	degree	10.452	CarboEuropeIP	3.595833	CarboEuropeIP
LL	leaf life span	months	5.21	GLOPNET	7.46	GLOPNET
LMA	leaf dry mass per area	g m-2	2.18	GLOPNET	2.29	GLOPNET
m	number of layers in the canopy	-	variable			
MA	fraction of vegetated cover	-				
Md	total mass of dry matter per unit ground area	kg				
me	parameter that define the shape of the relationship between λ and h(i)	-	variable			
mmCO2	molecular mass of CO2	g mol-1	44			
Mq	tissue water content per unit ground area	kg				
Mqx	potential tissue water content per unit ground area	kg				
mvG	empirical van Genuchten parameter	-				
n	number of of soil layers	-	20			
NCP	Net Carbon Profit	mol m-2 s-1				
nvG	empirical van Genuchten parameter	-	1.38	Schaap et al, 1998	1.28	Schaap et al, 1998
P	precipitation	mm				
P_a	barometric air pressure	hPa	1013			
P_b	tissue balance pressure	bar				
Q(i)	drainage flux	m s-1				

Symbol	Description	Units	Value	Reference	Puechabon	Reference
Q10,w	proportional increase in Rw with 10 K increase in wood temperature	-	1.92	Cernusak et al, 2006		
Qr(i)	root water uptake flux	m s-1				
r_a	aerodynamic resistance	s m-1				
RAI_{max}	maximum root area index	m2 m-2	1.8*LAImax	Gansert 1994	1.8*LAImax	Espelta et al, 2005
R_{ft}	foliage turnover costs per unit ground area	mol m-2 s-1				
R_l	leaf respiration per unit ground area	mol m-2 s-1				
R_{mol}	molar gas constant	J mol-1 K-1	8.314			
R_r	root respiration	mol m-2 s-1				
r_r	root radius	m	0.0003	Schymanski 2007		
R_s	soil respiration	µmol m-2 s-1				
r_s	surface resistance	s m-1				
$R_{s,ref}$	soil respiration at Tref and nonlimiting soil moisture	µmol m-2 s-1				
R_w	above-ground woody-tissue respiration	µmol m-2 s-1				
R_{w25}	respiration at reference temperature	µmol m-2 s-1	0.606			
$SA_{dr}(i)$	root surface area density	m2 m-3				
SA_r	root surface area	m2				
Ssc	solar constant	w m-2	1367			
su(i)	water saturation degree	-				
T_a	air temperature	K				
theta	geographic latitude	degree	51.0793	CarboEuropeIP	43.74139	CarboEuropeIP
T_{opt}	mean daytime temperature	K				
T_r	reference temperature for woody-tissue respiration	°C	25			
T_s	soil temperature	K				
Tw	wood temperature	°C				
u	wind speed	m s-1				
W_a	Molar fraction of water vapour in the atmosphere	mol mol-1				
W_l	Molar fraction of water vapour in the air spaces within a leaf	mol mol-1				
y_r	root depth	m				
Z	depth of pedosphere	m	5			
z_d	zero plane displacement height	m				
z_h	height at which the vapour pressure is measured	m				
z_m	height at which the wind speed is measured	m				
z_o	roughness length	m				
z_v	vegetation height	m	0.12			
z_v	vegetation height	m	0.12	Allen et al, 1998		
γ	psychometric constant	Pa °C-1				
Γ*	CO2-compensation point in the absence of respiration	mol mol-1				
δ	slope of the function of the saturation vapour pressure versus the air temperature	Pa °C-1				
θ	soil moisture content	m3 m-3				
$θ_b$	residual water content	m3 m-3	0.536	Schaap et	0.441	Schaap et al,

Symbol	Description	Units	Value	Reference	Puechabon	Reference
				al, 1998		1998
θ_s	saturated water content	m3 m-3	0.102	Schaap et al, 1998	0.081	Schaap et al, 1998
λ_v	latent heat of vaporization	J kg-1				
ρ_a	density of air	kg m-3	1.205			
ρ_w	density of water	kg m-3	1000			
Ω_r	root resistivity to water uptake per unit root surface area	s				
$\Omega_s(i)$	resistivity to water flow towards the roots in the soil	s				

Appendix 2: Original research proposal and planning

The ecohydrology of drought: what are the survival mechanisms of trees?
Carbon allocation in deciduous and evergreen oak species in Mediterranean France under drought
Student: Emma Daniels (0448257)
Supervision: Marc Bierkens (possibly Derek Karssenberg and/or Steven de Jong?), Physical Geography, UU

During the remainder of this project the following steps will be taken:

- Building a Matlab/Phyton/Fortran/PCRaster model that simulates tree growth and optimal behaviour during a drought (including assimilation, respiration and transpiration). The vegetation model simulates the growth of tree biomass using a CO2-assimilation module subject to water stress. The simulated trees choose between maximizing carbon gain by creating additional fine root mass at depth or reducing leaf area and respiration.
- The model will be compared to flux tower CO2 and evaporation measurements and reports of leaf vigor (health) assessed from hyperspectral remote sensing for the extreme and prolonged drought period in central Europe in the summer of 2003.
- The model will be validated further by a combination of meteorological time series and tree-ring data from Southern France. This will be done for a evergreen oak species (Quercus Ilex) and possibly compared to a deciduous species (Quercus Pubescens).
- After validation, the vegetation model will be run for different climate scenario's to investigate the influence of climate change on tree growth in forests in Mediterranean climates.

Time and planning	from	until
Literature research	now	15 July 2009
Field work	1 Sep	15 Sep
Model building	23 Aug	7 Oct
Reporting methods	7 Sep	15 Oct
Collect flux & rs data	15 Sept	15 Oct
Field data	15 Sept	15 Oct
Model tuning (2003)	1 Oct	23 Oct
Tree ring data	15 Oct	1 Nov
Model building	23 Oct	23 Nov
Model validation	7 Nov	15 Nov
Reporting results	15 Nov	23 Nov
Climate Scenario's	23 Nov	7 Dec
Reporting research	23 Nov	23 Dec
Writing thesis	1 Jan	31 Jan

(Abroad: 23-31 Aug Milan, 1-15 Sep Peyne, 7-12 Oct Molmo, 7-18 Dec Cop15)

The fieldwork will take place in the La Peyne area in Southern France. I hope to get an overview of the different methods that can be used to measure conditions in the field that will be used as parameters in the model. I would like to measure biomass distribution and moisture content in 2 tree species (Quercus Ilex and Pubescens), get an impression of the field conditions and reliability of the measurements. I will use some of the measurements done in this area by other students to calibrate the model for the specific tree species and make estimations of tree ring width during growth. Potentially the model could be used over larger forest areas to predict transpiration and respiration